JPRS 67047

29 March 1976

FBIS

USSR

THEORETICAL PRINCIPLES OF TORPEDO WEAPONS

By

G. M. Podobriy, et al.

U. S. JOINT PUBLICATIONS RESEARCH SERVICE

NOTE

JPRS publications contain information primarily from foreign newspapers, periodicals and books, but also from news agency transmissions and broadcasts. Materials from foreign-language sources are translated; those from English-language sources are transcribed or reprinted, with the original phrasing and other characteristics retained.

Headlines, editorial reports, and material enclosed in brackets [] are supplied by JPRS. Processing indicators such as [Text] or [Excerpt] in the first line of each item, or following the last line of a brief, indicate how the original information was processed. Where no processing indicator is given, the information was summarized or extracted.

Unfamiliar names rendered phonetically or transliterated are enclosed in parentheses. Words or names preceded by a question mark and enclosed in parentheses were not clear in the original but have been supplied as appropriate in context. Other unattributed parenthetical notes within the body of an item originate with the source. Times within items are as given by source.

The contents of this publication in no way represent the policies, views or attitudes of the U.S. Government.

PROCUREMENT OF PUBLICATIONS

JPRS publications may be ordered from the National Technical Information Service, Springfield, Virginia 22151. In ordering, it is recommended that the JPRS number, title, date and author, if applicable, of publication be cited.

Current JPRS publications are announced in Government Reports Announcements issued semi-monthly by the National Technical Information Service, and are listed in the Monthly Catalog of U.S. Government Publications issued by the Superintendent of Documents, U.S. Government Printing Office, Washington, D.C. 20402.

Correspondence pertaining to matters other than procurement may be addressed to Joint Publications Research Service, 1000 North Glebe Road, Arlington, Virginia 22201.

BIBLIOGRAPHIC DATA SHEET	1. Report No. JPRS 67047	2.	3. Recipient's Accession No.
4. Title and Subtitle THEORETICAL PRINCIPLES OF TORPEDO WEAPONS			5. Report Date 29 March 1976 6.
7. Author(s) G. M. Podobriy, V. S. Beloborodyy, V.V. Khalimonov, A. I. Nozov			8. Performing Organization Rept. No.
9. Performing Organization Name and Address Joint Publications Research Service 1000 North Glebe Road Arlington, Virginia 22201			10. Project/Task/Work Unit No. 11. Contract/Grant No.
12. Sponsoring Organization Name and Address As above			13. Type of Report & Period Covered 14.

15. Supplementary Notes

TEORETICHESKIYE OSNOVY TORPEDNOGO ORUZHIYA, 1969, Moscow

16. Abstracts

The report contains the theoretical fundamentals of present-day torpedo weapons: dynamics, destructive effect, proximity fuzes, gas-steam energy sources and engines, electric energy sources and motors, guidance control and homing systems.

17. Key Words and Document Analysis. 17a. Descriptors

USSR
Ordnance
Underwater Ordnance
Torpedoes

17b. Identifiers/Open-Ended Terms

17c. COSATI Field/Group 19H

18. Availability Statement	19. Security Class (This Report)	21. No. of Pages
Unlimited Availability. Sold by NTIS Springfield, Va. 22151	UNCLASSIFIED	366
	20. Security Class (This Page) UNCLASSIFIED	22. Price

FORM NTIS-35 (10-70)

USCOMM-DC 40329-P71

JPRS 67047

29 March 1976

THEORETICAL PRINCIPLES OF TORPEDO WEAPONS

Moscow TEORETICHESKIYE OSNOVY TORPEDNOGO ORUZHIYA in Russian 1969 signed to press 7 Mar 69 pp 1-359

[Book by G. M. Podobriy, V. S. Beloborodyy, V. V. Khalimonov, A. I. Nosov, Voyenizdat, 4,000 copies, UDC 623.946 (01)]

CONTENTS

[III - USSR - 4]
[II - USSR]

CONTENTS (Continued)

PUBLICATION DATA

Author(s)	:	Grigoriy Mikhaylovich Podobriy Vasiliy Sergeyevich Beloborodyy Vladimir Viktorovich Khalimonov Andrey Ivanovich Nosov
Editor(s)	:	S. A. Vyzvilko
Technical reviewer(s)	:	Ye. N. Sleptsova
Copies	:	4,000
Printing plant	:	Voyenizdat, 2nd Printing Plant, Leningrad

INTRODUCTION

World War I demonstrated and World War II confirmed that the torpedo is a potent weapon in offensive and defensive operations at sea. The effectiveness of torpedo utilization was determined first and foremost by the element of surprise in employing new models, by tactics of employment, by concealment of attack, as well as by the difficulties involved in evading torpedo attacks.

Today, in the age of nuclear energy and missile hardware, foreign navies are continuing to devote continuous attention to the improvement of torpedo weapons. The high level of development of modern torpedo weapons makes it possible to fire torpedoes from surface, submerged and airborne platforms and to employ torpedoes from considerable distances against transports, cargo ships, surface warships, submarines and port facilities. Outstanding Russian and Soviet engineers and scientists have made a great contribution toward the development of torpedo weapons: A. I. Shpakovskiy, I. I. Nazarov, N. A. Datskov, P. V. Bukhalo, N. N. Azarov, L. G. Goncharov, A. V. Trofimov, Yu. A. Dobrotvorskiy, N. N. Shamarin, D. P. Skobov, and A. K. Vereshchagin.

More than 100 years has passed since gifted Russian inventor I.F. Aleksandrovskiy proposed the first torpedo design in Russia in 1865.

While the first torpedo was an underwater unguided missile, today's torpedo is a complex aggregate of propulsion, directional control, homing and warhead detonation systems designed on the basis of modern achievements of science and technology.

The authors of this volume set for themselves the task of presenting the theoretical principles of torpedo weapons in the most comprehensible form possible. The authors do not examine specific torpedo models. For the sake of greater clarity some points of theory are illustrated by examples, the numerical values and quantities in which are hypothetical and are of a purely illustrative nature. We have been unable to present in this volume many elements elaborated in torpedo theory. But if this book assists the reader in comprehending the physical principles of torpedo weapons and comprehending hte the principles applied in designing torpedo assemblies and systems, the

authors will consider their task accomplished. In working on this book the authors utilized Soviet and foreign published materials available to the public.

This book was written by a team of authors: Professor G. M. Podobriy, Doctor of Technical Sciences (chapters 1, 7, 8); Docent V. S. Beloborodyy, Candidate of Technical Sciences (Introduction, chapters 4, 5); Docent V. V. Khalimonov, Candidate of Technical Sciences (Chapter 6); Docent A. I. Nosov, Candidate of Technical Sciences (chapters 2, 3); Chapter 9 was written in collaboration by G. M. Podobriy (sections 12-18) and V. V. Khalimonov (sections 1-11).

The authors would like to express their sincere gratitude to A. G. Pukhov, I. I. Trubitsyn, A. P. Vorob'yev and S. A. Vyzvilko, who were kind enough to inspect the manuscript and who offered a number of valuable comments, and will be grateful for any comments aimed at correcting the book's deficiencies and at improving its content.

CHAPTER 1. DYNAMICS OF TORPEDOES

1.1. General Information. Kinematic Parameters of the Torpedo

A theoretical examination of the dynamic properties of a torpedo, its stability of motion, controllability and maneuverability is based primarily on an analysis of torpedo motion equations.

The structure of differential equations of torpedo motion, as of any other body, is determined by that system of coordinates in which this motion is studied. Therefore coordinate systems are usually selected in such a manner that the equations are maximally simple in form and convenient for analysis.

In torpedo dynamics one employs for the most part Cartesian coordinate systems, primarily right-hand systems. In a right-hand coordinate system those angles, angular velocities and moments which are figured or which operate counter-clockwise are considered positive.

Coordinate Systems

The following are employed in dynamics of torpedoes (Figure 1.1):

a coordinate system linked to the earth — $OX_gY_gZ_g$, arbitrarily called a fixed or stationary system; it is used in determining the parameters of the trajectory of a torpedo's movement;

a coordinate system coupled to the torpedo — OXYZ. Axis OX runs along the longitudinal axis of the torpedo, axis OY runs upward and is located in the torpedo's centerplane, while axis OZ is perpendicular to axis XY. The origin of the coordinates is located either at center of gravity CG or at the center of buoyancy CB. In contrast to the center of gravity, which is defined as the point of application of the force of the torpedo's weight, the center of gravity constitutes the point of application of its displacement force. It is advantageous to use the center of buoyancy as origin of coordinates when the CG position changes within a substantial range; in this coordinate system it is convenient to define the components of inertial hydrodynamic force;

velocity coordinate system $OX_1Y_1X_1$, where axis OX_1 runs along the velocity vector, axis OY_1 is placed in the centerplane, while axis OZ_1 is perpendicular to axis X_1Z_1. This coordinate system is usually employed in determining the components of hydrodynamic force caused by viscosity of the medium.

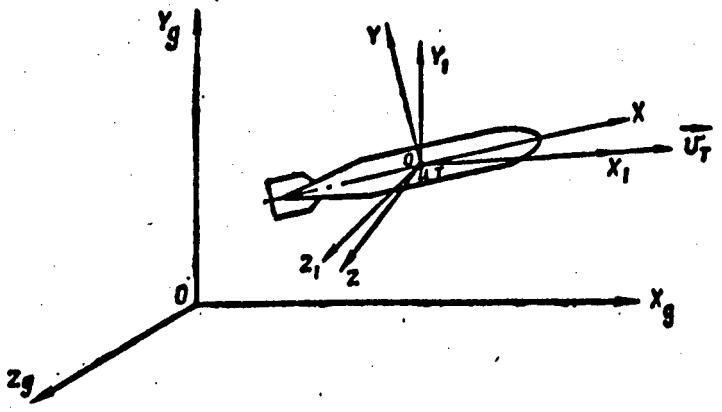

Figure 1.1. Fixed or Stationary ($OX_gY_gZ_g$), Coupled (OXYZ) and Velocity ($OX_1Y_1Z_1$) Coordinate Systems

Coordinates Determining a Torpedo's Position in a Fixed and Velocity Coordinate System

A torpedo's motion is considered known if at any moment in time t one can find the position in space of each point of the torpedo.

We shall designate the coordinates of point M (Figure 1.2) in a fixed coordinate system by x_g, y_g, z_g, in a coupled system with x, y, and z, and polar coordinates (point C),— x_{og}, y_{og}, z_{og}.

	x_g	y_g	z_g
X	$\cos\vartheta\cos\psi$	$\sin\vartheta$	$-\cos\vartheta\sin\psi$
Y	$\sin\gamma\sin\psi-\cos\gamma\sin\vartheta\cos\psi$	$\cos\gamma\cos\vartheta$	$\sin\gamma\cos\psi+\cos\gamma\sin\vartheta\sin\psi$
Z	$\cos\gamma\sin\psi+\sin\gamma\sin\vartheta\cos\psi$	$-\sin\gamma\cos\vartheta$	$\cos\gamma\cos\psi-\sin\gamma\sin\vartheta\sin\psi$

Table 1.1. Direction Cosines Between the Axes of a Coupled and Fixed Coordinate System

We shall project dashed line OABCPQM onto each of the axes OX_g, OY_g, OZ_g and, employing Table 1.1, we shall obtain expressions for the coordinates of point M in a stationary coordinate system [1.5]:

$$
\begin{aligned}
x_g &= x_{0g} + x\cos\theta\cos\psi + y(\sin\gamma\sin\psi - \cos\gamma\sin\theta\cos\psi) + \\
&\quad + z(\cos\gamma\sin\psi + \sin\gamma\sin\theta\cos\psi); \\
y_g &= y_{0g} + x\sin\theta + y\cos\gamma\cos\theta - z\sin\gamma\cos\theta; \qquad (1.1) \\
z_g &= z_{0g} - x\cos\theta\sin\psi + y(\sin\gamma\cos\psi + \cos\gamma\sin\theta\sin\psi) + \\
&\quad + z(\cos\gamma\cos\psi - \sin\gamma\sin\theta\sin\psi).
\end{aligned}
$$

Any torpedo movement can be broken down into two motions: translational and rotational [1.5].

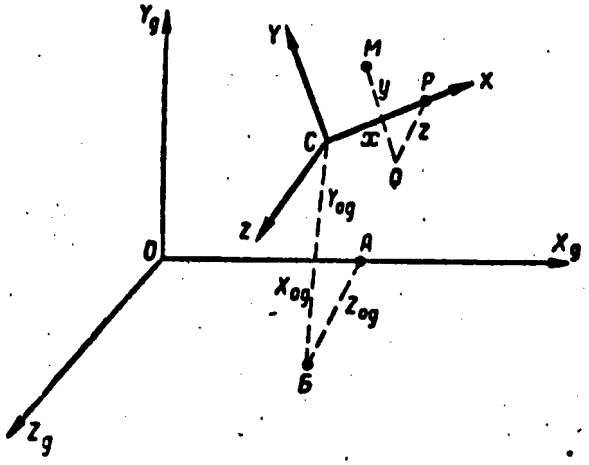

Figure 1.2. Deriving the Relationship Between the Coordinates of Point M in a Stationary and Coupled Coordinate System

Torpedo motion whereby only x_{0g}, y_{0g}, z_{0g} (current values of stationary coordinates) change is called translational motion, while all angles remain constant, that is, the coupled axes, displacing, remain constantly parallel to their original direction. In translational motion velocities, accelerations and trajectories are identical for all points of the torpedo.

Motion whereby only angles change is called rotary or rotational motion of the torpedo relative to any point (pole)*.

In conformity with expressions (1.1), the position of the torpedo in space is determined by six synthesized coordinates: by three polar coordinates x_{0g}, y_{0g}, z_{0g} and by three angles ϕ, θ, and γ, called the yaw angle, pitch angle, and heel angle respectively (Figure 1.3), that is, expressions (1.1) describe the torpedo's translational and rotary motions.

The angle between axis OX_g manned the torpedo's projected longitudinal axis onto plane X_gZ_g is called the yaw angle.

* The origin of a moving coordinate system is called the pole. Usually the torpedo's center of gravity is taken as the pole.

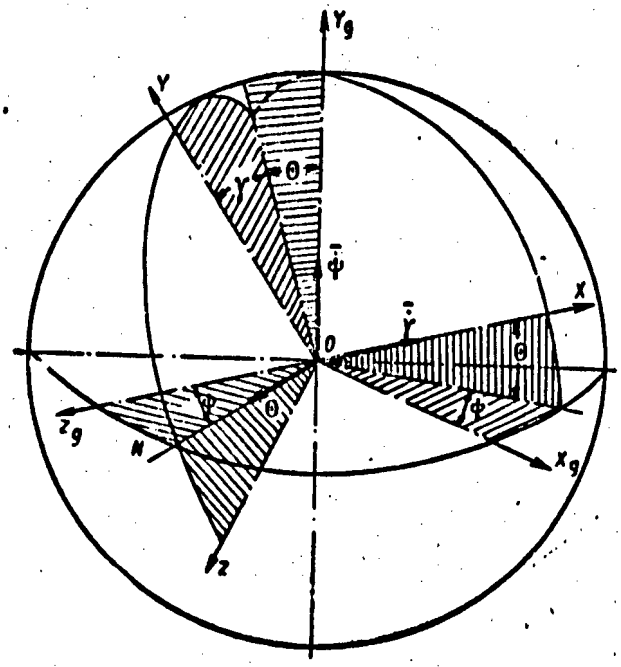

Figure 1.3. Torpedo Yaw Angle ψ, pitch angle θ, and heel angle γ

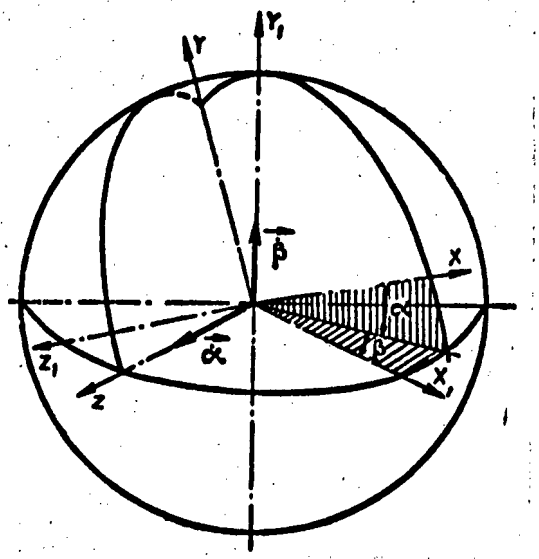

Figure 1.4. Torpedo Angle of Attack α and Drift Angle β

The angle between horizontal plane X_gZ_g and the torpedo's longitudinal axis is called the pitch angle.

The angle between vertical plane Y_gX and the torpedo's centerplane XY is called the heel angle.

A torpedo's position in a velocity coordinate system is determined by two angles: angle of attack α and drift angle β (Figure 1.4).

The angle between the velocity vector and the torpedo's centerplane is called the drift angle, while the angle between the velocity vector projected onto the centerplane and the torpedo's longitudinal axis is called the angle of attack.

	X_1	Y_1	Z_1
X	$\cos\alpha\cos\beta$	$\sin\alpha$	$-\cos\alpha\sin\beta$
Y	$-\sin\alpha\cos\beta$	$\cos\alpha$	$\sin\alpha\sin\beta$
Z	$\sin\beta$	0	$\cos\beta$

Table 1.2. Direction Cosines Between the Axes of a Coupled and Velocity Coordinate System

Principal Kinematic Ratios

In order to determine the parameters of a torpedo's trajectory it is necessary to know the projections of polar velocity onto axes $X_gY_gZ_g$; we shall designate them with the letters V_{Tx_g}, V_{Ty_g} and V_{Tz_g}.

The velocity projections are linked to the polar coordinates by the following ratios:

$$V_{Tx_g} = \frac{dx_{0g}}{dt}; \quad V_{Ty_g} = \frac{dy_{0g}}{dt}; \quad V_{Tz_g} = \frac{dz_{0g}}{dt}. \qquad (1.2)$$

Integrating expressions (1.2), we shall find the trajectory coordinates at any moment in time:

$$x_{0g} = x_0 + \int_0^t V_{Tx_g}\,dt;$$

$$y_{0g} = y_0 + \int_0^t V_{Ty_g}\,dt;$$

$$z_{0g} = z_0 + \int_0^t V_{Tz_g}\,dt,$$

where x_0, y_0, z_0 -- pole coordinates at an initial moment in time.

We shall determine velocity vector projections as follows: since $\vec{V}_T$ runs along axis OX_1, first we shall find its projections onto axes XYZ, utilizing Table 1.2:

$$V_{\tau x} = V_\tau \cos(\hat{X_\tau X_1}) = V_\tau \cos\alpha \cos\beta;$$
$$V_{\tau y} = V_\tau \cos(\hat{Y_\tau X_1}) = -V_\tau \sin\alpha \cos\beta; \qquad (1.3)$$
$$V_{\tau z} = V_\tau \cos(\hat{Z_\tau X_1}) = V_\tau \sin\beta.$$

Projecting V_{Tx}, V_{Ty}, V_{Tz} sequentially onto each axis of system $X_g Y_g Z_g$, we obtain:

$$V_{\tau x_g} = V_{\tau x} \cos(\hat{X_\tau X_g}) + V_{\tau y} \cos(\hat{Y_\tau X_g}) + V_{\tau z} \cos(\hat{Z_\tau X_g});$$
$$V_{\tau y_g} = V_{\tau x} \cos(\hat{X_\tau Y_g}) + V_{\tau y} \cos(\hat{Y_\tau Y_g}) + V_{\tau z} \cos(\hat{Z_\tau Y_g}); \qquad (1.4)$$
$$V_{\tau z_g} = V_{\tau x} \cos(\hat{X_\tau Z_g}) + V_{\tau y} \cos(\hat{Y_\tau Z_g}) + V_{\tau z} \cos(\hat{Z_\tau Z_g}).$$

The angle cosines contained in expression (1.4) can be found in Table 1.1.

In like manner we find the projections of the angular velocity of torpedo rotary motion vector onto the axes of a coupled and stationary coordinate system. Their expressions are in the following form: in a coupled system:

$$\omega_x = \dot{\gamma} + \dot{\psi} \sin\vartheta;$$
$$\omega_y = \dot{\vartheta} \sin\gamma + \dot{\psi} \cos\vartheta \cos\gamma; \qquad (1.5)$$
$$\omega_z = \dot{\vartheta} \cos\gamma - \dot{\psi} \cos\vartheta \sin\gamma;$$

in a stationary system:

$$\omega_{x_g} = \dot{\vartheta} \sin\psi + \dot{\gamma} \cos\psi \cos\vartheta;$$
$$\omega_{y_g} = \dot{\gamma} \sin\vartheta + \dot{\psi}; \qquad (1.6)$$
$$\omega_{z_g} = \dot{\vartheta} \cos\psi - \dot{\gamma} \sin\psi \cos\vartheta.$$

Utilizing expressions (1.3), (1.4), (1.5) and (1.6), we can find the kinematic ratios for particular instances of torpedo motion. As an example we shall examine torpedo motion in a vertical and horizontal plane separately.

Torpedo motion in a vertical plane occurs if the translational velocity vector is located at all times in plane $X_g Y_g$ and torpedo rotation takes place only in this plane relative to axis OZ_g.

In this case $V_{\tau z_g} = 0; \quad \omega_{x_g} = 0; \quad \omega_{y_g} = 0.$

Equations (1.4) and (1.6) are identically satisfied when

$$\psi = 0; \quad \gamma = \gamma_0 = \text{const} \quad \text{and} \quad \operatorname{tg}\beta = \sin\alpha \operatorname{tg}\gamma_0. \qquad (1.7)$$

Substituting these conditions in equations (1.3), (1.4), (1.5) and (1.6), we obtain the desired expressions for the kinematic parameters of torpedo motion in a vertical plane.

We should note that expressions (1.7) constitute the kinematic conditions of this motion.

With torpedo motion in a horizontal plane, the velocity vector continuously remains in plane X_gZ_g, while torpedo rotation takes place only relative to axis OY_g. Therefore

$$V_{z_g} = 0; \quad \omega_{x_g} = 0; \quad \omega_{z_g} = 0. \qquad (1.8)$$

Conditions (1.8) are identically satisfied when

$$\gamma = \gamma_0 = \text{const}; \quad \theta = \theta_0 = \text{const}; \quad \operatorname{tg}\theta_0 = \operatorname{tg}\alpha\cos\gamma_0 + \operatorname{tg}\beta\frac{\sin\gamma_0}{\cos\alpha}.$$

Utilizing the obtained conditions, we can find the kinematic ratios during torpedo motion in a horizontal plane.

General Description of Forces and Moments Acting on a Torpedo as It Moves Through the Water

A moving torpedo forms a complex hydrodynamic system together with the fluid medium. Therefore in an analytical study of its motion one introduces various assumptions which simplify solving a concrete problem. In order to construct an equation for a given type of torpedo motion, one must know the forces acting on it. These forces include the following: weight, displacement, force on the propellers, and hydrodynamic forces.

The force of displacement, in conformity with Archimedes law, is equal to the weight of the fluid contained within the volume of the torpedo and is directed upward, that is,

$$B = \gamma_B V_0$$

where γ_B — specific gravity of water; V_0 — torpedo volume.

Hydrodynamic forces and moments include forces and moments dictated by the inertia of the torpedo and the fluid, as well as the forces and moments occurring as a consequence of viscosity of the fluid medium. The latter in turn are subdivided into position and damping.

Forces and moments acting on the torpedo during translational steady-state motion with constant angles of attack and drift are called position forces and moments.

Forces and moments caused by torpedo rotary motion are called damping forces and moments [1.2].

Forces caused by inertia are determined either by theoretical means or with the aid of the method of analogies.

Hydrodynamic forces and moments of viscosity origin are determined chiefly by experimental means. Subsequently we shall examine both theoretical and experimental methods of determining hydrodynamic forces and their moments.

1.2. Position Hydrodynamic Forces

Fundamental Relations for Position Hydrodynamic Forces

Real fluids possess viscosity, which is caused by molecule cohesion. During heating, for example, when cohesive forces become weakened, the viscosity of a fluid diminishes.

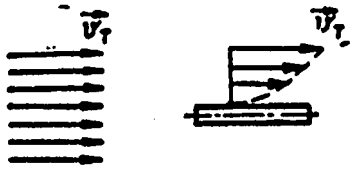

Figure 1.5. Motion of a Viscous Fluid Along a Plate

If a fluid were ideal, without viscosity, flow across a smooth plate* would be rectilinearly translational: velocity at all points in the flow would be identical, and the fluid particles would slip along the plate without experiencing drag. In a real fluid, possessing viscosity, distribution of velocities in the flow is as shown in Figure 1.5, that is, immediately adjacent to the plate surface the fluid moves at zero velocity, while with increasing distance from the plate the velocity of the particles of water in the adjacent layer increases to flow velocity V_T. The effect of viscosity here is manifested in deceleration of particles, that is, in the fact that the particles located in the various layers move at a somewhat different velocity relative to one another. Movement of particles at different velocities relative to one another is the result of action of internal forces of friction, or fluid viscosity. Frictional forces are defined as stresses τ tangential to the surface of the plate. When fluid particles move in parallel layers, tangential stress can be determined with Newton's formula [1.13].

$$\tau = -\mu \frac{\partial V}{\partial y}, \qquad (1.9)$$

where μ — coefficient of viscosity, the magnitude of which is determined by the nature of the fluid and its temperature;

$\frac{\partial V}{\partial y}$ — velocity gradient along external normal y.

Also acting on the torpedo, in additional to tangential stresses, are normal stresses which occur as a result of change in velocity of the fluid particles flowing around the body.

* Henceforth we shall apply the principle of reversibility of motion, according to which the nature of interaction between a body and medium is independent of whether the body is moving in the fluid or a homogeneous stream of fluid, with the same velocity but opposite in direction, will move onto motionless body.

Change in flow velocity in conformity with Bernoulli's law gives rise to hydrodynamic pressure along the torpedo hull. For points situated at one and the same depth, the Bernoulli equation can be written in the form

$$P = P_0 + \frac{\rho V_\tau^2}{2}\left[1 - \left(\frac{V}{V_\tau}\right)^2\right], \qquad (1.10)$$

where P_0 -- hydrostatic pressure at the given depth; V_τ -- velocity of incident flow; P, V — hydrodynamic pressure and velocity at the given point.

Thus with a torpedo moving in a real fluid, normal $Pd\Omega$ and tangential $\tau d\Omega$ to the area of force act on each elementary area $d\Omega$ (Figure 1.6). Let us project these forces onto the axes of the velocity coordinate system, and we obtain [1.13]:

$$\begin{aligned} dR_{x_1} &= [P\cos(P,\hat{}X_1) + \tau\cos(\tau,\hat{}X_1)]\,d\Omega; \\ dR_{y_1} &= [P\cos(P,\hat{}Y_1) + \tau\cos(\tau,\hat{}Y_1)]\,d\Omega; \\ dR_{z_1} &= [P\cos(P,\hat{}Z_1) + \tau\cos(\tau,\hat{}Z_1)]\,d\Omega. \end{aligned} \qquad (1.11)$$

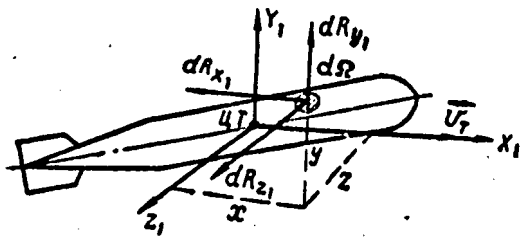

Figure 1.6. Hydrodynamic Forces Acting on the Elementary Area of a Torpedo

Integrating these expressions for the entire torpedo surface Ω_T we obtain formulas for drag R_{x1}, lift R_{y1}, and lateral force R_{z1}:

$$\begin{aligned} R_{x_1} &= \iint\limits_{(\Omega_\tau)} [P\cos(P,\hat{}X_1) + \tau\cos(\tau,\hat{}X_1)]\,d\Omega; \\ R_{y_1} &= \iint\limits_{(\Omega_\tau)} [P\cos(P,\hat{}Y_1) + \tau\cos(\tau,\hat{}Y_1)]\,d\Omega; \\ R_{z_1} &= \iint\limits_{(\Omega_\tau)} [P\cos(P,\hat{}Z_1) + \tau\cos(\tau,\hat{}Z_1)]\,d\Omega. \end{aligned}$$

In practice usually other formulas are used, for obtaining which subintegral expressions lead to a dimensionless form. We shall recall that quantities P, τ possess dimensionality $\frac{H}{M2}$, while Ω_T -- M^2.

To perform the indicated transformation we shall utilize dynamic pressure expression

$$\frac{\rho V_\tau^2}{2}\left[\frac{H}{M^3}\right],$$

where V_τ — velocity of torpedo steady-state motion, m/sec; ρ — water density, kg/m^3.

Since P and τ possess dimensionality of dynamic pressure, by dividing and multiplying subintegral expressions by

$$\frac{\rho V^2_\tau}{2},$$

we obtain them in dimensionless form.

In order to reduce $d\Omega$ to dimensionless form we shall divide and multiply it by some characteristic area, such as the torpedo wetted surface area Ω_τ. The relation for drag following transformation will assume the form

$$R_{x_1} = \frac{\rho V_\tau^2}{2}\Omega_\tau \int\limits_{(\Omega_\tau)}\int\left[\frac{P}{\frac{\rho V_\tau^2}{2}}\cos\left(P,\hat{X}_1\right) + \frac{\tau}{\frac{\rho V_\tau^2}{2}}\cos\left(\tau,\hat{X}_1\right)\right]\frac{d\Omega}{\Omega_\tau}.$$

We shall designate the subintegral expression in the formula with C_{x1}, upon which this formula and two others for R_{y1} and R_{z1} will be written in the form:

$$R_{x_1} = C_{x_1}\frac{\rho V_\tau^2}{2}\Omega_\tau; \qquad (1.12)$$

$$R_{y_1} = C_{y_1}\frac{\rho V_\tau^2}{2}\Omega_\tau; \qquad (1.13)$$

$$R_{z_1} = C_{z_1}\frac{\rho V_\tau^2}{2}\Omega_\tau. \qquad (1.14)$$

Dimensionless quantities C_{x1}, C_{y1}, C_{z1} are called coefficients of drag, lift and lateral force respectively.

It follows from the above formulas that forces R_{x1}, R_{y1}, R_{z1}, when the torpedo moves at constant velocity, are proportional to dynamic pressure

$$\frac{\rho V^2_\tau}{2}$$

and torpedo wetted surface Ω_τ; in addition they are determined by dimensionless coefficients characterizing the torpedo's shape and conditions of flow around it.

Elementary forces $Pd\Omega$ and $\tau d\Omega$ create hydrodynamic moments relative to the coordinate axes. We shall designate the coordinates of elementary area $d\Omega$ with x, y, z. Then the expression of moments of elementary forces, relative to axis OX_1, for example, will be

$$dM_{x_1} = dR_{z_1} y - dR_y z.$$

Integrating this expression for the torpedo's entire surface, we obtain

$$M_{x_1} = \iint\limits_{(\Omega_\tau)} (dR_{z_1} y - dR_{y_1} z).$$

In order to reduce to dimensionless form, it is necessary to multiply and divide the subintegral expression by constant quantities:

$$\frac{\rho V_\tau^2}{2},\ \Omega_\tau,\ L_\tau$$

(the torpedo's length). As a result the relation for M_X acquires the form

$$M_{x_1} = \frac{\rho V_\tau^2}{2} \Omega_\tau L_\tau \iint\limits_{(\Omega_\tau)} \left[\frac{dR_{z_1}}{\frac{\rho V_\tau^2}{2}} \frac{y}{L_\tau} - \frac{dR_{y_1}}{\frac{\rho V_\tau^2}{2}} \frac{z}{L_\tau} \right] \frac{d\Omega}{\Omega_\tau}.$$

Designating the dimensionless quantity defined by the double integral with C_{mx_1}, we obtain

$$M_{x_1} = C_{mx_1} \frac{\rho V_\tau^2}{2} \Omega_\tau L_\tau. \qquad (1.15)$$

Analogous expressions for M_{y1} and M_{z1} will assume the form:

$$M_{y_1} = C_{my_1} \frac{\rho V_\tau^2}{2} \Omega_\tau L_\tau; \qquad (1.16)$$

$$M_{z_1} = C_{mz_1} \frac{\rho V_\tau^2}{2} \Omega_\tau L_\tau. \qquad (1.17)$$

Moments M_{x1}, M_{y1}, M_{z1} are called the heeling moment, yawing moment and longitudinal moment respectively.

In an analogous manner we can obtain formulas for hydrodynamic forces and moments in projections onto the axes of the coupled coordinate system:

$$R_x = C_x \frac{\rho V_\tau^2}{2} \Omega_\tau;\quad R_y = C_y \frac{\rho V_\tau^2}{2} \Omega_\tau;\quad R_z = C_z \frac{\rho V_\tau^2}{2} \Omega_\tau;$$

$$M_x = C_{mx} \frac{\rho V_\tau^2}{2} \Omega_\tau L_\tau;\quad M_y = C_{my} \frac{\rho V_\tau^2}{2} \Omega_\tau L_\tau;$$

$$M_z = C_{mz} \frac{\rho V_\tau^2}{2} \Omega_\tau L_\tau. \qquad (1.18)$$

In a coupled coordinate system the forces and moments are called: R_X — longitudinal force; R_y — normal force; R_z — lateral force; M_x — heeling moment; M_y — yawing moment; M_z — longitudinal moment.

Dimensionless coefficients of forces and moments in a coupled coordinate system are determined with formulas [1.6]:

$$\begin{aligned} C_x &= (C_{x_1}\cos\beta + C_{z_1}\sin\beta)\cos\alpha - C_{y_1}\sin\alpha; \\ C_y &= (C_{x_1}\cos\beta + C_{z_1}\sin\beta)\sin\alpha + C_{y_1}\cos\alpha; \\ C_z &= -C_{x_1}\sin\beta + C_{z_1}\cos\beta; \\ C_{mx} &= (C_{mx_1}\cos\beta - C_{mz_1}\sin\beta)\cos\alpha + C_{my_1}\sin\alpha; \\ C_{my} &= -(C_{mx_1}\cos\beta - C_{mz_1}\sin\beta)\sin\alpha + C_{my_1}\cos\alpha; \\ C_{mz} &= C_{mx_1}\sin\beta + C_{mz_1}\cos\beta. \end{aligned} \qquad (1.19)$$

We shall note that the magnitude of hydrodynamic coefficients for one and the same torpedo depends on what area and length are taken as characteristic in the formulas for forces and moments. One must direct attention to this factor. When necessary the coefficients can easily be recomputed to other characteristic area and length.

We shall demonstrate the method of this conversion with the example R_X and M_X. Let $C_X=C_1$ and $C_{mx}=C_{m1}$ be known, in the determination of which midship section S_T is taken as characteristic area, and length $\underline{l}$ as length. We must determine coefficients C_{X2} and C_{mx2} for a case where torpedo surface Ω_T is taken as characteristic area, and torpedo length L_T as length. Then we can write:

$$R_x = C_1\frac{\rho V_T^2}{2}S_T = C_{x_2}\frac{\rho V_T^2}{2}\Omega_T;$$

$$M_x = C_{m_1}\frac{\rho V_T^2}{2}S_T l = C_{mx_2}\frac{\rho V_T^2}{2}\Omega_T L_T.$$

From these expressions we find:

$$C_{x_2} = \frac{C_1 S_T}{\Omega_T}; \quad C_{mx_2} = \frac{C_{m_1} S_T l}{\Omega_T L_T}. \qquad (1.20)$$

Concept of Mechanical Similarity

Determination of position hydrodynamic forces reduces essentially to finding dimensionless hydrodynamic coefficients. At the present time not all hydrodynamic coefficients can be theoretically determined with sufficient accuracy. In connection with this experimental methods of coefficient determination are widely used in torpedo hydrodynamics, whereby full-scale tests are of great importance, since the figures obtained from such tests are the most reliable. But since full-scale tests under actual conditions are very complex and require a considerable expenditure of time, effort and money, tests on models are practiced extensively, tests which are cheaper, technically more easily executed and which possess broader possibilities for completeness of

investigation and graphic demonstration. Experiments on models are performed in wind tunnels or flow channels at steady-state velocity of the advancing air flow and constant values of angles α, β, set angles of vertical δ_B and horizontal δ_Γ control surfaces. The forces acting on the model are measured on aerodynamic scales. Test results are usually presented as graphic relationships between the hydrodynamic coefficients and the above-indicated angles. But tests on models can be of practical significance only if the figures obtained in such tests can be applied to full-scale conditions. Such conversions are possible if certain conditions of mechanical similarity were observed in the process of testing, mandatory for which is fulfillment of the conditions of geometric, kinematic, and dynamic similarity [1.9].

Geometric similarity presupposes similarity of shape and constancy of relationship of corresponding dimensions of model and full-scale device, called scale of physical dimensions.

Kinematic similarity presupposes, alongside geometric similarity, constancy of ratios of velocity vector projections at any corresponding points in the flow. This relation is called the coefficient of kinematic similarity or scale of velocities.

Further, if the conditions of geometric similarity are satisfied and any forces acting on corresponding elements are proportional in both phenomena, such phenomena are called dynamically similar for these forces.

Various forces are in action in a fluid, and therefore there may be several conditions of similarity, each of which is called a condition of partial similarity. If all conditions of partial similarity are met, we say that we have full dynamic similarity.

We shall designate those quantities pertaining to the full-scale device with the subscript H, and those pertaining to the model with subscript M. Then the above-formulated conditions can be written as follows in mathematical form:

geometric similarity $$K_L = \frac{l_M}{L_H}; \qquad (1.21)$$

kinematic similarity $$K_v = \frac{V_M}{V_H}, \qquad (1.22)$$

if we introduce a time scale $$K_t = \frac{t_M}{t_H}, \qquad (1.23)$$

we can write the following ratio: $$K_v = \frac{K_L}{K_t}; \qquad (1.24)$$

dynamic similarity

$$K_F = \frac{F_M}{F_H}, \qquad (1.25)$$

where K_F — force scale F.

In conformity with Newton's law, force equals mass m times acceleration a, that is, F=ma.

Mass in turn is equal to the product of fluid density ρ and its volume V_0, that is, $m=\rho V_0$.

Proceeding from dimensionality, we can write

$$V_0 = L^3 \qquad \text{and} \qquad a = \frac{L}{T^2}.$$

Here L is length and T is time.

Consequently

$$F = \rho L^3 \frac{L}{T^2} = \rho V^2 L^2.$$

Thus for dynamic similarity it is necessary that the forces assume the following ratio:

$$K_F = \frac{\rho_M V_M^2 L_M^2}{\rho_H V_H^2 L_H^2}. \qquad (1.26)$$

Utilizing formula (1.26), we shall find the conditions of dynamic similarity for forces dictated by fluid viscosity. According to basic Newton law (1.9), the forces of viscosity can be expressed as follows:

$$F_{тр} = \mu \frac{V}{L} L^2 = \mu V L,$$

where $\frac{V}{L}$ — average velocity gradient value, and L^2 — body wetted surface area.

The principal dynamic similarity equation (1.26) assumes the form

$$\frac{\rho_M V_M^2 L_M^2}{\rho_H V_H^2 L_H^2} = \frac{\mu_M V_M L_M}{\mu_H V_H L_H}.$$

Hence we find

$$\frac{\rho_M V_M L_M}{\rho_H V_H L_H} = \frac{\mu_M}{\mu_H} \qquad \text{or} \qquad \frac{\rho_M V_M L_M}{\mu_M} = \frac{\rho_H V_H L_H}{\mu_H}.$$

Replacing ratio $\frac{\mu}{\rho}$ with kinematic viscosity ν, we finally obtain:

$$\frac{V_M L_M}{\nu_M} = \frac{V_H L_H}{\nu_H} \text{ или } Re(м) = Re(н). \qquad (1.27)$$

Dimensionless quantity $Re=\frac{vL}{\nu}$ is called Reynolds number.

Thus the Reynolds number equation is a condition for dynamic similarity between model and full-scale device under the effect of forces caused by fluid viscosity.

We shall now find the dynamic similarity condition for the forces of gravity. In this case we must substitute in equation (1.26) in place of force $\underline{F}$ the value of gravity:

$$F=mg=\rho L^3 g.$$

The equation assumes the following form thereby:

$$\frac{\rho_M V_M^2 L_M^2}{\rho_H V_H^2 L_H^2}=\frac{\rho_M L_M^3 g}{\rho_H L_H^3 g},$$

and after reduction

$$\frac{gL_M}{V_M^2}=\frac{gL_H}{V_H^2}. \qquad (1.28)$$

The resulting expression is called Froude's law, while dimensionless quantity

$$\frac{gL}{V^2}$$

is called the Froude number and is designated by Fr.

Consequently, if conditions of geometric and dynamic similarity are observed in model tests, the hydrodynamic coefficients will be identical for the model and the full-scale device.

1.3. Water Drag on the Torpedo

The water's resistance to torpedo motion consists of two parts: friction drag, and form drag.

Friction drag constitutes the resultant force of surface tangential forces, while form drag is the resultant force of standard pressure surface forces. Both are determined by fluid viscosity.

That part of the flow along the surface of the body where the forces of viscosity are most intensively manifested is called the boundary layer. The thickness of this layer decreases with an increase in fluid velocity. For practical purposes the thickness of the boundary layer is assumed equal to the distance from the wall at which velocity reaches 99% of undisturbed flow [1.1]. Beyond the boundary layer viscosity forces become so insignificant that one can apply the laws of hydromechanics of an ideal fluid to the flow.

This approach to a study of the motion of a viscous fluid makes it possible to divide the entire volume of fluid flowing around a solid into the following regions (Figure 1.7):

external potential flow region I, where viscosity forces are practically zero; one can apply the laws of an ideal fluid to study flow in this region;

boundary layer region II adjacent to the solid, in which frictional forces possess a substantial value;

wake region (zone) III; with fully-faired bodies this zone begins at the points of flow separation from the body surface, while with bodies with tapered lines (torpedo) it forms astern. Here the fluid flows from a lower-pressure region into a higher-pressure region (Figure 1.8, point B).

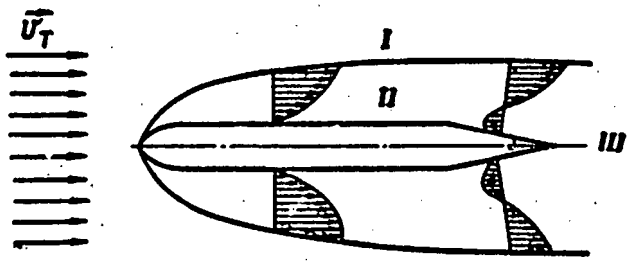

Figure 1.7. A Viscous Fluid Flowing Past a Torpedo

Figure 1.8. Distribution of Fluid Velocity and Hydrodynamic Pressure Along the Hull of a Torpedo

Since velocity is low adjacent to the surface, the kinetic energy of the fluid is insufficient to overcome the positive pressure differential. Therefore at this point the fluid flows in the opposite direction; boundary layer separation occurs, and a burble zone forms. The location of the point of separation is determined by the shape of the body and its attitude relative to the flow.

Friction Drag

Friction drag is determined chiefly by the character of fluid flow within the boundary layer. Two types of motion are distinguished: laminar and turbulent. With laminar motion the fluid flows in parallel, nonmixing layers; with turbulent flow fluid particles are in a random state, intermix and move along peculiar, constantly changing trajectories.

We should note that the above-mentioned motion conditions are stable only under certain definite conditions. These conditions were experimentally determined for the first time by Reynolds. He established that the conditions of fluid motion are determined by the value of dimensionless expression

$$\mathrm{Re} = \frac{V_{cp} d}{\nu},$$

where d -- characteristic linear dimension; V_{cp} -- average flow velocity; ν -- kinematic coefficient of viscosity.

There exists a critical Reynolds number. If R_e is less than critical, motion is laminar; if R_e exceeds critical, motion is turbulent.

Length L_T is employed as characteristic linear dimension for torpedoes; then R_e is determined with the formula

$$\mathrm{Re} = \frac{V_T L_T}{\nu}. \qquad (1.29)$$

The critical Reynolds number for torpedoes lies between 3×10^5 and 5×10^5.

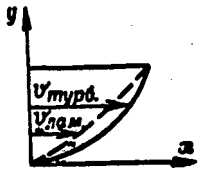

Figure 1.9. Distribution of Velocities Within the Boundary Layer During Fluid Laminar and Turbulent Flow

---

Figure 1.9 shows the distribution of velocities during laminar and turbulent flow. The increased swing of the velocity curve during turbulent flow is caused by the presence of intensive mixing. However, even here mixing of particles in a thin layer immediately adjacent to the body surface becomes impossible, since the hull prevents their lateral mixing. Consequently, even in a turbulent boundary layer laminar flow is retained adjacent to the hull, called laminar sublayer.

Tangential stresses within a laminar boundary layer and in a laminar sublayer can be computed with the Newton formula. But since we are interested in tangential stresses directly on the hull, this formula can also be applied in a case of turbulent motion. For these conditions we shall write formula (1.9) in the form

$$\tau_0 = \mu \left(\frac{dV}{dy}\right)_{y=0}, \qquad (1.30)$$

where $\left(\frac{dV}{dy}\right)_{y=0}$ is the velocity gradient for the normal to the body surface.

Employing formula (1.9), we shall analyze the possible methods of reducing friction drag.

It follows from this formula that a decrease in tangential stress can be achieved:

by reducing viscosity of the fluid in immediate contact with the torpedo hull;

by lessening the velocity gradient on the body surface.

Form Drag

Form drag constitutes a part of drag, the role of which is rather minor in the overall drag balance of highly-elongated bodies moving at high Reynolds numbers. However, form drag on bodies with a small fineness ratio may comprise the bulk of total drag.

Let us examine the causes of form drag. When an ideal fluid (without viscosity) flows around a symmetrical body, distribution of velocities is symmetrical relative to the maximum cross-section (Figure 1.8). As a consequence of full symmetry of pressure distribution, the resultant of these pressures projected onto any axis is zero. Consequently if the fluid were idea, form drag would also be zero.

When bodies move in a real fluid, the existence of a boundary layer and flow separation at the stern somewhat change the distribution of velocities in the outer part of the flow. In the nose section of the body, where the boundary layer is thin, the influence of viscosity on velocity is insignificant; as we approach the stern the difference in velocities in the ideal and real fluids becomes more significant. As a result of this there takes place redistribution of pressures, and a resultant force arises in the direction of flow, called form drag.

Approximate Determination of Coefficient of Drag

Coefficient C_{x1} consists of two parts -- coefficient of friction and coefficient of form drag, that is,

$$C_{x1}=C_f+C_w \qquad (1.31)$$

Coefficient C_f is determined with the Prandtl-Schlichting interpolation formula [1.1]

$$C_f=\frac{0{,}455}{(\lg \mathrm{Re})^{2{,}58}}. \qquad (1.32)$$

Formula (1.32) is derived for flat, ideally-smooth plates and applies to Reynolds numbers of 5×10^7 and higher. Flow around a torpedo does not correspond to plate flow due to the curvature of the hull, but this difference is negligible.

The (Papmel') formula, derived by him on the basis of an analysis of wind tunnel tests on airfoils and testing of ships [1.1], is used for an approximate determination of the value of coefficient of form drag C_w:

$$C_{\phi} = 0{,}09\frac{S_T}{\Omega_k}\sqrt{l}, \qquad (1.33)$$

where S_T — torpedo maximum cross sectional area, m^2; Ω_k — torpedo wetted surface, excluding fins, m^2; $\bar{l}$ — stern taper factor, determined with formula

$$\bar{l} = \frac{\sqrt{S_T}}{2l},$$

where l is the length of the tapered portion of the torpedo.

Special tests are performed for more precise determination of C_{x1}. We shall note that if equal Reynolds numbers are not observed for a model and a full-scale device in tests on models, it is necessary to convert C_{x1} with the formula

$$C_{f(н)} = C_{f(м)}\left(\frac{\lg Re_м}{\lg Re_н}\right)^{2,58}, \qquad (1.34)$$

whereby it is assumed that with a change in Reynolds number there occurs a change only in friction drag, while form drag remains unchanged.

1.4. Determination of Torpedo Motor Effective Output

Motor output is expended on turning the propellers, on overcoming friction in the motor and in the shaft bearings, and on operating attendant equipment. Motor effective output is defined as that portion of its output which is developed on the torpedo propeller shafts. This power can be determined theoretically in the following manner.

In order for a torpedo to travel at a specified velocity V_T, it is necessary to perform work equal to $R_{x1}V_T$ in a unit of time. If screw propellers are employed as propulsive device, effective motor horsepower will be determined with the expression

$$N_e = \frac{R_{x_1}V_T}{\eta_p}\,sm, \qquad (1.35)$$

where η_p — is the propulsive coefficient of the screw propellers, that is, propeller efficiency taking into account the influence of the torpedo hull.

Consequently the question of determining effective output reduces to determining torpedo drag.

Substituting in formula (1.35) quantity $C_{x_1}\frac{\rho V_T^2}{2}\Omega_T$ in place of R_{x1} we obtain

$$N_e = C_{x_1}\frac{\rho V_T^3}{2\eta_p}\Omega_T, \qquad (1.36)$$

that is, motor power output is proportional to the torpedo's velocity cubed.

Consequently, if power N_{e1} is necessary to obtain velocity V_{T1}, then for velocity V_{T2} we shall require

$$N_{e_2} = N_{e_1}\left(\frac{V_{T_2}}{V_{T_1}}\right)^3. \qquad (1.37)$$

1.5. Lift and Hydrodynamic Moment

When a torpedo is traveling in a real fluid with a certain angle of attack, substantial lift is generated. It is formed primarily by normal surface forces. An explanation of this should be sought in the difference between actual distribution of pressures and distribution of pressures in an ideal fluid.

Figure 1.10 contains an approximate distribution of normal stresses on the torpedo hull. As is evident from the figure, lift is generated by overpressure in the forward part of the torpedo and underpressure in the aft section of the torpedo.

Coefficient of lift C_{y_1} of a finned torpedo hull is found experimentally, chiefly by running wind tunnel tests on torpedo models.

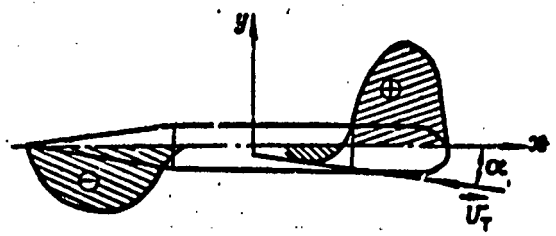

Figure 1.10. Generation of Torpedo Lift

In tests C_{y_1} is determined for a finned and unfinned-hull torpedo model at various angles of attack and at various angles of horizontal control surface setting δ_r.

Figure 1.11 contains the results of aerodynamic tests to determine a torpedo's coefficients of lift ($\delta_r>0$ corresponds to control deflection downward).

At low angles of attack α and low angles of horizontal control surface deflection δ_r, the relationship between C_{y1} and these angles can be assumed linear in a first approximation:

$$C_{y_1} = \frac{\partial C_{y_1}}{\partial \alpha}\Big|_{\delta_r=0}\alpha + \frac{\partial C_{y_1}}{\partial \delta_r}\Big|_{\alpha=0}(\delta_r + \alpha). \qquad (1.38)$$

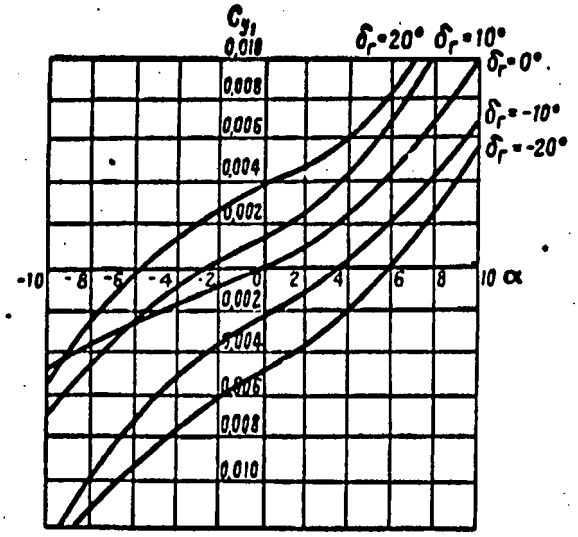

Figure 1.11. Relationship Between of Lift and Angle of Attack α and Angle of Horizontal Control Surface Deflection δ_r

Partial derivatives $\frac{\partial C_{y_1}}{\partial \alpha}$ and $\frac{\partial C_{y_1}}{\partial \delta_r}$ are determined as the ratios

$$\frac{C_{y_1}(\alpha)}{\alpha} \quad \text{and} \quad \frac{C_{y_1}(\delta_r)}{\delta_r}.$$

The value of coefficient C_{mz_1} of a finned torpedo hull is obtained from wind tunnel data. In testing, the coefficients of hydrodynamic moments of a finned and unfinned hull are determined at various angles of attack and control surface deflection angles. Figure 1.12 contains the results of determining C_{mz_1} for a torpedo. Hydrodynamic moments are given relative to its center of gravity. As is evident from the graph, the fins and control surface position appreciably influence the value of the hydrodynamic moment coefficient.

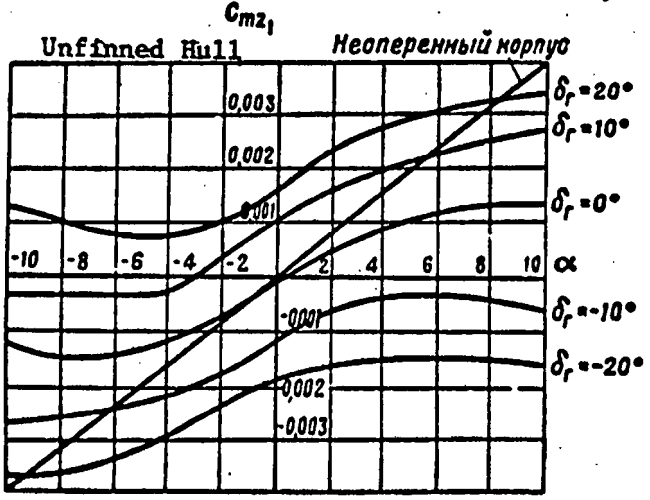

Figure 1.12. Relationship Between Coefficient of Longitudinal Moment and Horizontal Control Surface Angle of Deflection δ_r and Angle of Attack α

At small angles of attack α and small angles of horizontal control surface deflection δ_r, coefficient C_{mz_1} can be approximately represented with linear relation

$$C_{mz_1} = \frac{\partial C_{mz_1}}{\partial \alpha}\Big|_{\delta_r=0}\alpha + \frac{\partial C_{mz_1}}{\partial \delta_r}\Big|_{\alpha=0}(\delta_r + \alpha). \qquad (1.39)$$

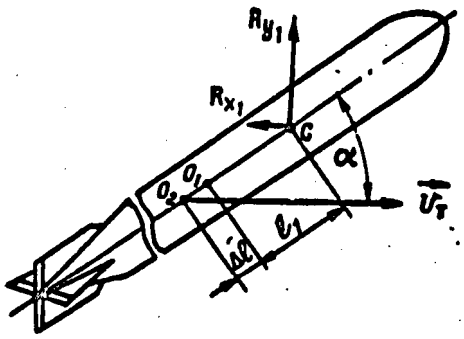

Figure 1.13. Deriving a Formula for Converting a Torpedo's Longitudinal Hydrodynamic Moment

Quantities $\frac{\partial C_{mz_1}}{\partial \alpha}$ and $\frac{\partial C_{mz_1}}{\partial \delta_r}$ are determined in the same manner as $\frac{\partial C_{y_1}}{\partial \alpha}$ and $\frac{\partial C_{y_1}}{\partial \delta_r}$.

We shall note that the above also applies in equal measure to force R_{z_1} and moment M_{y_1}.

In practical calculations the hydrodynamic moment must be converted for one and the same torpedo as a consequence of change in its center of gravity. Such a conversion for small angles of attack can be performed in an approximate manner with formula

$$M'_{z_1} = M_{z_1} + \Delta l R_{y_1}, \qquad (1.40)$$

where M_{z_1} -- hydrodynamic moment relative to the initial position of the center of gravity $ЦТ_0$; M'_{z_1} -- hydrodynamic moment relative to the new position of the torpedo's center of gravity $ЦТ_1$ (Figure 1.13); Δl -- distance between $ЦТ_0$ and $ЦТ_1$; Δl>0 with a shift of $ЦТ_1$ toward the aft end of the torpedo.

1.6. Hydrodynamic Heeling Moment

Moment M_x is generated with fin and control surface asymmetry. Assume the torpedo, for example, is moving with a positive angle β, while the rudder is deflected by angle $\delta_в$. Then lateral force $R_{zвр}$ will act on the upper vertical fin, $R_{zнп}$ on the lower vertical fin, $R_{zвр}$ on the upper rudder, and $R_{zнр}$ on the lower rudder (Figure 1.14). These forces generate a moment relative to axis OX, determined by equality

$$M_x = R_{z\,вп} Y_{вп} - R_{z\,вп} Y_{вп} + R_{z\,нр} Y_{нр} - R_{z\,вр} Y_{вр},$$

where $Y_{вп}$, $Y_{вп}$, $Y_{нр}$, $Y_{вр}$ — coordinates of points of application of the above-indicated forces.

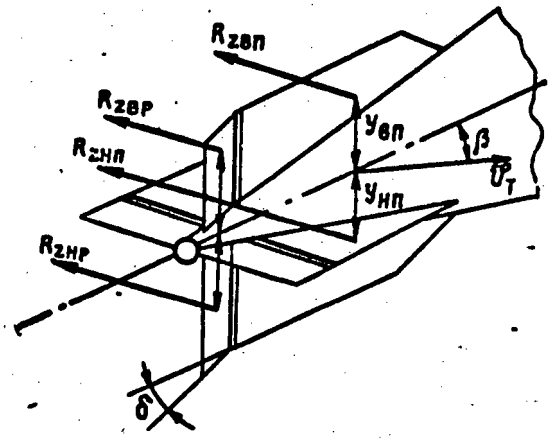

Figure 1.14. The Problem of Generation of a Torpedo's Lateral Hydrodynamic Moment

The final expression for determining heeling moment will be

$$M_x = d_3 \frac{\rho V_т^2}{2} \Omega_т L_т \beta + d_4 \frac{\rho V_т^2}{2} \Omega_т L_т \delta. \qquad (1.41)$$

From expression (1.41)

$$d_3 = d_1 \left(\frac{S_{нп}}{S_{вп} + S_{нп}} \bar{Y}_{нп} - \frac{S_{вп}}{S_{вп} + S_{нп}} \bar{Y}_{вп} \right);$$

$$d_4 = d_2 \left(\frac{S_{нр}}{S_{вр} + S_{нр}} \bar{Y}_{нр} - \frac{S_{вр}}{S_{вр} + S_{нр}} \bar{Y}_{вр} \right),$$

where $d_1 = \frac{\partial C_{z\,оп}}{\partial \beta}$; $d_2 = \frac{\partial C_{зр}}{\partial \delta}$;

$\bar{Y}_{нп}$, $\bar{Y}_{вп}$, $\bar{Y}_{вр}$, $\bar{Y}_{нр}$ -- distances of lines of corresponding forces relative to axis OX, in relation to torpedo length $L_т$;

$S_{нп}$, $S_{вп}$, $S_{вр}$, $S_{нр}$ -- areas of lower and upper vertical fin, upper and lower rudder respectively;

$C_{z\,оп}$ -- dimensionless coefficient of lateral force of vertical fin;

$C_{зр}$ -- dimensionless coefficient of rudder lateral force.

1.7. Damping Hydrodynamic Forces and Moments

We have examined above hydrodynamic characteristics under the condition that the torpedo moves only translationally at a constant velocity $V_т$. If the

torpedo is involved in rotary or oscillatory motion in addition to translational, its hydrodynamic characteristics will change appreciably, since there will be additionally generated hydrodynamic forces and moments called damping forces and moments [1.2]. We shall clarify their origin with a particular case of torpedo motion, that is, with circulation in a horizontal plane.

As a consequence of torpedo rotation, local linear fluid velocities arise at each point of the torpedo's hull, velocities which are normal to the torpedo's longitudinal axis and numerically equal to the product of angular velocity ω and the distance to point x. Consequently, sum velocity $\vec{V}$ of the incident flow will be equal to the geometric sum

$$\vec{V} = \vec{V}_r + \vec{x\omega}.$$

Since $\vec{x\omega}$ is a variable quantity, the fluid flow along the torpedo will be curvilinear and local drift angles will differ from those which would occur with rectilinear motion.

For the sake of an example Figure 1.15 contains local drift angles for two surface elements; with a positive angular velocity local drift angles in the aft section increase by quantity

$$\Delta\beta \approx \frac{x\omega}{V_r},$$

while in the nose section they decrease by the same amount.

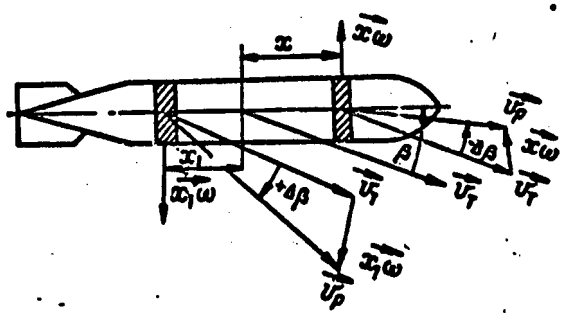

Figure 1.15.

Change in local angles of drift is the reason for the occurrence of damping forces and moments. These forces and moments can be determined both theoretically and experimentally. With the theoretical method they are determined separately for an unfinned and finned hull.

We shall first examine the method of determining damping force and moment for a torpedo's fins. With torpedo rotation relative to axis OZ the increase in angle of drift $\Delta\beta$ can be determined in approximate fashion as [1.7]

$$\Delta\beta \approx \frac{C_{on}\omega}{V_r},$$

where C_{on} is the distance from the torpedo's center of gravity to the center of hydrodynamic forces of the fins.

As a consequence of this an additional lateral force and an additional yawing moment arise on the fins or, as they are usually called, a damping force and a damping moment.

Coefficient of fin lateral force C_{zon} can be determined with the formula

$$C_{z\,on} = C_z - C_{zk},$$

where C_z is the coefficient of lateral force of a finned hull; C_{zk} -- coefficient of lateral force of an unfinned hull. Assuming $\Delta\beta$ to be a small quantity, we can write

$$\frac{\partial C_{z\,on}}{\partial \beta} = \frac{\partial C_z}{\partial \beta} - \frac{\partial C_{zk}}{\partial \beta};$$

$$R^{\omega}_{z\,on} = \frac{1}{2}\frac{\partial C_{z\,on}}{\partial \beta}\cdot\frac{\rho V_T^2}{2}\Omega_T \Delta\beta = \frac{1}{2}\frac{\partial C_{z\,on}}{\partial \beta}\rho\Omega_T C_{on} V_T \omega = A^{\omega}_{z\,on} V_T \omega, \qquad (1.42)$$

where $A^{\omega}_{z\,on} = \frac{1}{2}\frac{\partial C_{z\,on}}{\partial \beta}\rho\Omega_T C_{on}$.

The fin damping moment can be computed approximately with the formula

$$M^{\omega}_{z\,on} \approx R^{\omega}_{z\,on} C_{on} \approx A^{\omega}_{my\,on} V_T \omega, \qquad (1.43)$$

where $A^{\omega}_{my\,on} = \frac{1}{2}\frac{\partial C_{z\,on}}{\partial \beta}\rho\Omega_T C_{on}^2$.

For an unfinned hull damping forces and moment are determined with the formulas of K. K. Fedyayevskiy:

$$R^{\omega}_{zk} = A^{\omega}_{zk} V_T \omega; \qquad M^{\omega}_{yk} = A^{\omega}_{myk} V_T \omega, \qquad (1.44)$$

where

$$A^{\omega}_{zk} = \rho L_T^3 \bar{r}\,(\bar{\eta} - \bar{\eta}_0)\left(\frac{\partial C_{z_k}}{\partial \alpha}\right)_{\alpha=0};$$

$$A^{\omega}_{myk} = \rho L_T^4 \bar{r}\,(\bar{\eta} - \bar{\eta}_0)^2\left(\frac{\partial C_{z_k}}{\partial \alpha}\right)_{\alpha=0}, \qquad (1.45)$$

where $\bar{\eta}$ is a section relative (to L_T) coordinate figured from the torpedo nose; η_0 -- relative (to L_T) coordinate of the center of rotation (origin of coordinates), figured from the torpedo nose; $\bar{r}$ -- relative (to L_T) radius of the profile of the torpedo's meridional section at distance $\bar{\eta}$ from the torpedo's nose.

Calculation of synthesized coefficients employing formulas (1.45) is performed in the following sequence.

We determine quantity $\bar{r}$, for which we first compute the torpedo's fullness coefficient, equal to the ratio of the volume of the torpedo hull V_0 to the displacement of a cylinder of equal size, that is,

$$\varphi = \frac{V_0}{\frac{\pi D_т^2}{4} L_т}.$$

From the fullness coefficient in the graph (Figure 1.16) we obtain the ratio of radii

$$\frac{r}{r_{мак}} = K,$$

where r_{mak} — torpedo radius; r — running radius of the target section in the afterpart of the torpedo.

We then determine $r=Kr_{mak}$ and relative radius

$$\bar{r} = \frac{r}{L_т}.$$

We compute quantity $\bar{\eta}_0$ with the formula

$$\bar{\eta}_0 = \frac{x_{цт}}{L_т},$$

where $x_{цт}$ is the distance from the torpedo nose to its center of gravity.

In order to determine $\bar{\eta}$ we determine on the drawing distance l_1 from the torpedo nose to the section in the after part with a radius of r. Then

$$\bar{\eta} = \frac{l_1}{L_т}.$$

On the basis of known values of $\bar{\eta}$ and $\bar{r}$ from the graph (Figure 1.16) for force R_{z0}, assuming in section $\beta=0-5°$ C_{z0} is a linear function of angle β, we compute partial derivative

$$\frac{\partial C_{z_0}}{\partial \beta}.$$

Then we determine R^{ω}_{zk} and $R^{\omega}_{zоп}$ as well as M^{ω}_{yk} and $M^{\omega}_{yоп}$.

Total damping forces and damping moment are equal to:

$$R^{\omega}_z = R^{\omega}_{zк} + R^{\omega}_{zоп};$$
$$M^{\omega}_y = M^{\omega}_{yк} + M^{\omega}_{yоп}.$$

In like manner we can determine damping force R^{ω}_y and moment M^{ω}_z during torpedo rotation (oscillation) in a vertical plane.

In the case of torpedo rotation on its longitudinal axis with angular velocity ω_x, a damping moment also occurs, the approximate value of which is determined with the formula

$$M^{\omega}_{xк} = A^{\omega}_{mxк} V_т \omega_x, \qquad (1.46)$$

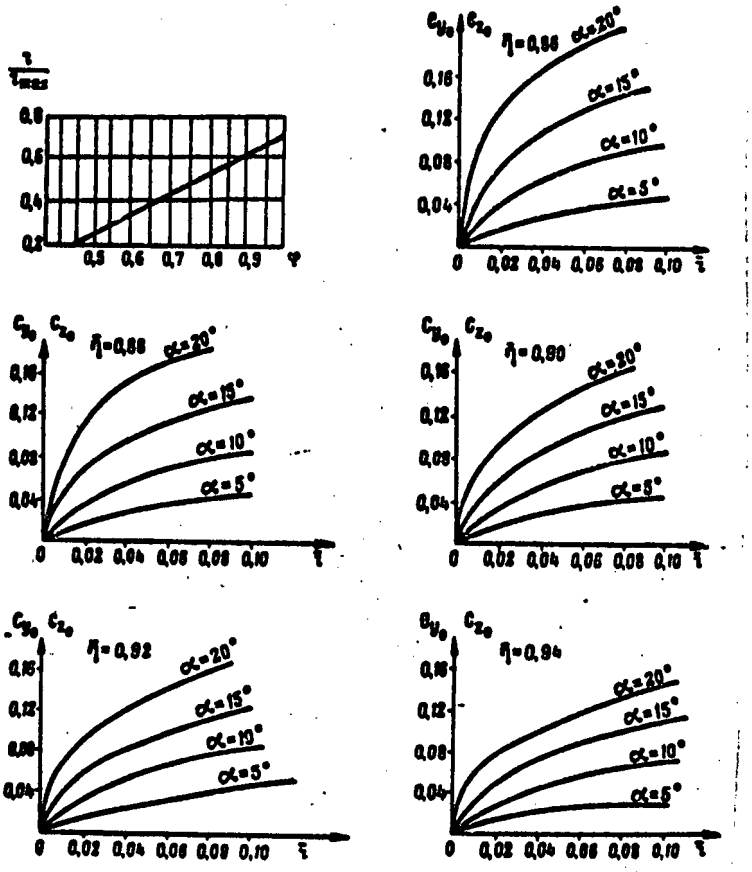

Figure 1.16. Graphs for Determining Lift Coefficients of an Unfinned Torpedo Hull (C_{y0})

where

$$A^{\omega}_{mx\,\kappa} = \frac{C_x \rho \Omega_\kappa r^6}{2};$$

r -- torpedo radius.

Utilizing expression (1.46), we can determine in a first approximation the damping moment of an unfinned hull during torpedo rotation on its longitudinal axis.

When a torpedo rotates on its longitudinal axis, a damping moment also arises on the fins. For theoretical determination of the magnitude of this moment, one can employ the formula

$$M^{\omega_x}_{x\,\text{on}} = \frac{2}{3} A^{\omega_x}_{mx\,\text{on}} V_\tau \omega_x, \qquad (1.47)$$

whereby $$A^{\omega}_{mx\,on} = \left(\frac{\partial C_y}{\partial \alpha}\right)_{on} l\left(d^3 - d_0^3\right)\rho.$$

where l — is the average length of the fin plate (Figure 1.17); d — distance between the outer edge of the fin to the axis of rotation; d_0 — distange from the inner edge of the fin to the axis of rotation.

In conclusion we should note that the above formulas make it possible only approximately to determine damping characteristics. Special tests must be performed in order to obtain more precise values. One experimentally determines thereby rotational derivatives

$$C^{\omega}_{y} = \frac{\partial C_y}{\partial \omega}\Big|_{\omega=0} \quad \text{and} \quad C^{\omega}_{mz} = \frac{\partial C_{mz}}{\partial \omega}\Big|_{\omega=0},$$

connected with damping forces and moments by the following relations:

$$R^{\omega}_{y} = C^{\omega}_{y}\Omega_{\tau}\frac{\rho V_{\tau}^2}{2}\omega; \quad M^{\omega}_{z} = C^{\omega}_{mz}\Omega_{\tau}\frac{\rho V_{\tau}^2}{2}L_{\tau}\omega.$$

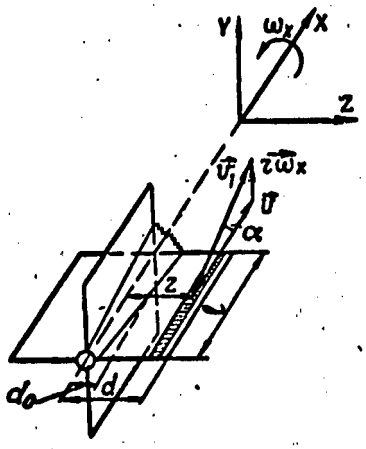

Figure 1.17. Determining Damping Forces and Moments of Torpedo Fins

There exist two methods of determining these derivatives. One is the testing of a model on a rotation testing unit. The model travels in a circle. Measuring the hydrodynamic forces and moments at various angular velocities, one can determine rotational derivatives by subsequent numerical or graphic differentiation. Another method of determining these derivatives is based on recording small model oscillations in the flow. On the basis of these tests one determines the damping constant and subsequently rotational derivatives proper.

1.8. Force Effect of a Nonviscous Fluid on a Torpedo Traveling Through It

Up to the present we have been examining hydrodynamic forces caused by fluid viscosity. As noted above, beyond the limits of the boundary layer a fluid can be assumed ideal, nonviscous. Let us examine the force effect exerted on a torpedo by a nonviscous fluid.

During torpedo motion certain momentum is imparted to the particles of the ambient fluid. If the torpedo moves at a constant velocity, this momentum will possess a constant value. In conformity with the laws of momentum and the moment of momentum, in this case the fluid will not exert force on the torpedo.

With torpedo unsteady motion, the momentum of the fluid continuously changes, and forces and moments of an inertial nature arise. Indeed, the pressure of the external surface of the torpedo on the fluid should overcome only its inertia; there will not be other forces, since the fluid is assumed nonviscous.

We shall examine these forces and moments in greater detail [1.3]. Let us assume, for example, that a torpedo is in unsteady translational motion along axis OX and is rotating on that axis. The reaction force with unsteady translational motion in the general case will not coincide with the direction of velocity $\vec{V}_{TX}$. The value of this force will be determined by its three projections onto the axes of the coupled coordinate system:

$$R_{1x} = -\lambda_{11}\dot{V}_{Tx};\quad R_{1y} = -\lambda_{12}\dot{V}_{Tx};\quad R_{1z} = -\lambda_{13}\dot{V}_{Tx}.$$

Since force $\vec{R}_1$ does not pass in the general case through the origin of coordinates, it forms a moment the projections of which onto the coordinate axes are equal to

$$M_{1x} = -\lambda_{14}\dot{V}_{Tx};\quad M_{1y} = -\lambda_{15}\dot{V}_{Tx};\quad M_{1z} = -\lambda_{16}\dot{V}_{Tx}.$$

With torpedo rotation on axis OX with angular acceleration ω_X, inertial forces also arise, which can be reduced to main vector $\vec{R}_2$ and a pair of forces the vector of which is equal to $\vec{M}_2$. Projections $\vec{R}_2$ and $\vec{M}_2$ onto the coordinate axes are determined by the expressions:

$$R_{2x} = -\lambda_{41}\dot{\omega}_x;\quad R_{2y} = -\lambda_{42}\dot{\omega}_x;\quad R_{2z} = -\lambda_{43}\dot{\omega}_x;$$
$$M_{2x} = -\lambda_{44}\dot{\omega}_x;\quad M_{2y} = -\lambda_{45}\dot{\omega}_x;\quad M_{2z} = -\lambda_{46}\dot{\omega}_x.$$

In like manner one could write expressions for inertial forces and moments for the two other axes. As a result we shall have 36 expressions of projections of forces and moments and correspondingly 36 coefficients λ_{ik} which, at the suggestion of N. Ye. Zhukovskiy, are called apparent masses and apparent moments of inertia respectively. One should not define apparent mass thereby as a certain fluid mass moving together with the torpedo. In actuality fluid particles possess velocity and accelerations which are

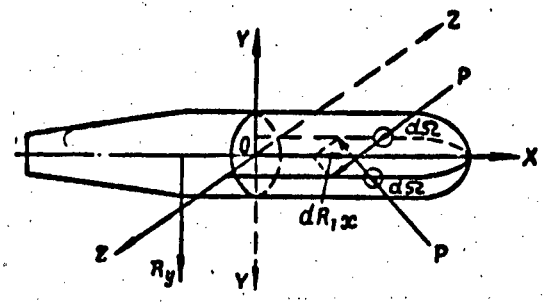

Figure 1.18. Analysis of Coefficients of Torpedo Apparent Masses

not equal to the velocity and acceleration of the solid body. Therefore apparent mass is defined as a fictitious fluid mass which, moving at the same velocity as the torpedo, would have the same momentum which is in fact possessed at the given moment by the fluid surrounding the torpedo.

The number of quantities λ_{ik} diminishes significantly if the body possesses planes of symmetry. In particular, the torpedo can be assumed to be a body which is symmetrical relative to planes XOY and XOZ (Figure 1.18).

Let us first see what λ_{ik} become zero when the torpedo moves along axis OX.

Flow along the torpedo is symmetrical, and because of this fluid pressures P on elementary surfaces dΩ to the right and left of plane XOY are identical. Resultant dR_{1x} of both these forces is directed along axis OX. Therefore its projections onto axes OY and OZ will be equal to zero. It follows from this that $\lambda_{12}=\lambda_{13}=0$.

Force dR_{1x} does not create moments relative to the coordinate axes, and therefore should be $\lambda_{14}=\lambda_{15}=\lambda_{16}=0$.

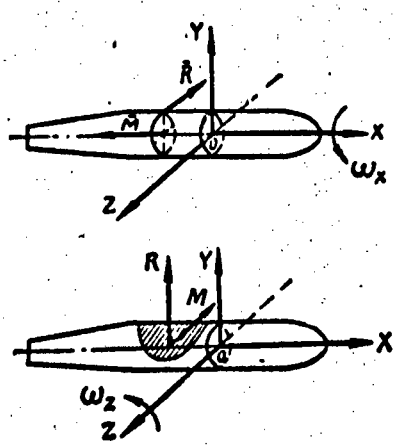

Figure 1.19. Analysis of Coefficients of Torpedo Apparent Masses

When a torpedo moves along axis OY, the resultant pressure R_y will lie in the plane of symmetry XOY, but it will not pass through the origin of coordinates. Projections of this force onto axes OX and OZ are equal to zero, and consequently $\lambda_{21}=\lambda_{23}=0$. Force R_y generates a moment only relative to axis OZ, and therefore $\lambda_{24}=\lambda_{25}=0$.

In the case of the torpedo motion along axis OZ, the following four coefficients become zero: $\lambda_{31}=\lambda_{32}=\lambda_{34}=\lambda_{36}=0$.

When the torpedo rotates on axis OX, the main vector of inertial forces should lie in plane YOZ, while the vector of the main moment should coincide with axis OZ (Figure 1.19). If we ignore fin asymmetry, the torpedo can be assumed to be a solid of revolution. In this case the main vector of inertial forces becomes zero. Consequently, $R_{4x}=R_{4y}=R_{4z}=M_{4y}=M_{4z}=0$. It follows from this that $\lambda_{41}=\lambda_{42}=\lambda_{43}=\lambda_{45}=\lambda_{46}=0$.

In the case of torpedo rotation relative to axis OZ, the main vector of inertial forces should be positioned symmetrically to plane XOY, and the main moment parallel to axis OZ, since plane YOZ is not a plane of symmetry. Then $R_{5x}=R_{5y}=M_{5y}=M_{5x}=0$ and $\lambda_{61}=\lambda_{63}=\lambda_{64}=\lambda_{65}=0$.

When the torpedo rotates relative to axis OY, $\lambda_{51}=\lambda_{52}=\lambda_{54}=\lambda_{56}=0$.

In general courses in hydrodynamics it is proven that $\lambda_{ik}=\lambda_{ki}$. If one takes this into account, then only eight of 36 coefficients remain for the torpedo, namely: λ_{11}, λ_{22}, λ_{33}, λ_{44}, λ_{55}, λ_{66}, λ_{26} and λ_{35}.

The values of apparent mass coefficients λ_{ik} are usually determined in a coupled coordinate system with the origin at the center of buoyancy. If the origin of coordinates is placed at any other point, at the torpedo's center of gravity, for example, the necessity arises to recalculate the apparent mass coefficients. This recalculation can be performed with the following formulas [1.12]:

$$\lambda_{11}=\lambda'_{11};\quad \lambda_{22}=\lambda'_{22};\quad \lambda_{33}=\lambda'_{33};$$
$$\lambda_{44}=\lambda'_{44}+\lambda'_{33}y^2_{цв};$$
$$\lambda_{55}=\lambda'_{55}+\lambda'_{33}x^2_{цв}-2\lambda'_{35}x_{цв};$$
$$\lambda_{66}=\lambda'_{66}+\lambda'_{22}x^2_{цв}+2\lambda'_{26}x_{цв};$$
$$\lambda_{35}=-\lambda'_{33}x_{цв}+\lambda'_{35};$$
$$\lambda_{26}=\lambda'_{26}+\lambda'_{22}x_{цв},$$

where λ'_{ik} and λ_{ik} are apparent mass coefficients computed relative to the center of buoyancy and relative the center of gravity respectively; we shall note that coefficients λ_{11}, λ_{22}, λ_{33} possess the dimension of mass, coefficients λ_{44}, λ_{55} and λ_{66} — the dimension of moment of inertia, and λ_{26}, λ_{35} — the dimension of static moment of mass.

For an approximate determination of coefficients of apparent mass one usually employs the method of plane sections [1.2]. The essence of this method consists in the fact that with lateral flow across an elongated body, each of its frames is considered to be in a plane flow without longitudinal fluid spreading. The apparent mass of the entire body in the direction of the lateral axis is determined by adding together the apparent masses of the separate sections. The coefficients are calculated separately thereby for an unfinned hull and for the torpedo fins. We shall cite the formulas for determining λ_{22}, λ_{26} and λ_{66}, while the remaining apparent mass coefficients are determined in analogous manner.

When an unfinned torpedo moves along axis OY

$$\lambda_{22}^{к} = \pi\rho \int_{x_1}^{x_2} r^2(x)\,dx = \rho V_0; \tag{1.48}$$

$$\lambda_{26}^{к} = \pi\rho \int_{x_1}^{x_2} xr^2(x)\,dx = \rho V_0 x_0, \tag{1.49}$$

where x_1, x_2 are the coordinates of the nose and aft end; x_0 -- coordinate of the torpedo center in a coupled coordinate system; V_0 -- volume of the unfinned torpedo hull; $r(x)$ -- variable hull radius.

In the case of torpedo rotation relative to axis OZ we have

$$\lambda_{66}^{к} = \pi\rho \int_{x_1}^{x_2} x^2 r^2(x)\,dx; \tag{1.50}$$

$$\lambda_{62} = \lambda_{26}.$$

We shall note and in a first approximation $\lambda_{22}^{к}$ and $\lambda_{66}^{к}$ can also be determined by substituting for the unfinned torpedo hull an ellipsoid of revolution the axes of which are equal to the torpedo's length and diameter. Coefficients of apparent mass for ellipsoids of revolution have been computed and are contained in a number of courses on hydrodynamics [1.14].

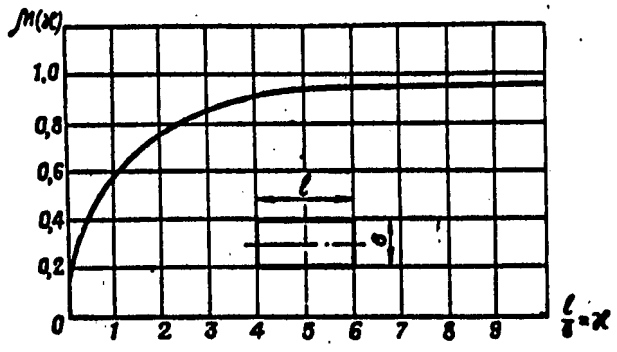

Figure 1.20. Graph for Determining Correction Factor $\mu(x)$ for Finiteness of Fin Span

With an approximate determination of fin apparent mass coefficients, the fins can be replaced by isolated plates with an aspect ratio

$$x=\frac{l}{b},$$

where l -- plate length, b -- plate width. Then the values of apparent mass coefficients, for horizontal fins, for example, with movement along axis OY, are determined with the following formulas:

$$\lambda_{22}^{on}=2\mu(x)\frac{\pi}{4}\rho b^2 l;$$
$$\lambda_{26}^{on}=\lambda_{22}^{on}x_{on}, \qquad (1.51)$$

where $\mu(x)$ -- correction for finiteness of span, determined from the graph (Figure 1.20); x_{on} -- fin center coordinate in a coupled coordinate system.

In the case of torpedo rotation relative to axis OZ, the coefficients of apparent fin mass are respectively equal to:

$$\lambda_{66}^{on}=\pi\rho\int_{x_n}^{x_k} b^2x^2\,dx;$$
$$\lambda_{62}^{on}=\lambda_{26}^{on}, \qquad (1.52)$$

where x_H and x_k -- coordinates of fin starting and end points in a coupled system.

Knowing the apparent mass coefficients for the hull and fins, one can easily obtain their values for the entire torpedo by means of addition.

1.9. Principal Dynamic Properties of a Torpedo

Torpedo movement in the water consists of spatial maneuvers of various kind. The capability and position of execution of these maneuvers are determined chiefly by the dynamic properties of the torpedoes, particularly their maneuverability, controllability, and stability. These properties are interlinked and are determined by the specifications, performance capabilities and hydrodynamic properties of torpedoes. We shall briefly examine the content of the fundamental dynamic properties of torpedoes.

The maneuverability of a torpedo reflects its ability to change direction, speed and depth or, which amounts to the same thing, to change its position in space. Following are the standard torpedo maneuvers: acceleration and deceleration, movement along inclined trajectories, and turning in a horizontal plane. Each of these maneuvers is evaluated by its indices, which are the following: time and path of acceleration or deceleration, maximum permissible angle of inclination of trajectory, range of change in velocities during torpedo movement at various cruising depths, minimum turning radius or maximum angular velocities.

Quantitative indices of the various maneuvers are in the final analysis determined by the accelerations which can be imparted to the torpedo as it moves through the water. Therefore maximum linear and angular accelerations can be viewed as the indices of torpedo maneuverability in general.

As it moves through the water a torpedo is subjected to various kinds of disturbing influences which disrupt the equilibrium of the forces and moments acting on it. As a result of this the torpedo diverges from the originally calculated mode of movement. Deviations of this kind also take place as a consequence of a difference between the actual parameters and characteristics of the torpedo and its control systems and their values employed in calculations. Usually all parameter deviations from computed values are viewed as disturbing influences.

In stability theory standard rated conditions are called undisturbed motion. Generated motion in respect to standard (undisturbed) is called torpedo disturbed motion. Following are characteristic undisturbed motions for torpedoes: rectilinear motion at a specified depth, circling motion, and inclined rectilinear or nonrectilinear motion.

We should note that undisturbed motion can be both steady-state and unsteady. It is important that it constitutes one of a torpedo's physically possible motions, taking place under specific given circumstances. Let us assume, fo_ example, that a torpedo is moving on a rectilinear trajectory. At some moment in time it diverges from undisturbed motion under the influence of external disturbing forces (Figure 1.21).

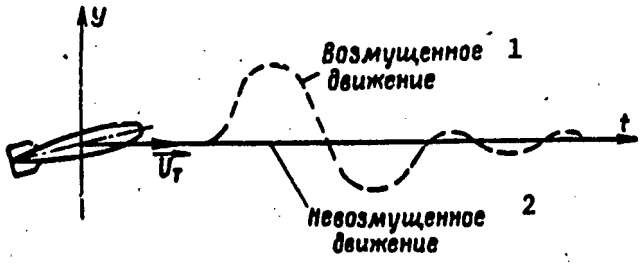

Figure 1.21. Torpedo Disturbed and Undisturbed Motion

Key to figure: 1 -- disturbed motion; 2 -- undisturbed motion

If after cessation of the disturbing forces the torpedo returns to the original conditions of motion (within the limits of allowable precision of travel), its undisturbed motion is stable. On the other hand, if after cessation of disturbing forces the torpedo does not return to the original mode, its undisturbed motion is unstable.

Consequently, stability is a torpedo's ability to reestablish its original undisturbed motion mode in all or separate kinematic parameters; depth, trim, yaw angle, heeling angle, and velocity. The more rapidly undisturbed motion is reestablished, the greater the degree of stability.

A torpedo's turning ability is its ability to change its direction of movement. Quantitatively turning ability is defined by angular velocity or turning radius. The greater the angular velocity or the smaller the turning radius, the greater is the torpedo's turning ability.

Controllability is a torpedo's ability to execute commands (signals) proceeding from the control system to the torpedo controls (control surfaces), and thus to alter direction of motion in strict conformity with a specified program (trajectory) or to follow a signal from a homing system.

Torpedo controllability and turning ability are closely-related terms. They are not identical, however. It may happen that a torpedo which possesses a high degree of turning ability will control poorly and will be unable to follow input signals which change with a specified frequency. Essentially controllability unifies two opposite torpedo properties: turning ability and stability.

Degree of stability of torpedo movement decreases with an increase in turning ability and, on the other hand, an increase in degree of stability results in diminished turning ability. Therefore in substantiating hydrodynamic design parameters (torpedo relative elongation, fin surface, control surface area), one proceeds from the necessity of ensuring an efficient combination of torpedo basic dynamic properties.

1.10. Conditions of Torpedo Rectilinear Motion in a Vertical Plane

Rectilinear motion is one of the simplest and at the same time the most common type of motion. A torpedo executes this kind of motion on the horizontal segment of its trajectory as well as when surfacing and diving.

Center of gravity rectilinear motion is possible under the condition that the velocity vector does not change during the entire time of torpedo travel, that is,

$$\vec{V}_\tau = \text{const} \tag{1.53}$$

or

$$\psi_1 = \theta - \alpha = \text{const},$$

where ϕ_1 is the angle between the velocity vector and the horizon.

In order to satisfy condition (1.53) it is necessary and sufficient to ensure constant angle of attack α and trim angle θ during the entire time of torpedo motion.

Constancy of angle θ is ensured by the system controlling torpedo motion in a vertical plane. The angle of attack is determined by many factors: negative buoyancy, torpedo hydrodynamic characteristics and speed. In order to determine this relation it is necessary to construct an equation of equilibrium of forces and moments acting on the torpedo.

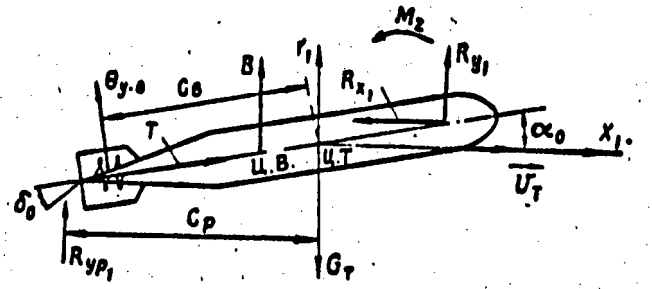

Figure 1.22. Diagram of Forces Acting on a Torpedo in the Vertical Plane

During rectilinear motion a torpedo is acted on by a number of hydrodynamic forces and moments. If these forces and moments are mutually balanced or, as is usually stated, the torpedo is balanced, under this and only under this condition is it possible to ensure constancy of angle of attack.

In steady-state rectilinear motion a torpedo is acted upon by the following forces (Figure 1.22).

Drag

$$R_{x_1} = C_{x_1} \frac{\rho V_\tau^2}{2} \Omega_\tau = A_{x_1} V_\tau^2,$$

where $A_{x_1} = C_{x_1} \frac{\rho \Omega_\tau}{2}$ — synthesized coefficient of drag.

Lift

$$R_{y_1} = C_{y_1} \frac{\rho V_\tau^2}{2} \Omega_\tau.$$

For small angles of attack and angles of horizontal control surface deflection, lift can be represented by a linear relationship between these angles

$$R_{y_1} = \frac{\partial C_{y_1}}{\partial \alpha} \cdot \frac{\rho V_\tau^2}{2} \Omega_\tau \alpha_0 + \frac{\partial C_{y_1}}{\partial \delta_r} \cdot \frac{\rho V_\tau^2}{2} \Omega_\tau \delta_{r0}.$$

The first term of this relationship defines the torpedo's lift without horizontal control surfaces $R_{y_1 T}$, and the second — lift of horizontal control surfaces R_{yp}.

Consequently

$$R_{y_1 \tau} = \frac{\partial C_{y_1}}{\partial \alpha} \cdot \frac{\rho V_\tau^2}{2} \Omega_\tau \alpha_0 = A_{y_1} V_\tau^2 \alpha_0;$$

$$R_{yp} = \frac{\partial C_{y_1}}{\partial \delta_r} \cdot \frac{\rho V_\tau^2}{2} \Omega_\tau \delta_{r0} = A_p V_\tau^2 \delta_{r0},$$

where $A_{y_1} = \frac{\partial C_{y_1}}{\partial \alpha} \cdot \frac{\rho \Omega_T}{2}$ — synthesized coefficient of torpedo lift;

$A_p = \frac{\partial C_{y_1}}{\partial \delta_r} \cdot \frac{\rho \Omega_T}{2}$ — synthesized control surface lift coefficient, characterizing their effectiveness.

The torpedo's longitudinal hydrodynamic moment without taking into consideration horizontal control surfaces is

$$M_{z_1} = C_{mz_1} \frac{\rho V_T^2}{2} \Omega_T L_T.$$

For small angles of attack the coefficient of longitudinal moment is expressed by linear relation

$$C_{mz_1} = \frac{\partial C_{mz_1}}{\partial \alpha} \cdot \alpha.$$

Consequently,

$$M_{z_1} = \frac{\partial C_{mz_1}}{\partial \alpha} \cdot \frac{\rho V_T^2}{2} \Omega_T L_T \alpha_0 = A_{mz_1} V_T^2 \alpha_0,$$

where $A_{mz_1} = \frac{\partial C_{mz_1}}{\partial \alpha} \cdot \frac{\rho \Omega_T}{2} L_T$ — synthesized coefficient of longitudinal hydrodynamic moment.

Propeller thrust T. It is usually assumed that force T is directed along the torpedo's longitudinal axis.

Propeller lateral force Q_{yB}. It arises on the propellers when the torpedo moves at a certain angle of attack and is directed perpendicular to the torpedo's longitudinal axis:

$$Q_{yB} = KV_T^2 \alpha_0,$$

where K — synthesized coefficient of propeller lateral force.

Torpedo weight G.

Torpedo displacement force B.

The moments of forces R_{yp}, T, Q_{yB}, B are determined according to the general rules of mechanics.

In order to determine angles α_0 and δ_{r0} we shall construct equations of equilibrium of the enumerated forces and moments acting on the torpedo in steady-state motion.

1. Equation of equilibrium of forces in projections onto axis OX_1

$$-R_{x_1} + T \cos \alpha_0 - Q_{yB} \sin \alpha_0 - (G_T - B) \sin \psi_1 = 0.$$

2. Equation of equilibrium of forces in projections onto axis OY_1

$$R_{y_1} + B - G_T + T\sin\alpha_0 + Q_{ys}\cos\alpha_0 + R_{yp} = 0.$$

3. Equation of equilibrium of moments of forces relative to the torpedo's center of gravity

$$M_{z_1} - B(l\cos\alpha_0 + \Delta\sin\alpha_0) - T\Delta - Q_{ys}C_B - C_pR_{yp} = 0,$$

where l -- distance between center of gravity and center of buoyancy; Δ -- lowering of center of gravity; C_B -- distance from center of gravity to plane of propellers; C_p -- distance from center of gravity to center of control surface pressure.

During torpedo motion the angle of attack does not exceed 5-7°.

Therefore we can assume that $\cos\alpha_0 \approx 1$ и $\sin\alpha_0 \approx \alpha_0$.

Terms $Q_{ys}\sin\alpha_0$ and $\Delta\sin\alpha_0$ are small and can be ignored. Taking these assumptions into consideration, the equations of equilibrium of forces and moments during torpedo rectilinear motion can be presented in the form

$$\begin{aligned} A_{x_1}V_T^2 &= T - (G_T - B)\sin\psi_1; \\ (A_{x_1} + A_{y_1} + K)V_T^2\alpha_0 + A_pV_T^2\delta_{r0} &= G_T - B; \\ (A_{mz_1} - KC_B)V_T^2\alpha_0 - A_pC_pV_T^2\delta_{r0} &= Bl + T\Delta. \end{aligned} \qquad (1.54)$$

One determines velocity of torpedo steady motion from the first equations, with specified propeller thrust.

Solving together the second and third equations of system (1.54), we obtain

$$\begin{aligned} \alpha_0 &= \frac{C_p(G_T - B) + Bl + T\Delta}{[(A_{x_1} + A_{y_1} + K)C_p + A_{mz_1} - KC_B]V_T^2}; \\ \delta_{r0} &= \frac{(A_{mz_1} - KC_B)(G_T - B) - (A_{x_1} + A_{y_1} + K)(Bl + T\Delta)}{[(A_{x_1} + A_{y_1} + K)C_p + (A_{mz_1} - KC_B)]A_pV_T^2}. \end{aligned} \qquad (1.55)$$

Angles α_0 and δ_{r0}, at which all forces and moments are mutually balanced, are called balance angles. Angle α_0 is called the balance angle of attack and angle δ_{r0} -- the balance angle of control surface deflection. As is evident from expressions (1.55), they are determined by the torpedo's hydrodynamic characteristics, velocity and trim dive -- $(G_T - B)$ and l.

If during torpedo motion the position of its center of gravity does not change, the moments of forces remain constant. Consequently, condition $\alpha_0 = \text{const}$ will be satisfied only if velocity V_T does not change in magnitude and the torpedo's trim dive remains constant during the entire time of motion.

We should note that the balance angle values can be changed in the required direction. In particular, a decrease in the balance angle can be achieved by displacing the center of gravity toward the nose of the torpedo. In this case the arm of forces R_{x1} and R_{y1} is reduced, as a consequence of which there occurs a decrease in the longitudinal hydrodynamic moment. Obviously the control surfaces must be deflected to a smaller angle in order to balance a hydrodynamic moment of smaller magnitude.

This same problem can be solved by increasing fin surface area, as a consequence of which there takes place a shift in the center of drag (point of application of forces R_{x1} and R_{y1}) in the direction of the torpedo center of gravity, which also decreases the magnitude of the pitching moment.

A decrease in angles α_0 and δ_{r0} is advisable, since it leads to a certain decrease in torpedo drag and, in addition, increases control surface effectiveness.

There exists for each torpedo a maximum allowable value δ_{rOM}, at which it still possesses controllability. If δ_{rOM} is known, one can determine critical velocity, that is, the minimum allowable velocity value at which the torpedo does not lose controllability. For this we must substitute δ_{rOM} in expression (1.55) in place of δ_{r0}.

1.11. Change in Torpedo Velocity

When torpedoes move in complex space trajectories, their velocity changes within certain limits. This change is dictated by the trajectory angle of inclination, by the influence of negative buoyancy, and decrease in reciprocating engine output with depth.

We shall analyze change in velocity during surfacing (diving) and motion on rectilinear trajectories at various depths.

We shall assume that a torpedo rises from firing depth to a specified depth with a trajectory angle of inclination ψ (Figure 1.22).

Under stable conditions of rising the equation of forces in a projection onto axis OX_1 is in the form

$$T\cos\alpha-(G_т-B)\sin\psi_1-A_{x_1}V_т^2=0. \qquad (1.56)$$

The angle of attack is small, so that we can assume $\cos\alpha\approx 1$. From formula (1.56) we find

$$V_т=\sqrt{\frac{T-(G_т-B)\sin\psi_1}{A_{x_1}}}. \qquad (1.57)$$

This relationship is characteristic of torpedoes the propeller thrust of which is independent of operating depth.

As is evident from expression (1.57), torpedo velocity is not a constant value; it changes during maneuvering in a vertical plane.

We shall examine velocity change in torpedoes the propeller thrust of which is determined by depth. This relation can be approximately represented with the following expression:

$$T = T_0 - \beta H_T, \qquad (1.58)$$

where T_0 — rated thrust; β — a factor which takes into account change in thrust as a consequence of decreased engine output with depth; H_T — torpedo depth.

Since thrust continuously changes as the torpedo rises or descends, its velocity on inclined segments of the trajectory is not a constant value. However, inertial forces dictated by change in torpedo velocity are small and can be ignored.

In this case we can utilize in order to determine torpedo velocity formula (1.57), which assumes the following form, taking into account formula (1.58):

$$V_T = \sqrt{\frac{T_0 - \beta H_T - (G_T - B)\sin\psi_1}{A_{x_1}}}. \qquad (1.59)$$

1.12. Method of Substantiating Torpedo Hydrodynamic Design

A torpedo's excellent dynamic properties are secured by a number of measures, and chiefly by selecting an efficient hydrodynamic design. We shall define efficient design as a combination of tail fin and control surface characteristics whereby the torpedo will rapidly and sufficiently precisely respond to control surface deflection or, in other words, will possess a high degree of reaction to control surface deflection. A torpedo's ability to respond to control surface deflection can be qualitatively appraised by its amplitude and phase frequency characteristics.

Phase frequency characteristics define a torpedo's delay in responding to control surface deflection, while amplitude-frequency characteristics define its quickness of action.

We shall examine this question in greater detail, employing the example of torpedo lateral motion. We shall construct equations of torpedo motion in projections onto the axes of a coupled coordinate system, applying the d'Alembert principle. According to this principle, the sum of projections of all forces and moments applied to a torpedo, including inertial, should equal zero. During motion in a horizontal plane the following forces and moments act on a torpedo (Figure 1.23).

Longitudinal force

$$R_x = -A_x V_T^2 \cong A_{x_1} V_T^2 \qquad (1.60)$$

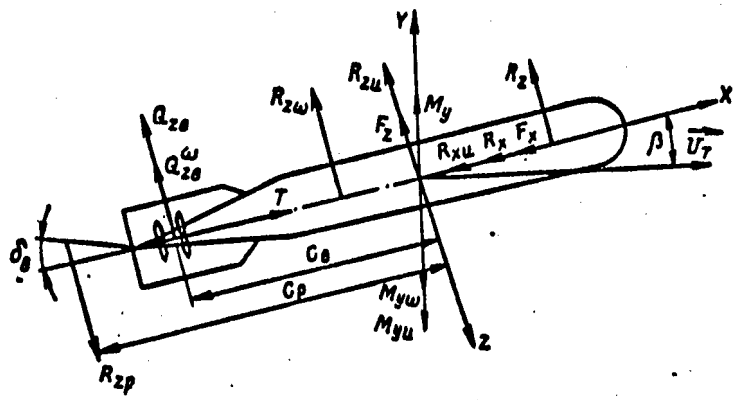

Figure 1.23. Diagram of Forces Acting on a Torpedo in a Horizontal Plane

Lateral force

$$R_z = -C_{z_1}\frac{\rho V_T^2}{2}\Omega_T - C_{x_1}\frac{\rho V_T^2}{2}\Omega_T\beta.$$

For small angles of displacement β and angles of control surface deflection δ_B, coefficient C_{z_1} can be represented as a linear relation between the specified angles

$$C_{z_1} = \left.\frac{\partial C_{z_1}}{\partial\beta}\right|_{\delta_B=\delta_{B0}}\beta + \left.\frac{\partial C_{z_1}}{\partial\delta_B}\right|_{\beta=\beta_0}\delta_B$$

or

$$C_{z_1} = \left.\frac{\partial C_{z_1}}{\partial\beta'}\right|_{\delta_B=0}\beta + \left.\frac{\partial C_{z_1}}{\partial\delta_B}\right|_{\beta=0}(\delta_B-\beta).$$

The first term determines the torpedo's coefficient of lateral force without control surfaces, and the second — the control surface coefficient of lateral force. If linearization is effected relative to $\delta_B=0$; $\beta=0$, one must employ in the second term the control surface true angle of attack $\delta_B-\beta$ in place of δ_B.

Thus the expression for lateral force will assume the form

$$R_z = -A_{z_1}V_T^2\beta + A_\rho V_T^2(\delta_B-\beta) - A_{x_1}V_T^2\beta, \qquad (1.61)$$

where $A_{z_1} = \left.\frac{\partial C_{z_1}}{\partial\beta}\right|_{\delta_B=0}\cdot\frac{\rho\Omega_T}{2}$ — synthesized coefficient of torpedo lateral force;

$A_\rho = \left.\frac{\partial C_{z_1}}{\partial\delta_B}\right|_{\beta=0}\cdot\frac{\rho\Omega_T}{2}$ — synthesized coefficient of torpedo control surface lateral force.

Torpedo yawing moment, not taking into account vertical control surface moment

$$M_y = C_{my}\frac{\rho V_\tau^2}{2}\Omega_\tau L_\tau \cong C_{my_1}\frac{\rho V_\tau^2}{2}\Omega_\tau L_\tau.$$

For small angles β M_y can be represented by the linear relation

$$\dot{M}_y = \left.\frac{\partial C_{my}}{\partial\beta}\right|_{\delta_в=0}\cdot\frac{\rho V_\tau^2}{2}\Omega_\tau L_\tau\beta = A_{my}V_\tau^2\beta \cong A_{my_1}V_\tau^2\beta. \qquad (1.62)$$

where

$A_{my_1} = \left.\frac{\partial C_{my}}{\partial\beta}\right|_{\delta_в=0}\cdot\frac{\rho\Omega_\tau}{2}L_\tau$ — synthesized coefficient of moment M_y.

Moment of force of vertical control surfaces. It is determined by expression

$$M_{zp} = R_{zp}C_p = A_pC_pV_\tau^2(\delta_в - \beta). \qquad (1.63)$$

Damping hydrodynamic force R_z^ω and moment M_y^ω

$$R_z^\omega = A_z^\omega V_\tau\omega; \quad M_y^\omega = -A_{my}^\omega V_\tau\omega. \qquad (1.64)$$

Inertial force and moment generated by torpedo nonuniform motion. They are determined on the basis of Newton's second law

$$\vec{F} = -m\frac{d\vec{V}_\tau'}{dt}; \qquad \vec{M}_и = -J\frac{d\vec{\omega}}{dt}, \qquad (1.65)$$

where m, J — torpedo mass and moment of inertia; $\frac{d\vec{V}_\tau'}{dt}; \frac{d\vec{\omega}}{dt}$ — torpedo linear and angular accelerations in a fixed coordinate system.

Rate of change of vector $\vec{V}_\tau$ relative to a moving coordinate system is equal to [1.13]

$$\frac{d\vec{V}_\tau'}{dt} = \frac{d\vec{V}_\tau}{dt} + \vec{\omega}\times\vec{V}_\tau. \qquad (1.66)$$

where $\frac{d\vec{V}_\tau}{dt}$ — a local derivative computed in the assumption that the coordinate system is fixed, while $\vec{\omega}$ is the angular velocity of rotation of the coordinate system.

Projecting (1.65) onto the axes of a movable coordinate system, we find

$$F_x = -m\frac{dV_{\tau x}}{dt} - mV_{\tau z}\omega_y;$$
$$F_z = -m\frac{dV_{\tau z}}{dt} + mV_{\tau x}\omega_y; \qquad (1.67)$$
$$M_{yи} = -J\frac{d\omega_y}{dt}.$$

Components of inertial resistance. During translational motion the resultant force of inertial resistance $\vec{R}_и$ is directed at some angle to the direction of torpedo motion. In order to determine the components of force $\vec{R}_и$ on axes X and Z, we shall apply the theorem of momentums. According to this theorem momentum of force $\vec{R}_и$ can be equated to a change in quantity of motion of associated mass taken with the opposite sign [1.13]:

$$\vec{R}_и dt = -d\left(\lambda_{11} V_{тx} \vec{i} + \lambda_{33} V_{тy} \vec{k}\right),$$

where $\vec{i}$, $\vec{k}$ — unit vectors along axes X and Z. From this it follows that

$$\vec{R}_и = -\frac{d}{dt}\left(\lambda_{11} V_{тx} \vec{i}\right) - \frac{d}{dt}\left(\lambda_{33} V_{тz} \vec{k}\right) =$$

$$= -\lambda_{11} \frac{dV_{тx}}{dt} \vec{i} - \lambda_{33} \frac{dV_{тz}}{dt} \vec{k} - \lambda_{11} V_{тx} \frac{d\vec{i}}{dt} - \lambda_{33} V_{тz} \frac{d\vec{k}}{dt}.$$

Derivatives $\frac{d\vec{i}}{dt}$ and $\frac{d\vec{k}}{dt}$ in turn are determined by

$$\frac{d\vec{i}}{dt} = \vec{\omega} \times \vec{i} = -\omega \vec{k}; \quad \frac{d\vec{k}}{dt} = \vec{\omega} \times \vec{k} = \omega \vec{i}.$$

Consequently the expression for force $\vec{R}_и$ will assume the form

$$\vec{R}_и = \left(-\lambda_{11} \frac{dV_{тx}}{dt} - \lambda_{33} V_{тz} \omega_y\right) \vec{i} - \left(\lambda_{33} \frac{dV_{тz}}{dt} - \lambda_{11} V_{тx} \omega_y\right) \vec{k}.$$

Terms with unit vectors constitute projections of force $\vec{R}_и$ onto axes X and Z, that is,

$$R_{xи} = -\lambda_{11} \frac{dV_{тx}}{dt} - \lambda_{33} V_{тz} \omega_y;$$

$$R_{zи} = -\lambda_{33} \frac{dV_{тz}}{dt} + \lambda_{11} V_{тx} \omega_y.$$

Terms containing λ_{11} are small, and henceforth we shall not consider them. Then

$$R_{xи} = -\lambda_{33} V_{тz} \omega_y;$$

$$R_{zи} = -\lambda_{33} \frac{dV_{тz}}{dt}. \qquad (1.68)$$

Moment of force of inertial resistance. During torpedo rotation on axis OY and translational movement along axis OZ, there arise moments of inertial resistance (see 1.8), the projections of which onto axis OY are determined by expression

$$M_{yи} = -\lambda_{55} \frac{d\omega_y}{dt} - \lambda_{35} \frac{dV'_{тz}}{dt}. \qquad (1.69)$$

To determine projection $\frac{dV'_{тz}}{dt}$ it is necessary to project vector equation

$$\frac{d\vec{V}'_т}{dt} = \frac{d\vec{V}_т}{dt} + \vec{\omega} \times \vec{V}_т \qquad (1.70)$$

onto axis OZ.

As a result of projection (1.70) onto axis OZ, we obtain

$$\frac{dV'_{\tau z}}{dt} = \frac{dV_{\tau z}}{dt} - V_{\tau x}\omega_y. \qquad (1.71)$$

Substituting the value of equation (1.71) into equation (1.69), we shall have

$$M_{yn} = -\lambda_{55}\frac{d\omega_y}{dt} - \lambda_{35}\frac{dV_{\tau z}}{dt} + \lambda_{33}V_{\tau x}\omega_y \qquad (1.72)$$

Forces and moments generated by the propellers (Figure 1.23):

propeller thrust T;

lateral force on propellers $Q_{zB} = KV_\tau^2\beta$;

damping force of propellers $Q^{\omega}_{zB} = KC_B V_\tau \omega_y$;

moments of forces Q_{ZB} and Q^{ω}_{ZB}, equal to

$$Q_{zB}C_B = KC_B V_\tau^2\beta; \qquad (1.73)$$
$$Q^{\omega}_{zB}C_B = KC_B^2 V_\tau \omega_y.$$

Projections of forces of weight G_T and displacement B. During torpedo motion with heeling angle γ, projections of the above forces onto axis OZ are equal to

$$G_\tau \sin\gamma - B\sin\gamma = (G_\tau - B)\sin\gamma. \qquad (1.74)$$

Moment of force of displacement B. Force B forms a moment relative to axis OY only in the case of torpedo heeling. To determine the magnitude of this moment, we must project force B onto axis OZ and multiply the projection of the force by the distance from center of displacement ЦВ to center of gravity ЦТ.

The magnitude of this moment is equal to

$$B\sin\gamma l. \qquad (1.75)$$

Adding together the projections of forces and moments (Figure 1.23) onto the axes of a coupled coordinate system, we obtain the following equations of torpedo lateral motion:

$$m\frac{dV_{\tau x}}{dt} + (m + \lambda_{33})V_{\tau z}\omega_y = \hat{T} - A_x V_\tau^2;$$

$$(m + \lambda_{33})\frac{dV_{\tau z}}{dt} + \lambda_{35}\frac{d\omega_y}{dt} - mV_\tau\omega_y = -A_{z_1}V_\tau^2\beta + A_p V_\tau^2(\delta_B - \beta) -$$
$$- A^{\omega}_z V_\tau\omega_y - A_{x_1}V_\tau^2\beta - KV_\tau^2\beta - KC_B V_{\tau x}\omega_y + (G_\tau - B)\sin\gamma;$$
$$(J_{yy} + \lambda_{55})\frac{d\omega_y}{dt} - \lambda_{35}V_\tau\omega_y + \lambda_{35}\frac{dV_{\tau z}}{dt} =$$
$$= A_{my_1}V_\tau^2\beta + A_p C_p V_\tau^2(\delta_B - \beta) - A^{\omega}_{my}V_\tau\omega_y - KC_B V_\tau^2\beta -$$
$$- KC_B^2 V_\tau\omega_y + Bl\sin\gamma. \qquad (1.76)$$

Here

$$V_{\tau z} = V_\tau \sin\beta \approx V_\tau \beta;$$

$$\frac{dV_{\tau z}}{dt} = \frac{dV_\tau}{dt}\beta + \frac{d\beta}{dt}V_\tau;$$

$$V_{\tau x} = V_\tau \cos\beta \approx V_\tau.$$

Torpedo controllability can be examined in the assumption that its speed of motion does not change appreciably, that is, assuming

$$\frac{dV_\tau}{dt} = 0.$$

In addition, we shall assume that there is no heel ($\gamma = 0$).

For these conditions we write equations (1.76) in the following form:

$$m_0 V_\tau \frac{d\beta}{dt} + A_{zn} V_\tau^2 \beta + \lambda_{35}\frac{d\omega}{dt} + A^{\omega}_{z_1} V_\tau \omega = A_p V_\tau^2 \delta_B;$$

$$\lambda_{35} V_\tau \frac{d\beta}{dt} - A_{myn} V_\tau^2 \beta + J_0 \frac{d\omega}{dt} + A^{\omega}_{my_1} V_\tau \omega = A_p C_p V_\tau^2 \delta_B. \quad (1.77)$$

Here

$$A_{zn} = A_{z_1} + A_p + A_{x_1} + K; \quad A^{\omega}_{z_1} = A^{\omega}_z + KC_a - m; \quad J_0 = J + \lambda_{55};$$

$$A_{myn} = A_{my_1} - KC_a - A_p C_p; \quad A^{\omega}_{my_1} = A^{\omega}_{my} + KC_a^2 - \lambda_{35}; \quad m_0 = m + \lambda_{33}.$$

Proceeding from expressions (1.77), we shall determine first of all the torpedo's transfer function at angular velocity $W_\omega(p)$.

Toward this end we shall write (1.77) in representations under zero initial conditions

$$(m_0 V_\tau p + A_{zn} V_\tau^2)\bar{\beta}(p) + (\lambda_{35} p + R^{\omega}_{z_1} V_\tau)\bar{\omega}(p) = A_p V_\tau^2 \bar{\delta}_B(p);$$

$$(\lambda_{35} p - A_{myn} V_\tau^2)\bar{\beta}(p) + (I_0 p + A^{\omega}_{my_1} V_\tau)\bar{\omega}(p) = A_p C_p V_\tau^2 \bar{\delta}_B(p). \quad (1.78)$$

We shall recall that the ratio of the output quantity representation to input quantity representation under zero initial conditions is called transfer function.

Taking as our input quantity control surface deflection angle $\delta_B(\text{вх})$, and as our output quantity torpedo angular velocity $\omega_{\text{вых}}$, from (1.78) we obtain

$$W_\omega(p) = \frac{\bar{\omega}_{\text{вых}}(p)}{\bar{\delta}_{B\,\text{вх}}(p)} = \frac{B_0 p + 1}{B_1 p^3 + B_2 p + B_3}, \quad (1.79)$$

where

$$B_0 = \frac{m_0 C_p - \lambda_{35}}{(A_{zn} C_p + A_{myn}) V_\tau}; \quad B_1 = \frac{m_0 I_0 - \lambda_{35}^2}{(A_{zn} C_p + A_{myn}) A_p V_\tau^3};$$

$$B_2 = \frac{m_0 A^{\omega}_{my_1} + A_{zn} I_0 + A_{myn}\lambda_{35} - \lambda_{35} A^{\omega}_{z_1}}{(A_{zn} C_p + A_{myn}) A_p V_\tau^2};$$

$$B_3 = \frac{A_{zn} A^{\omega}_{my_1} + A_{myn} A^{\omega}_{z_1}}{(A_{zn} C_p + A_{myn}) A_p V_\tau}.$$

An analysis of the coefficients of characteristic equation

$$B_1p^2+B_2p+B_3=0$$

shows that the requisite and sufficient conditions of stability are met if $B_3>0$. Therefore we shall call coefficient B_3 a coefficient of stability.

Substituting $j\omega$ in place of p in expression (1.79), we obtain expressions for torpedo amplitude-frequency $A(\omega)$ and phase-frequency $\phi(\omega)$ characteristics

$$A(\omega)=\sqrt{\frac{1+(B_0\omega)^2}{(B_3-B_1\omega^3)+(B_2\omega)^2}}; \qquad (1.80)$$

$$\varphi(\omega)=\operatorname{arc\,tg} B_0\omega-\operatorname{arc\,tg}\frac{B_2\omega}{B_3-B_1\omega^2}. \qquad (1.81)$$

In this case the amplitude-frequency characteristic determines the torpedo's angular velocity per unit of control surface deflection angle.

Consequently $A(\omega)$ characterizes torpedo turning ability. With an increase in $A(\omega)$, torpedo turning ability increases. The phase-frequency characteristic determines phase lag in torpedo response to control surface deflection. Thus torpedo controllability can be evaluated on the basis of amplitude and phase-frequency characteristics $A(\omega)$ and $\phi(\omega)$. The less the lag and the greater the turning ability, the greater torpedo controllability will be. Of substantial significance is the inclination of the amplitude-frequency characteristic toward the X axis, which characterizes torpedo inertia.

In substantiating the hydrodynamic design of a homing torpedo it is necessary to select a combination of tail fin and control surface characteristics whereby $A(\omega)$ has a minimum inclination to the X axis, so that the torpedo will respond to signals from the homing system within the specified range of frequencies.

The quantitative value of $A(\omega)$ should be established on the basis of an analysis of the relationship between dynamic errors on the one hand and homing system parameters as well as torpedo dynamic properties on the other. In a first approximation tail fin and control surface parameters can also be determined according to the allowable value of coefficient of stability B_3. With an increase in B_3 torpedo turning ability decreases and the degree of stability of its motion increases.

1.13. Influence of Hydrodynamic Design Parameters on Torpedo Controllability

The principal design elements are the following: the ratio of torpedo length t o diameter, usually called torpedo aspect ratio λ, control surface area, and tail fin area.

Influence of Tail Fin Surface Area and Control Surface Effectiveness

Figure 1.24 indicates $A(\omega)$ for a torpedo with varying fin area. Fin characteristics were assumed proportional to their areas.

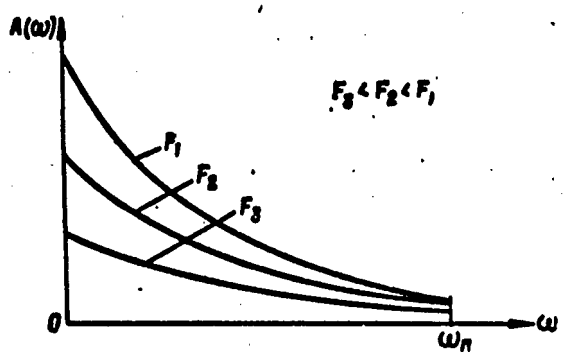

Figure 1.24. Amplitude-Frequency Characteristics of Torpedoes with Differing Fin Area

The curves show that a torpedo with standard fins (F_1) constitutes a filter which does not pass frequencies $\omega>\omega_п$. An increase in fin area worsens torpedo turning ability but increases the degree of stability of its motion.

When $\omega>\omega_п$ and $A_р$ is constant, torpedo turning ability is practically independent of fin area.

It is important to note that with an increase in fin area there occurs a decrease in inclination of $A(\omega)$ to the X axis, that is, torpedo lag decreases.

As is indicated by calculations, by means of simultaneously changing fin area and control surface effectiveness $A_р$, one can substantially improve torpedo dynamic properties and, in particular, increase the band of frequencies passed by the torpedo.

Influence of Torpedo Aspect Ratio

As calculations show, with a decrease in λ a torpedo becomes more maneuverable, and its turning radius $R_т$ decreases substantially, but at the same time the torpedo's controllability substantially decreases. It is true that the controllability of torpedoes with a low ratio of length to diameter can be secured by employing more effective fins. In this case the center of resistance is displaced aft, moment M_y decreases, and control surface effectiveness increases.

In solving the problems of torpedo controllability, scientists increasingly turned to examples in the animal world, some representatives of which possess sophisticated control and stabilization organs. Fish, for example, execute complex three-dimentional maneuvers with ease. This is achieved thanks to the existence of a highly-developed system of fins as well as body flexing. Fish can alter the parameters of their control and stabilization organs in relation to the desired maneuver.

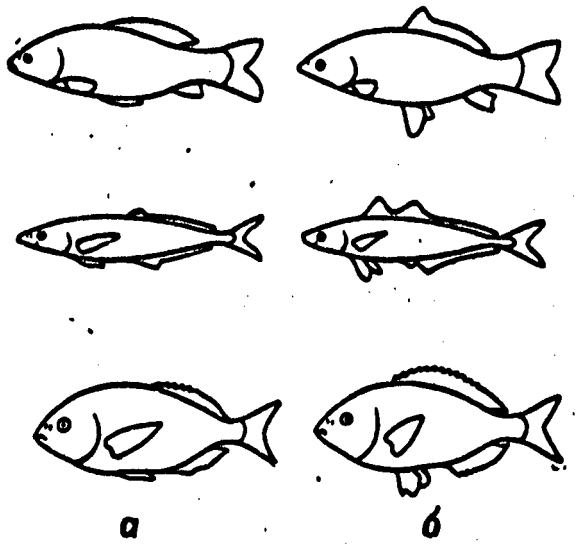

Figure 1.25. Fin Configuration on Fish During Straight-Line Motion (a) and During Turns (b)

Figure 1.25 shows the configuration of the fins of fish during straight-line movement (a) and during turning movement (b). Fin extension and body flexure generates a control force, achieving certain destabilization, which is caused by an increase in effectiveness of the fins located closer to the fish's center of gravity. The center of resistance is displaced forward, thanks to which the fish's turning ability increases.

1.14. Torpedo Steady-State Turning Motion in a Horizontal Plane

Turning motion is possible only when a centripetal force acts on the torpedo, a force which generates normal acceleration which changes the direction of the torpedo's motion. A centripetal force can be obtained with various methods.

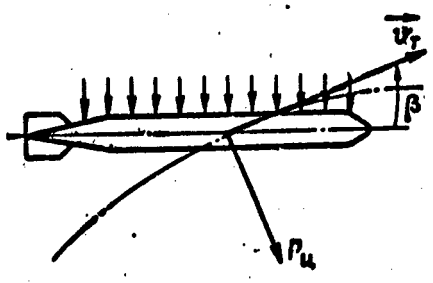

Figure 1.26. Generation of Torpedo Centripetal Force

Some fish species generate centripetal force by bending the forward half of their body in the direction of the turn, while the rear half of the body displaces in a direction opposite to the turn; thus the entire fish is positioned at an angle to the direction of motion.

Centripetal force for a torpedo can be obtained by means of control surface deflection or by heeling. In the former case (Figure 1.26) the torpedo turns to drift angle β, as a consequence of which centripetal force $P_Ц$ is generated. In the latter case centripetal force is the projection of forces G_T and B onto the Z axis, that is, $(G_T-B)\sin\gamma$.

Of all the possible turning motions, steady-state motion in a circle can realistically occur only in horizontal plane XZ.

For a steady turn, from system of equations (1.76) we find

$$V_т = \sqrt{\frac{T}{A_{x_{11}}}}, \qquad (1.82)$$

where

$$A_{x_{11}} = (m + \lambda_{22})\frac{\beta_0}{R_т} + A_x;$$

$$R_т = \frac{\left(A_{myn}R^{\omega}_{z_1} + A_{zn}A^{\omega}_{my_1}\right)V^2_т \cos\gamma}{A_p\left(A_{myn}+A_{zn}C_p\right)V^2_т\delta_в + \left[(G_т-B)A_{myn}-BlA_{zn}\right]\sin\gamma}; \qquad (1.83)$$

$$\beta_0 = \frac{\left(A^{\omega}_{my_1} - R^{\omega}_{z_1}C_p\right)A_pV^2_т\delta_в + \left[(G_т - B)A^{\omega}_{my_1} + BlA^{\omega}_{z_1}\right]\sin\gamma}{\left(A_{zn}A^{\omega}_{my_1} + A_{myn}A^{\omega}_{z_1}\right)V^2_т}. \qquad (1.84)$$

$\delta_в$ is positive when the rudder deflects to port, while heeling angle γ is positive with a heel to starboard.

Analyzing the relationship between a torpedo's turning radius on the one hand and velocity and heeling angle on the other, we see from formula (1.84) that an increase in torpedo velocity leads to a decrease in R_T. This is true only in the absence of elastic deformations of the rudder control rods. In actuality the rods possess elastic deformations, which in turn are determined by torpedo velocity. The character of this relationship is in the form

$$\delta_в = \frac{\delta_0}{1 + K_д A_p V^2_т}. \qquad (1.85)$$

where δ_0 — angle of deflection without load on control surfaces; $K_Д$ — coefficient characterizing rudder control rod elastic deformations.

CHAPTER 2. DESTRUCTIVE EFFECT OF TORPEDOES

2.1. Warheads

Warheads comprise the nose section of a torpedo (Figure 2.1.) and contain explosive charge 1 and detonating devices 3-4 [2.6].

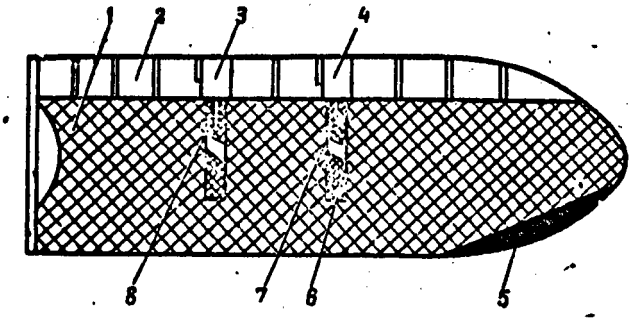

Figure 2.1. Warhead

Torpedo warheads also frequently contain homing system receiver-amplifier devices and influence firing mechanism sensing devices.

The warhead is in the form of a cylinder with a tapered nose of ogival shape.

The warhead cavity can be either completely or partially filled. With partial filling air box-displacer 2 is placed at the top of the cavity, which lowers the warhead's center of gravity. With complete filling (and with partial filling as well), the warhead's center of gravity is lowered with lead weights placed at location 5.

Complex high explosives are employed as charge in the warhead. They comprise mixtures of individual (pure) TNT-base explosives. Compounds of TNT with hexogen are the most common.

	1 Тип ВВ	2 Состав ВВ или формула	3 Плотность ρ, $кг/м^3$	4 Скорость детонации D, $м/сек$	5 Тротиловый эквивалент для 1 кг ВВ, K	6 Чувствительность к удару, $кгс/м^2 \times 10^{-4}$	7 Восприимчивость к детонации или инициирующая способность
8 Чистые бризантные ВВ	10 Тротил	$C_6H_2(NO_2)CH_3$	1600	7000	1,0	3—4	19 Удовлетворительная
	Тетрил 11	$C_6H(NO_2)_3N(NO_2)CH_3$	1630	7500	1,1	1,6	20 Выше, чем у тротила
	Гексоген 12	$C_3H_6O_6N_6$	1600	8100	1,3	1,3	21 Выше, чем у тетрила
	ТЭН 13	$C(CH_2ONO_2)_4$	1600	7900	1,4	0,8	22 Выше, чем у гексогена
9 Инициирующие ВВ	14 Гремучая ртуть	$Hg(ONC)_2$	4000	5050	0,41	0,08	19 Удовлетворительная
	Азид свинца 15	$Pb(N_3)_2$	4000	5100	0,39	0,12	Высокая 23
	Тенерес 16	—	2900	5200	0,37	17 18 Очень чувствительны к лучу пламени	Очень низкая 24
	Тетразен 17	$C_2H_6ON_{10}$	1470	5000	0,55		Невысокая 25

Table 2.1. Characteristics of Several Explosives

Key to table: 1 -- type of explosive; 2 -- composition of explosive or formula; 3 -- density ρ, kg/m^3; 4 -- rate of detonation D, m/sec; 5 -- TNT equivalent for 1 kg of explosive, K; 6 -- sensitivity to impact, $kg/m^2 \times 10^{-4}$; 7 -- susceptibility to detonation or initiation capability; 8 -- pure high explosives; 9 -- initiators; 10 -- TNT; 11 -- Tetryl; 12 -- hexogen; 13 -- TEN; 14 -- Mercury fulminate; 15 -- lead azide; 16 -- (Teneres); 17 -- tetrazene; 18 -- very sensitive to flame; 19 -- satisfactory; 20 -- greater than TNT; 21 -- greater than Tetryl; 22 -- greater than hexogen; 23 -- high; 24 -- very low; 25 -- low

Retarders are added to explosives to reduce sensitivity and at the same time to improve pressability. A retarder reduces friction between particles of explosive and fills in uneven spots and cracks in the particles, which improves the plasticity of the charge as a whole. In addition, a retarder absorbs part of energy of external origin, reduces local stress concentrations and also hinders the spread of detonation to the entire charge from point detonation foci.

Metal powders are added to explosives to increase their effectiveness. This enhances their blast effect.

In order to increase the density and consequently the weight of an explosive, it is poured into the warhead section of a torpedo in molten form. The warhead compartment should be rigged in such a manner as totally to eliminate explosive charge displacement.

For safety of warhead handling, detonation of the explosive charge in a live-fire operation is effected by stages.

The primary detonator (7 and 8), consisting of a friction primer and a detonator, contains highly-sensitive (fulminating) explosives, such as fulminate of mercury, lead azide, [teneres] and tetrazene, which explode from a light impact or slight heating. Types of explosives and their characteristics are contained in Table 2.1 [2.3].

To reduce the danger of explosion on board ship, a small quantity of explosive, insufficient to detonate the main charge, is placed in the primary detonator.

The primary detonator is placed in detonator intrusion tube 6, the secondary detonator, which contains an explosive which is less sensitive to impact, such as Tetryl, in an amount weighing 600-800 g. This amount of Tetryl is sufficient to detonate the main charge. Tetryl is placed in the detonator intrusion tube in the form of pressed charges.

The safest igniter devices are those in which a primary detonator is forced home into a secondary detonator after the torpedo is launched.

The weight of the secondary detonators, their quantity (there are usually two) and placement in the warhead compartment should ensure complete warhead detonation when the torpedo strikes the target.

Detonation of the primary detonator is effected with contact or influence fuzes [2.1].

2.2. Conditional Law of Target Damage

Before every torpedo firing exercise a mission is assigned to inflict certain damage on the enemy. This may involve disabling or destroying an enemy ship. A torpedo attack may result either in accomplishment of the assigned mission or failure to accomplish the mission. The success of the attacking ship can be estimated by probability of target damage or destruction. If n torpedoes are fired at the target, and m torpedoes hit the target, the probability that these torpedoes will hit the target will be $P_{m,n}$. Torpedoes, upon impacting with the target, will explode and inflict certain damage.

The probability of damage being inflicted on an enemy ship under the condition that it is struck by m torpedoes will be $G(m)$. This probability is conditional. Then the overall probability of target damage or destruction will be [2.4]

$$W(n) = \sum_{m=0}^{n} P_{m,n} G(m). \qquad (2.1)$$

Hit probability $P_{m,n}$ is determined by a great many factors investigated in gunnery theory, but it is not determined by the destructive effect of the torpedoes. Conditional probability G(m) is determined only by the destructive effect of the torpedoes and therefore constitutes a numerical characteristic of this damage or destructive effect. The relationship between probability of target damage or destruction G(m) on the one hand and number of hits m on the other is called the conditional law of damage or simply the law of target damage. This law is a two-way characteristic, that is, a characteristic of torpedo destructive force and target survivability.

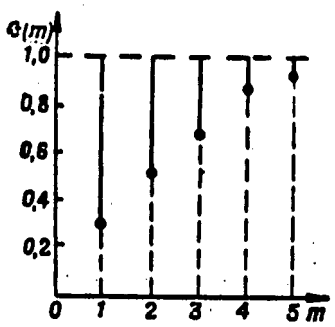

Figure 2.2. Conditional Law of Target Damage

If one hit is sufficient to damage or destroy a target, the law of damage is designated as 1 — G(1)=1. Only in this case are a target hit and target destruction equivalent events.

The law of target destruction possesses the following general properties:

as any probability, G(m) can assume values $0 < G(m) < 1$;

in the absence of a hit, the target is not damaged or destroyed, that is G(0)=0;

with a large number of hits, target damage or destruction always occurs, that is, $\lim_{m \to \infty} G(m)=1$;

the law constitutes a nondecreasing function of its argument, that is, $G(m+1) \geq G(m)$. This is quite understandable, since an increase in the number of hits does not offer the target ship additional possibilities of remaining undamaged.

Ovbiously only those torpedoes which destroy targets with a comparatively small number of hits m, if not when m=1, should be accepted into the navy's arsenal.

Since function G(m) makes sense only for whole values of m, graphically it should be represented in the form of discrete points with nondecreasing ordinates (Figure 2.2). However, for convenience, which is usually revealed when placing on one and the same diagram representations of several laws of damage, points G(m) are joined by a smooth curve (Figure 2.3).

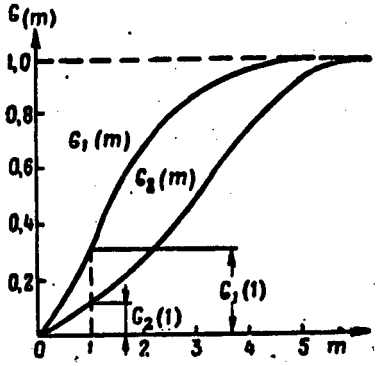

Figure 2.3. Comparison of Two Laws of Effective Target Hit

Since all the points on curve $G_1(m)$ lie above curve $G_2(m)$, with action against one and the same target a more powerful torpedo warhead corresponds to the first curve, while with torpedoes of equal destructive power employed against different targets, the poorer-survivability target corresponds to the first curve.

In computations one frequently employs the law of target destruction in the form of an exponential function

$$G(m)=1-e^{-\alpha m}, \qquad (2.2)$$

where

$$\alpha=-\ln[1-G(1)]. \qquad (2.3)$$

Coefficient α is determined by the weight and type of explosive, by the conditions of detonation (contact or influence, at what depth, at what location under the ship, etc) and target survivability. This relation is of a diversified character. Therefore the law of target destruction cannot always be defined with acceptable precision. As a consequence of this the first numerical characteristic of this law is employed in practice -- the mathematical expectation of the number of hits required for target destruction ω:

$$\omega = \sum_{m=0}^{\infty} [1 - G(m)]. \qquad (2.4)$$

It is evident from this that quantity ω is determined from the graph G(m) as the sum of segments complementing the ordinates of the law of destruction to 1 (Figure 2.2).

For the exponential law

$$1 - G(m) = [1 - G(1)]^m.$$

Then

$$\omega = \sum_{m=1}^{\infty} [1 - G(1)]^m = \frac{1}{G(1)}.$$

Hence

$$G(1) = \frac{1}{\omega}, \qquad (2.5)$$

while the exponential law formula can be written in the form

$$G(m) = 1 - \left(1 - \frac{1}{\omega}\right)^m. \qquad (2.6)$$

Table 2.2 [2.5] contains the approximate average number of torpedo hits ω* to inflict specific types of damage on target ships (based on the experience of World War II).

№ пор.	9 Класс корабля	10 Водоизмещение стандартное, т	Количество торпедных попаданий ω*, необходимых 11	
			для потопления 12	для вывода из строя 13
1	Легкий АВ (авиатранспорт)	7000—8000	1	—
2	АВ	До 30 000 14	2—3	1
3	Тяжелый АВ	До 60 000 14	6	1
4	ЛК постройки периода первой мировой войны	25 000—30 000	2—3	1—2
5	Малый ЛК постройки периода второй мировой войны	30 000—35 000	4—6	3—4
6	Крупный ЛК постройки периода второй мировой войны	45 000—60 000	8—10	4—6
7	КР		2—3	1—2
8	ЭМ		1 в районе миделя 15	1 в районах носа и кормы 16

Table 2.2. Number of Torpedo Hits ω* Required to Inflict Effective Damage on Target Ships (Based on the Experience of World War II)

Key to table: 1 — light carrier (aircraft transport ship); 2 — aircraft carrier; 3 — heavy aircraft carrier; 4 — battleship of World War I vintage; 5 — small battleship of World War II vintage; 6 — large battleship of World War II vintage; 7 — cruiser; 8 — destroyer; 9 — type of ship; 10 — standard displacement; 11 — number of torpedo hits ω* required; 12 — to sink; 13 — to disable; 14 — up to; 15 — amidships; 16 — bow and stern

The weight of explosives carried by torpedoes of that period was 300 kg of TNT. With a greater weight of explosives, obviously the number of requisite hits to inflict effective damage on the target will be less. The number of hits will also be less if torpedo detonation is of an influence type.

2.3. Physical Description of an Underwater Explosion

The law of target destruction is determined in large measure by the conditions of detonation of the torpedo warhead. This detonation always takes place under water. An underwater explosion is a complex combination of thermodynamic, gas-dynamic and hydrodynamic processes. It is extremely difficult to examine them separately. Therefore in practice an underwater explosion is characterized by summary parameters.

The parameters of an explosion in an unbounded water medium differ from the parameters of an explosion with the presence of a free surface and bottom.

We shall first examine the physical picture of an explosion in an unbounded liquid.

An explosion constitutes a process of extremely rapid chemical transformation of an explosive. It is accompanied by a practically instantaneous transition by the explosive from solid to gaseous state. A large quantity of heat energy is released thereby.

At the initial moment of an explosion gaseous products occupy the warhead space and possess high pressure and temperature. The blast energy is transmitted to adjacent water layers. A so-called blast wave is formed due to the compressibility of water at high pressures. The forward boundary of the blast wave is called the wave front. The explosion products, expanding, form a gas bubble.

The blast wave front displaces through the water. It leads the spread of gaseous explosion products. As the blast wave propagates, its velocity drops off sharply. Energy density also decreases sharply. Blast wave attenuation occurs. At a considerable distance it transitions to an acoustic wave. The qualitative character of pressure change in the blast wave in time and space is shown in Figure 2.4 [2.7].

The blast wave diagram includes regions of positive and negative pressures -- compression zone (+) and underpressure zone (-). The spatial extent of the compression zone is called blast wavelength λ. It is considerably less than the extent of the underpressure zone. The total time of effect of overpressure is called wave period τ or t_+.

Pressure at wave front $p_m(r)$ is a principal characteristic of a blast wave. The area bounded by the pressure curve and the X axis in the compression zone is called the full pressure impulse at the given point. With increasing

distance from blast center, pressure at the blast wave front gradually decreases and its length somewhat increases. At a very great distance the shock wave transitions to a sound wave.

It has been calculated that the thickness of a blast wave front is approximately equal to the length of a free molecular path (10^{-5}-10^{-6} cm). Therefore mathematically a blast wave front is viewed as a surface of discontinuity.

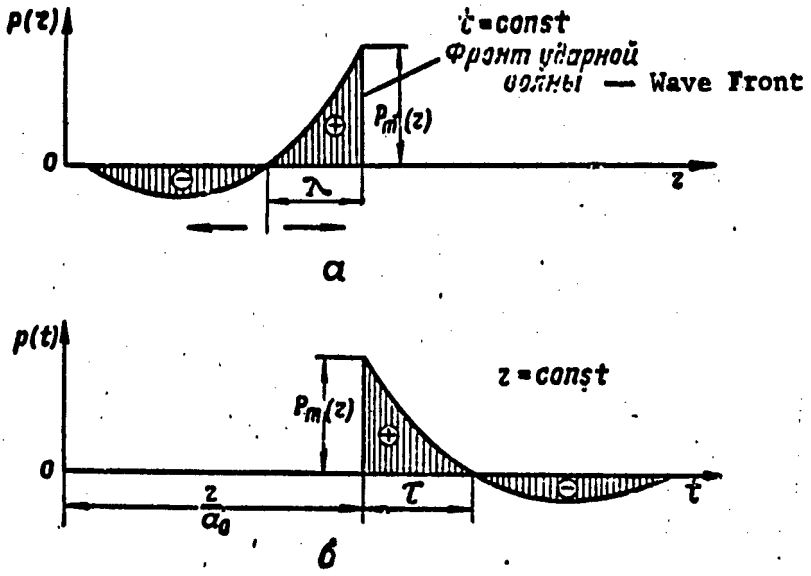

Figure 2.4. Pressure Change in Blast Wave

The generated gas bubble expands. At a certain moment pressure in the bubble becomes equal to ambient pressure. Bubble expansion will continue as a consequence of the water's inertia. Finally reverse motion of the liquid will begin under the influence of forces of hydrostatic pressure, and the bubble will begin to compress. So-called gas bubble pulsations occur. The energy of each succeeding pulsation will differ from the preceding pulsation by the amount of dissipated energy.

It has been established that approximately 59% of stored energy is lost in the first pulsation (bubble expansion and compression), approximately 20% in the second, and approximately 7% in the third. These quantities characterize the energy of the shock waves forming at the beginning of each pulsation.

The effect of an underwater explosion on ships is comprised of the effect of the blast wave and the movement of water masses. The character of action will differ between contact and influence detonations.

With a contact detonation the principal role is played by gas pressure against the target ship's hull plates, which rapidly collapse, and the gases surge into the ship. A small but deep (into the ship's interior) hole is formed. The compartment in which the hole was formed usually fills with water.

With an influence detonation a portion of the blast energy is transformed into the kinetic energy of moving masses of water. A blast wave and water in motion act upon the ship's hull. The overall time of effect of the underwater explosion on the ship increases thereby. The resulting hole is large in area but not always deep (penetration into the ship). It is impossible to plug such a hole. This results in the flooding of several compartments and as a rule threatens the ship with sinking.

Secondary expansion of the gas bubble produces a general "concussion" to the ship's hull. Local vibrations are generated which lead not only to separation of equipment and weapons from their mounts but also to a displacement of the ship's main propulsion machinery, twisting of propeller shafts, etc.

Thus an influence-type underwater explosion in a certain zone in the vicinity of the target ship is considerably more effective than a contact detonation.

The degree of damage inflicted on the target ship will be determined not only by the weight of explosive, its type, and conditions of occurrence of the underwater explosion (contact, influence, place of explosion, etc), but also the ability of the target ship's hull to resist an underwater blast. The latter is determined by its structural features.

2.4. Quantitative Characteristics of the Destructive Effect of an Explosion

The greater the blast pressure and the longer the time of application of this pressure, the greater the destructive effect of torpedoes. The pressure pulse is the quantity which takes both these parameters into account. Its current value for a given point is

$$I(t, r) = \int_0^t p(t, r)\, dt, \qquad (2.7)$$

where p(t, r) is pressure change in the blast wave on a time axis at a given point, which is located at distance r from blast center.

It has been established as a result of a large number of experiments that pressure at the blast wave front in the absence of bottom and free surface influence is determined by the following formula [2.7]:

$$p_m(r) = 533 \cdot 10^4 \left(\frac{\sqrt[3]{q_э}}{r}\right)^{1{,}13} \frac{кгс}{м^2}, \qquad (2.8)$$

where $q_э$ — torpedo warhead TNT equivalent, kg:

$$q_э = Kq, \qquad (2.9)$$

K — TNT equivalent of 1 kg of explosive; q — quantity of explosive, kg; r — distance from blast center, m.

Relation (2.8) for dimensionless distances possesses the form

$$p_m(r) = \frac{14700 \cdot 10^4}{\bar{r}^{1,13}} \frac{\kappa z c}{M^2}, \qquad (2.10)$$

where

$$\bar{r} = \frac{r}{R_{03}}; \qquad (2.11)$$

R_{03} — radius of equivalent charge of spherical shape:

$$R_{03} = 0{,}053 \sqrt[3]{q_0}\ M. \qquad (2.12)$$

To estimate change in blast wave pressure in its acoustic continuation, we employ exponential relation

$$p(t, r) = p_m(r)\, e^{-\frac{1}{\theta}\left(t - \frac{r}{a_0}\right)} \sigma_0\left(t - \frac{r}{a_0}\right), \qquad (2.13)$$

where a_0 — speed of sound in water, equal to approximately 1500 m/sec; θ — pressure drop time constant:

$$\theta = q_0^{0,253} \rho^{0,24} 10^{-4}\ сек; \qquad (2.14)$$

$\sigma_0\left(t - \frac{r}{a_0}\right)$ — unit separation function of zero order, indicating that pressure increases with a sudden jump upon approaching a given point.

$$\sigma_0\left(t - \frac{r}{a_0}\right) = \begin{cases} 0 & \text{when} \quad t < \frac{r}{a_0}, \\ 1 & \text{when} \quad t > \frac{r}{a_0}. \end{cases} \qquad (2.15)$$

With an increase in distance r, pressure drop time constant θ increases, thus taking into account extension of the pressure curve on a time axis as the blast wave moves away from blast center.

In conformity with expression (2.13), the pressure impulse according to formula (2.7) will be

$$I(t, r) = p_m(r)\,\theta\left[1 - e^{-\frac{1}{\theta}\left(t - \frac{r}{a_0}\right)}\right] \sigma_0\left(t - \frac{r}{a_0}\right). \qquad (2.16)$$

In actuality the pressure curve differs from an exponential function.

Pressure curve deformation is usually taken into account by means of approximation of the pressure drop curve with a hyperbolic relation [2.7].

Effective overpressure time

$$\tau \approx \frac{20 R_{03}}{a_0}. \qquad (2.17)$$

A full pressure impulse can be obtained if we substitute $t = \frac{r}{a_0} + \tau$ in expression (2.16).

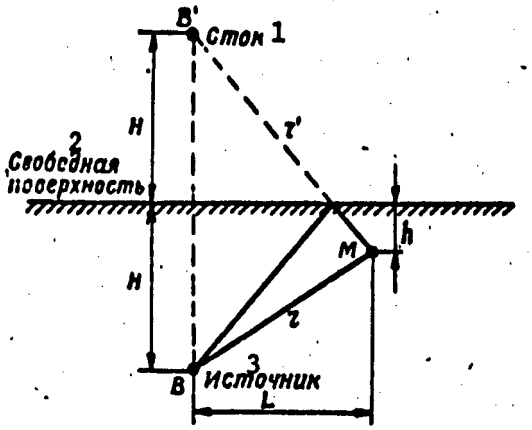

Figure 2.5. Diagram of Mirror Image of Source and Discharge

Key to figure: 1 — discharge; 2 — free surface; 3 — source

Then

$$I_+(r) = p_m(r)\,\theta\left[1 - e^{-\frac{\tau}{\theta}}\right] \approx p_m(r)\,\theta. \qquad (2.18)$$

The above relation applies to the first pulsation of the gas bubble in unbounded water or at great depth. Shock waves also are generated with succeeding pulsations, but their intensity is less. Impulse magnitude is 5-6 times less on the second pulsation than the first, and on the third three times less than on the second.

The free surface exerts considerable influence on the pressure field parameters with explosions at shallow depths. The character of wave reflection from it is determined by the demands that pressure above the interface remain unchanged (atmospheric). As a consequence of this the reflected wave should be a negative pressure wave. This conclusion permits a simple and graphic geometric interpretation called a diagram of mirror-image representation of source B and discharge B' (Figure 2.5).

Pressure at any point M under the free surface is equal to the algebraic sum of pressures in two waves, taking into account difference in amplitude and in arrival time. The resultant pressure remains the same as in the initial wave from the source, right up to arrival of reflected negative pressure at subsequent moments in time. Obviously the tail end of the incident wave will be reflected (Figure 2.6).

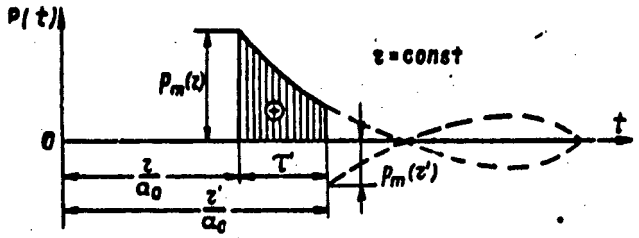

Figure 2.6. Pressure Change in Blast Wave Taking Free Surface Influence into Account

Effective time of the positive pressure phase will be equal to the difference in times of arrival at a given point of the direct and reflected waves:

$$\tau = \frac{1}{a_0}\left[\sqrt{L^2+(H+h)^2}-\sqrt{L^2+(H-h)^2}\right], \qquad (2.19)$$

where L -- difference between blast center and point of pressure measurement on the horizontal; H — charge depth; h — depth of pressure measurement point.

It follows from (2.19) that the effective time of positive pressure in the presence of a free surface in an acoustic approximation is determined only by the blast geometry and is independent of warhead charge weight. In actuality, when an explosion occurs pressure at the wave front proves to be less at the water surface than in an unbounded liquid, while the effective time of its positive phase is greater than that computed in an acoustic approximation. The shape of the pressure-time curve also changes. This occurs because part of the blast energy at shallow depth passes into the air and the rarefaction wave cannot have a discontinuous front.

This theory applies to relative warhead depth , where

$$\bar{H} = \frac{H}{R_{os}} \text{ и } \bar{H}^* = \frac{H^*}{R_{os}} = 1{,}66^{0{,}44}. \qquad (2.20)$$

When $\bar{H}<\bar{H}^*$ it is necessary to take into account the nonlinear effect of influence of a free surface on the pressure field with an underwater explosion.

The greatest full pressure inpulse value is observed with a charge explosion at a specific depth. This depth is called optimal blast depth and comprises

$$\bar{H}_{опт} = \frac{H_{опт}}{R_{os}}. \qquad (2.21)$$

It is obvious that $\bar{H}_{опт} > \bar{H}^*$.

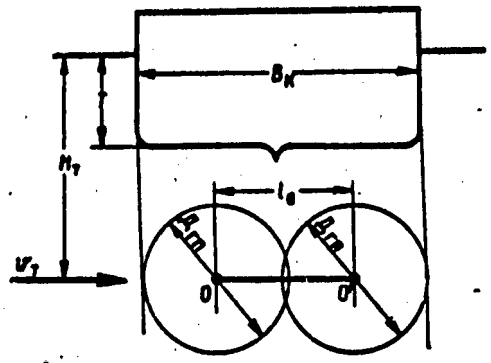

Figure 2.7. Diagram of Position of Gas Bubbles from Underwater Explosion under a Ship

Damage to surface units and submarines in surfaced positions is estimated on the basis of magnitude of pressure pulse per unit of vessel draft

$$\frac{I+(r)}{T} \text{ kg·sec/m}^3$$

for the entire length of the target.

The destructive effect (this can be pierced hole area, number of pierced bulkheads or bottom plates, etc) with a bottom influence underwater blast increases in comparison with the effect with a contact detonation with increasing distance from blast center and possesses a maximum value at a certain distance from the vessel's bottom. This distance is called effective distance $r_{эф}$:

$$r_{эф} \approx K_0 \sqrt[3]{q_э} \text{ м.} \qquad (2.22)$$

Coefficient K_0 depends on the type of ship and the construction of its hull bottom protection. When $r>r_{эф}$ the destructive effect is diminished and at a distance of approximately $2r_{эф}$ corresponds to the effect with a contact detonation. Then the torpedo influence fuze detonation distance $d_{нв}$ (proceeding from destructive effect) should be

$$d_{нв} < 2r_{эф} \qquad (2.23)$$

Tests have established that the maximum value of full pressure impulse with detonation under the target ship is obtained when the gas bubble does not go beyond a projection of the ship's hull onto a horizontal plane (Figure 2.7).

The diameter of the gas bubble can be determined from the following formula:

$$D_{гп} = \frac{60R_{оз}}{\sqrt{1+0{,}1H_т}}. \qquad (2.24)$$

Consequently the optimal torpedo detonation point should be a segment of its trajectory under the target ship $\overline{OO'} = l_B$:

$$l_B = B_K - D_{TH}. \qquad (2.25)$$

It may be, however, that $l_B < 0$. Therefore the following detonation localization requirement is imposed on the influence fuze: it is considered satisfactory when an influence fuze actuates and detonates the torpedo at any point under a target ship's hull.

CHAPTER 3. TORPEDO PROXIMITY FUZES

3.1. General Principles

Proximity fuzes are automatic devices that are tripped and detonate the charge in a torpedo's warhead when the torpedo passes near the target ship but does not touch its hull.

Torpedo proximity fuzes are classified, according to their operating principle, as electromagnetic, magnetic, acoustical, and so on; that is, they are classified according to the physical field that, when distrubed, triggers them.

Electromagnetic and magnetic proximity fuzes have been used in torpedoes by almost every navy in the world, and were used during World War II. The possibility of using acoustical and other types of proximity fuzes has been repeatedly pointed out in the literature [2.1] and confirmed by patents issued in the United States and Germany.

According to the location of the physical field's source, proximity fuzes are subdivided into two types: passive and active. If the field is created by the target ship, then the proximity fuze that reacts to it is called passive. If the source is located in the torpedo, however, the proximity fuze that reactions to the distortion of this field by the target ship is called active.

The main characteristic of a proximity fuze is its triggering distance; that is, the maximum distance from the ship at which the fuze operates reliably. In connection with this, it is assumed that at all distances less than the maximum, the proximity fuze's triggering action is also flawless. For the proximity fuzes of torpedoes used against the surface ships, this distance is computed along the normal to the bottom of the ship and is called the vertical triggering distance (d_{pf})

As is the case with any other part in a torpedo, there are certain requirements for proximity fuzes. For each specific fuze, they take into consideration its operating characteristics and combat application and utilization [3.4].

These requirements include ease of operation, simple design, cheapness and simplicity of the manufacturing process, the use of materials that are not scarce, and so forth.

The diversity and complexity of the requirements that the fuzes must satisfy has led to a situation where modern torpedo proximity fuzes are quite complex automatic devices containing mechanical, electrical, and electronic instruments and assemblies.

3.2. The Triggering Distance of Fuzes

Where surface ships are concerned, the conditional probability of destruction G(m) is increased when the torpedo is detonated on a proximity basis. When contact detonation is involved, that same probability can be attained by increasing the amount of explosive. Torpedoes equipped with proximity fuzes carry less explosive for this very reason, but in connection with this the following fact must be taken into consideration.

In order to prevent torpedoes from running on the surface and deviating from their course because of the sea swell, they are set to run at a certain depth. This is especially necessary when they are equipped with acoustical homing systems, since it reduces interference by a great deal. However, increasing the running depth leads to a situation where torpedoes can pass underneath the target ships without striking them; that is, the probability of the torpedo's hitting its target ($P_{m,n}$) is reduced.

Hit probability $P_{m,n}$ is determined by the hit probabilities in the horizontal and vertical planes and is equal to their product, since the torpedo's movements in these planes are independent of each other.

For a single torpedo,

$$P_{1,1} = P_h P_v. \qquad (3.1)$$

where P_h=torpedo hit probability in the horizontal plane;
P_v=torpedo hit probability in the vertical plane.

P_h depends on a multitude of factors, which are discussed in firing theory, but is independent of the dispersion of the torpedo's running depth and the target ship's draft.

P_v depends only on the torpedo's and target ship's dispersions with respect to depth. A proximity fuze helps to increase this probability.

Torpedo and target location depth dispersions are caused by a larger number of cumulative effects that are almost independent of each other and are quite small in comparison with the final result. Research has shown that this type of dispersion is governed by the normal distribution law.

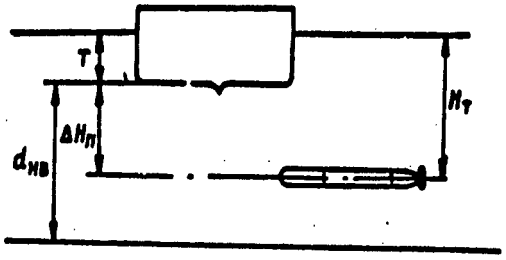

Figure 3.1. Diagram of the passage of a torpedo under a target ship.

Using Figure 3.1, we can write

$$d_{нв} = 5{,}4E_{тс} + \Delta H_n, \qquad (3.2)$$

where E_{ts}=total mean depth deviation of the torpedo and the target ship; H_p=minimum difference between the specified torpedo running depth H_t and the ship's draft T.

Distance H_p is regulated by the instruction for the use of torpedoes:

$$E_{тс} = \sqrt{E_т^2 + E_к^2}, \qquad (3.3)$$

where E_t=mean deviation of the torpedo with respect to depth; E_s=mean deviation of the target ship's draft;

$$E_т = \sqrt{E_{т_1}^2 + E_{т_2}^2}, \qquad (3.4)$$

where E_{t1}=mean deviation of the torpedo's true running depth from its average value H_t; E_{t2}=mean deviation of the torpedo average running depth from the specified depth H_t.

3.3 Electromagnetic Proximity Fuzes

Operating Principle

Electromagnetic fuzes are active fuzes. The fuze's radiating unit I (Figure 3.2), which is a solenoid in the afterbody that is either coaxial with the torpedo's axial line or tilted at a slight angle to it, creates an electromagnetic field around the torpedo. The solenoid's winding is powered by alternating current at a given frequency (the

operating frequency). The torpedo's variable field is sensed by one or two (identical) receiving coils C, which are located in its nose.

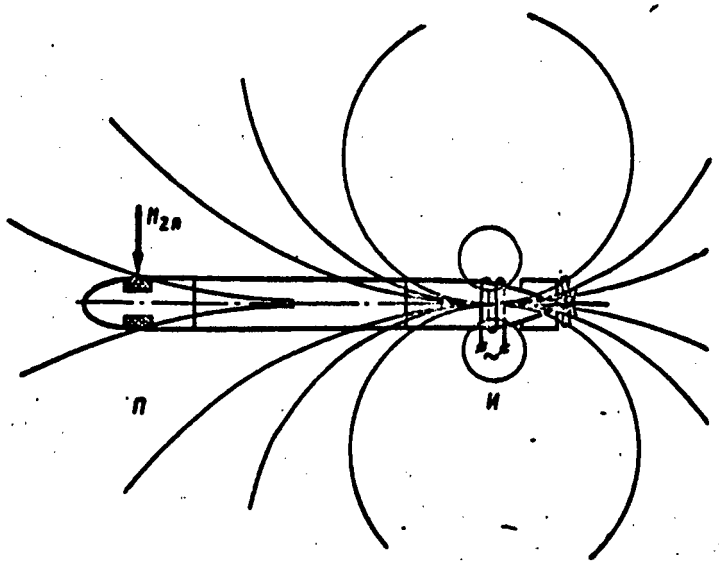

Figure 3.2. Magnetic field of an electromagnetic fuze.

The radiating unit and the receiving coils are situated in such a fashion that the electrical link between them is minimal, while the residual electromotive force that is induced in the receiving coils (the electromotive force of disbalance) is neutralized by compensating voltage that is formed in the fuze's circuitry.

When the torpedo passes under the target ship, eddy currents arise in the latter's hull. They create a reflected variable electromagnetic field, in which the magnetic component's vertical component H_{zp} creates an electromotive force in the receiving coils. This force is also the operating (or effective) signal that triggers the fuze under the ship [3.1].

Propagation of the Electromagnetic Field in Sea Water

The propagation of electromagnetic oscillations in sea water takes place at a certain velocity, although in a limited spatial area in close proximity to the radiator and for a comparatively slowly changing field; the propagation time can be ignored.

At any moment of time, the magnetic field of the radiator's alternating current will have the same value it would have in the presence of direct current equal to the instantaneous value of the alternating current. This condition is called the quasi-stability condition. It is effective at distances not exceeding one-tenth the length of an electromagnetic wave in the given medium ($r \leq 0.1\lambda$)[3.5]. The wavelength of the electromagnetic

oscillations used in torpedo proximity fuzes are numbered in the tenths and hundredths of meters. From this, it follows that the magnetic field of a proximity fuze's radiator is equivalent to a permanent magnet's field.

When compared with a ship's hull, a radiating coil's dimensions are extremely small. Therefore, a radiator's actual dimensions are usually ignored.

It has been established that, at distances of 1.5 m and more, a proximity fuze's radiator can be regarded as a dipole (since the change in its field with respect to distance also takes place according to a cube law, as is the case with a dipole).

Assuming a proximity fuze's radiator to be a magnetic dipole with moment M (Figure 3.3), which is changing according to a harmonic law, we obtain the well-known expressions for the radial and tangential components of the intensity of this dipole's magnetic field in polar coordinates [3.6,3.7]:

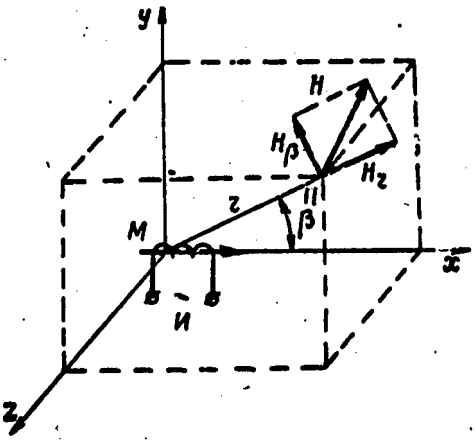

Figure 3.3. Toward a determination of the components of an electromagnetic field in sea water.

$$\left.\begin{aligned} \dot{H}_r &= \frac{2M\cos\beta}{r^3}\, e^{-r^*(1+j)}\,[1 + r^* + jr^*]; \\ \dot{H}_\beta &= \frac{M\sin\beta}{r^3}\, e^{-r^*(1+j)}\,[1 + r^* + jr^*(1 + 2r^*)], \end{aligned}\right\}^* \qquad (3.5)$$

where r* is called the numerical distance. This is a slightly reduced value that characterizes not only the true distance, but also the properties of the medium:

*H given in terms of a/m, where $1(a/m)=4\pi 10^{-3}$ oe; B given in terms of am^2, where $1am^2=4\pi 10^3$ oe·cm^3.

$$r^* = r\sqrt{\frac{\mu_a \sigma \omega_p}{2}}. \qquad (3.6)$$

where μ_a=absolute magnetic permeability of water: $\mu_a=\mu_0=4\pi 10^{-7}$ h/m; σ=electrical conductivity of sea water: σ=1-5(1/ohm·m); ω_p=frequency of the field.

One specific feature of the operating conditions of proximity fuzes is their relatively small operating distance. For such a distance in air, the damping is no more than 1 percent; consequently,

$$\left.\begin{aligned} H_r &\approx \frac{2M\cos\beta}{r^3}, \\ H_\beta &\approx \frac{M\sin\beta}{r^3}. \end{aligned}\right\} \qquad (3.7)$$

From a comparison of (3.5) and (3.7), it is obvious that electromagnetic oscillations in sea water are subject to damping and phase shifts. As the field's frequency increases, so do the intensities of the damping and phase shifts.

Reflection of the Electromagnetic Field From a Ship's Hull

As the torpedo passes under a ship, the field intensity at the point where the proximity fuze's receiving coils are located changes to the intensity of the field reflected from the target's hull.

In order to calculate the reflected field, let us replace the ship's hull with an infinite, conducting plane.

The actual outlines of the ship's hull and the effect of the medium on the performance of a proximity fuze are accounted for by empirical coefficients. In this case, as the torpedo passes under the ship, the effective signal in the proximity fuze will change according to the following rule:

$$H_{zp}(l) = H_{z\delta p} K_z K_k(l), \qquad (3.8)$$

where $H_{zp}(1)$=effective signal (it is sometimes called the receiving effect or the ship's longitudinal characteristics with respect to the torpedo's direction of movement); $H_{z\delta p}$=vertical component of the intensity of the fuze's magnetic field, as reflected from the conducting infinite plane; K_z=damping factor of the field's vertical component $H_{z\delta p}$; $K_k(1)$=coefficient allowing for the width of the ship and the shape of its outlines with respect to the torpedo's direction of movement.

In order to determine the amount of electromagnetic energy reflected by the infinite plane, we use the geometry of the radiator's and receiver's positions, as shown in Figure 3.4. The distance between the radiator and the receiver (2) is called the fuze base.

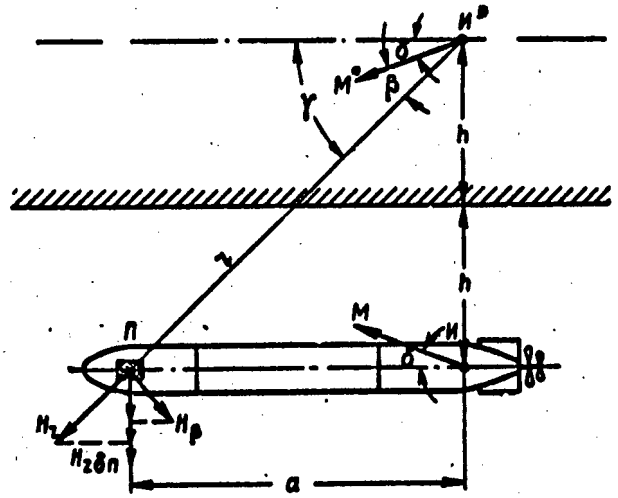

Figure 3.4. Diagram for calculating the electromagnetic field reflected by the infinite conducting plane.

Since the electromagnetic field is reflected by a conducting plane, this indicates the absence of a normal component of field intensity at the water-plane is replaced by an equivalent magnetic dipole M* that is a mirror image of dipole M, such that M*=M. Thus, the calculation of the additional field at point C that is created by the infinite conducting plane reduces to defining the field of dipole M*.

Without allowing for damping and phase shift,

$$H_{z\delta n} = H_r \cos\gamma + H_\beta \sin\gamma. \tag{3.9}$$

From the figure, it is obvious that

$$\left.\begin{aligned} \sin\gamma &= \frac{2h}{r};\ r = \sqrt{a^2 + 4h^2};\\ \cos\gamma &= \frac{a}{r};\ \gamma = \beta + \delta. \end{aligned}\right\} \tag{3.10}$$

Substituting (3.7) and (3.10) into (3.9), we obtain

$$H_{z\delta n} = \frac{M}{\sqrt{(a^2 + 4h^2)^5}}\,[6ah\cos\delta + (8h^2 - a^2)\sin\delta]. \tag{3.11}$$

When the proximity fuze's radiator is situated coaxially, $\delta=0$.

It is then the case that

$$H_{z\delta n} = \frac{6Mah}{\sqrt{(a^2 + 4h^2)^5}}. \tag{3.12}$$

A study of formula (3.12) at the extremum shows that when a is constant, the maximum signal is obtained from the infinite plane when h=½a, while when h is constant, it is obtained when a=h.

This means that the signal in the proximity fuze when the torpedo is passing under a ship at distance h will be maximal when the fuze base equals this distance.

The damping of the variable electromagnetic field in sea water is described by the damping factor K_z, which is the ratio of the field intensity in water to the intensity of the field in air (or a vacuum) for the same coordinate points.

When the radiator is situated coaxially, the damping factor K_z and the phase shift ϕ_z for $H_z\delta_p$ can be derived by substituting (3.5) into (3.9) and dividing the result by (3.12):

$$K_z = e^{-r^*}\sqrt{1 + 2r^* + 2r^{*2} + \frac{4}{3}r^{*3} + \frac{4}{9}r^{*4}}; \qquad (3.13)$$

$$\varphi_z = -r^* + \operatorname{arc\,tg}\frac{r^*}{1 + r^*}\left(1 + \frac{2}{3}r^*\right). \qquad (3.14)$$

Coefficient $K_k(l)$ is essentially the ship's normalized longitudinal characteristic, since at K_z=1.0,

$$K_k(l) = \frac{H_{zp}(l)}{H_{z\delta n}}. \qquad (3.15)$$

$K_k(l)$ is a function of the ship's width and outlines and the torpedo's angle of impact θ with the target, and is practically independent of the distance at which the torpedo passes under the ship. Table 3.1 shows the values of $K_k(l)$ for B_k=8-9 m and θ=90°.

l м	10	8	6	4	2	0	−2
$K_k(l)$	0,03	0,06	0,13	0,28	0,62	0,79	0,87
l м	−4	−6	−8	−10	−12	−14	
$K_k(l)$	0,68	0,47	0,32	0,20	0,11	0,01	

Table 3.1. Some Values of a Ship's Normalized Longitudinal Characteristic $K_k(l)$

The general form of the change in $K_k(l)$ is shown in Figure 3.5. If a transition from l to t is made in formula (3.8) (since $l=V_T t$), then $H_{zp}(t)$ will be the ship's perturbing function or -- as it is frequently called -- its passage characteristic.

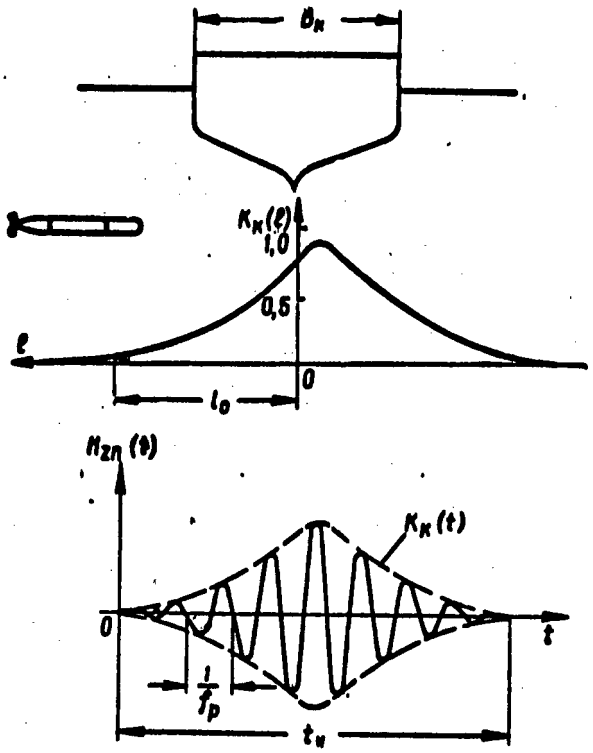

Figure 3.5. Normalized longitudinal and passage characteristics of a target ship.

When the change in the proximity fuze radiator's magnetic moment is governed by a harmonic law, the expression for the passage characteristic will have the form

$$H_{zn}(t) = H_{znm}(t)\sin(\omega_p t + \varphi_z), \tag{3.16}$$

where

$$H_{znm}(t) = H_{z0n}K_z K_к(t). \tag{3.17}$$

This is the field amplitude change law.

The form of the effective signal under the ship is also shown in Figure 3.5.

Here, l_0 is the initial distance reading.

It is then the case that

$$t = \frac{l_0 - l}{V_\tau}.$$

For an approximate description of the effective signal's envelope, we can use the formula (from [3.1])

$$K_x(t) = \beta e^{-\alpha |V_\tau (t - t_0)|^n},$$

where α and β=coefficients depending on the conditions of the torpedo's impact with the target;

$$t_0 = \frac{l_0}{V_\tau}.$$

Reflection of the Electromagnetic Field by the Water's Surface

The process by which the electromagnetic field is reflected from the water's surface, which is caused primarily by the difference in conductivity of the two mediums (air and water), has a rather complex physical nature.

A comparison of the intensities of fields reflected from the ocean's free surface and from a conducting plane shows that in salt water, the intensity at the sea surface itself reaches a value that is commensurate with the fuze's triggering parameter. The phase of a field that is reflected from the water's surface differs considerably from the phase of a signal under the conducting plane.

In order to eliminate self-triggering of the proximity fuze when the torpedo approaches the water's surface or jumps out of the water, phase discrimination is built into it.

3.4. Block Diagram and Characteristics of Fuzes

Figure 3.6 is a typical proximity fuze block diagram without power sources and safety devices.

The effective signal, which is caused by the distortion of the fuze's natural field by the ship's hull $H_{zp}(t)$, is sensed by receiving coil C. The receiving coil, together with the parallel-connected condenser C_k, forms an input (or receiving) circuit. Resistor R_k, into which compensating voltage U_k is fed, is connected in series with the coil. This voltage is introduced into the circuit in order to balance the so-called electromotive force of disbalance. Voltage U_k has the same frequency and amplitude as the electromotive force of disbalance, but its phase is reversed.

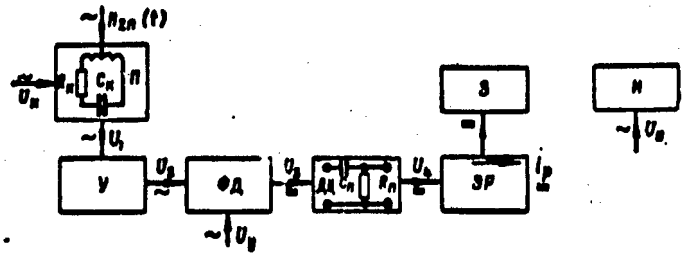

Figure 3.6. Block diagram of an electromagnetic fuze: I=radiator (generating coil); C=receiver (receiving coil); Y=voltage amplifier; PD=phase discriminator; DC=differentiating circuit; ER=electronic relay; Z=ignition device.

In order to regulate the phase and amount of voltage U_k, the proximity fuze's circuitry has a compensating device in the form of a phase-shifting bridge.

Voltage U_1 forms at the receiving circuit's output and enters the voltage amplifier, where it is boosted to U_2.

Alternating voltage U_2 is sent to the input of phase (or balancing) discriminator PD.

The discriminator's circuitry has the feature that at its output, voltage U_3 depends on the phase of U_2. The phase reading is taken with respect to the phase of some controlling voltage U_y, which is introduced into the discriminator's circuitry and is rigidly related to the phase of the current in radiator I.

Rectified voltage U_3 is sent to differentiating circuit DC, which consists of a separating (or transitional) capacitor C_t and a resistor R_t.

The purpose of the differentiating circuit is as follows. Under actual conditions — even when the proximity fuze is very carefully equalized (or balanced) — some electromotive force of disbalance is present. This disbalance leads to the appearance of a direct voltage at the phase discriminator's output, the amount of which may be sufficient to trigger electronic relay ER. Because of the inclusion of the transitional capacitor in the circuit, the direct disbalance voltage does not reach the relay's input.

When the torpedo passes under a ship at a relatively high speed, the effective signal $H_{zp}(t)$ leads to the abrupt appearance at the phase discriminator's output of voltage U_3, under the effect of which capacitor C_t begins to charge. The charging current passes through resistor R_t and causes a voltage drop U_4 in it. Voltage U_4, which is the electronic relay's input voltage, causes it to be triggered.

The electronic relay is a direct current amplifier, the anode circuit of which contains electromagnetic relays.

When the relay's contacts close, a direct voltage is sent from current i_p to ignition device Z that causes the warhead to detonate.

The electronic relay serves as the proximity fuze's actuating device.

If the torpedo's relative velocity when it encounters the target is low, then capacitor C_t will be charged more slowly (in comparison with the discharge through resistor R_t and the phase discriminator) and the relay will not be triggered. The minimum relative velocity at which electromagnetic proximity fuzes are triggered is a total of several subvelocities.

The proximity fuze triggering area is determined by the amount of time it takes a signal to pass through its circuitry. If this period is short or the torpedo runs slowly, then a special delay circuit is added to actuating device ER in order to increase the fuze's total triggering time.

Proximity fuzes have frequency, amplitude, phase, and time characteristics.

The fuze's frequency characteristic is frequently taken to mean the amplifier's frequency characteristic.

The amplifier's frequency characteristic is the dependence of the amplitude of output voltage U_{2m} on the frequency (f) of input voltage U_1 when the latter's amplitude is constant:

$$U_{2m} = F(f) \text{ при}$$
$$U_{1m} = \text{const.}$$

The general form of this characteristic is shown in Figure 3.7.

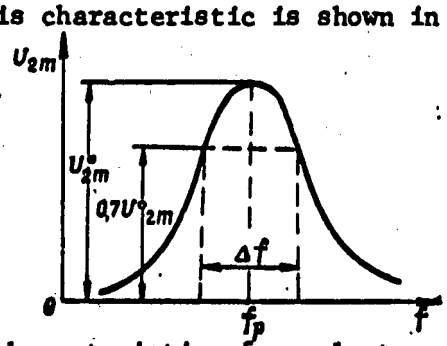

Figure 3.7. Frequency characteristic of an electromagnetic fuze.

The amplifier's resonance tuning frequency f_t, at which the value of U_{2m} is maximal, is close to the proximity fuze's operating frequency ($f_t \approx f_p$).

The amplifier's transmission band (Δf) corresponds to amplifier Y's output voltages, which are 0.7 times their maximum values U_{2m}. The narrower the

transmission band, the better the proximity fuze's frequency selectivity, but the longer must be the effective signal that is capable of triggering the fuze.

The amplitude characteristic (Figure 3.8) determines the voltage amplifier's amplifying properties. It is a function of the dependence of the amplitude of output voltage U_{2m} on the amplitude of input voltage U_{1m}, which changes with the operating frequency:

$$U_{2m} = F(U_{1m}) \text{ when } f = f_p = \text{const}.$$

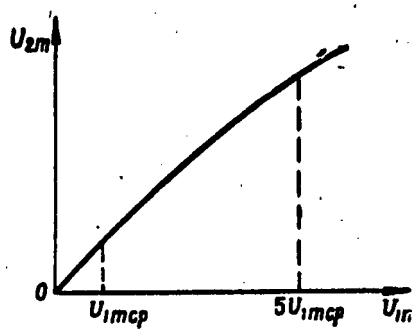

Figure 3.8. Amplitude characteristic of an electromagnetic fuze.

For electromagnetic fuzes, the amplitude characteristic is linear (for all practical purposes) within the limits of the change in input voltage U_{1m} up to a value equaling five triggering parameters.

The phase characteristic (Figure 3.9) is the dependence of voltage U_3 (at the phase discriminator's output) on the phase of the working frequency's variable input voltage U_1:

$$U_3 = F(\varphi) \text{ when } f = f_p = \text{const};$$
$$U_{1m} = \text{const}.$$

The input voltage phase at which phase discriminator's positive output voltage will be maximal is called the optimal phase (ϕ_{opt}).

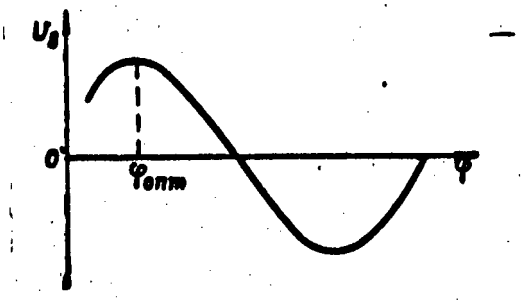

Figure 3.9. Phase characteristic of an electromagnetic fuze.

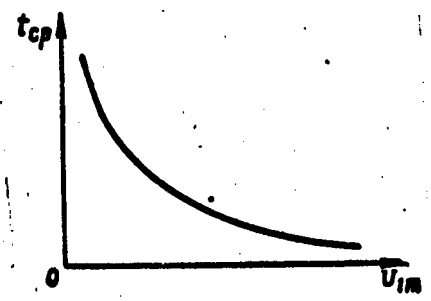

Figure 3.10. Time characteristic of an electromagnetic fuze.

The time characteristic (Figure 3.10) establishes the dependence of the fuze's triggering time on the amount of voltage at the input that is transmitted after being boosted in the optimum phase and at the operating frequency. It shows that the larger the input signal, the shorter the fuze's triggering time:

$$t_{ср} = F(U_{1m}) \quad \underset{\text{when}}{\text{при}} \quad f = f_р = \text{const};$$
$$\varphi = \varphi_{опт}.$$

3.5. Fuze Radiating and Receiving Devices

According to the relative positions of the radiator and receiver, all electromagnetic proximity fuzes are divided into two groups: those with mutually perpendicular, and those with coaxial positioning of these units.

A comparison of various alternatives for the positioning of the radiator and receiver shows that the expected maximum effective signal values for these variants differ by no more than 100-150 percent. This difference has an insignificant effect on changing the triggering distance. When selecting the radiating and receiving system, therefore, special attention is given to the question of what direct effect the field of a radiator in a free medium has on the receiver.

When the radiator and receiver are mutually perpendicular, theoretically the radiator's primary field does not induce an electromotive force in the receiver. Practically, the result of inaccuracy in the relative positioning of the two induces in the receiver some electromotive force. The proximity fuze is balanced in order to compensate for this.

The maximum link between the radiator and the receiver occurs in coaxial systems. Any change in the primary field can result in interference.

In order to reduce the primary field's effect on the receiver, the latter should be located in an area where the absolute value of the primary field's complexor voltage component, as taken in by the receiver, will be minimal; that is, it is necessary to place the receiver as far away from the radiator as possible. For structural considerations, it is possible to place the receiver at a distance from the radiator equal to the length of the torpedo only when they are mutually perpendicular to each other. When they are located coaxially, the distance between them can be no more than the torpedo's diameter.

Radiators

Two types of radiators are used in electromagnetic proximity fuzes: ring and rod.

A ring-type radiator is a coil that is made of relatively thick wire wound around the afterbody. The coil's core is the body of the torpedo itself.

This coil's ampere-turns must be

$$I_{\text{и}} W_{\text{и}} = \frac{4\pi M}{\mu_{\text{и}} S_{\text{и}}}, \tag{3.18}$$

where $I_{\text{и}}$=current in the radiator; $W_{\text{и}}$=number of turns in the radiator's coil; $\mu_{\text{и}}$=reduced magnetic permeability of the torpedo body's casing ($\mu_{\text{и}}$=2-3); $S_{\text{и}}$=area of an average turn in the coil:

$$S_{\text{и}} = \frac{\pi \bar{D}_{\text{и}}^2}{4}, \tag{3.19}$$

where $\bar{D}_{\text{и}}$=average diameter of the coil.

A core-type radiator is an electromagnetic with a transformer-steel core that is magnetized by a current passing through a winding having a large number of turns made of thin wire. The winding's thickness is small in comparison with the core's lateral dimensions.

This type of radiator is placed on top of the conical part of the afterbody.

Between the magnetic moment M and the radiator core volume V_c that can create this moment, there exists the relationship

$$V_c = \frac{4\pi\mu_0 M}{B}, \tag{3.20}$$

where B=magnetic induction inside the core.

When selecting the size of the core, the normal starting point is that the induction should be $B \leq 0.2$-0.3 teslas.

After fixing the length of the core at l_c, because of structural considerations, its cross-section area is determined:

$$S_c = \frac{V_c}{l_c}. \tag{3.21}$$

The solenoid's ampere-turns can be calculated from the following formula:

$$I_{\text{и}} W_{\text{и}} = \frac{4\pi M}{\mu_d S_c}, \tag{3.22}$$

where μ_d is the core's choke (or averaged) magnetic permeability, which allows not only for the core material's permeability, but also for the permeability of its shape [3.2]:

$$\mu_d = \frac{m_d \mu}{m_d + \mu}, \tag{3.23}$$

where μ=initial magnetic permeability of the core substance, as found in tables (for transformer steel, μ=560); m_d=magnetic permeability of the core shape, which depends on the core's relative length μ:

$$\lambda = \frac{l_c}{d_c}, \tag{3.24}$$

where d_c=diameter of the core.

Table 3.2 is a list of m_d permeability values.

λ	m_d	λ	m_d	λ	m_d	λ	m_d
5	18,4	14	80,8	22	162	30	273
7	29,5	15	89,5	24	181	40	458
8	35,5	17	108	25	200	50	688
10	49,2	18	118	27	228	60	960
12	64,5	20	140	28	242	70	1270

Table 3.2. Magnetic Permeability (m_d) of the Shape of Cylindrical Cores (Rods)

The Receiving Circuit

The receiving circuit is a resonance circuit. Figure 3.11 is an equivalent circuit of the receiving circuit.

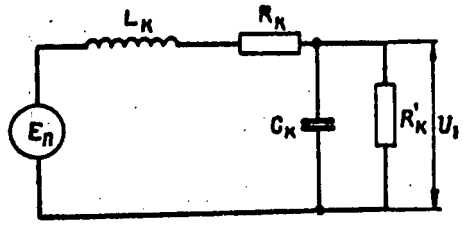

Figure 3.11. Equivalent circuit of the receiving circuit: L_k=inductance of the receiving coils; C_k=circuit capacitance; R_k=resistance of the receiving coils; R_k=circuit load resistance — grid leak resistance of the voltage amplifier's first tube; E_c=electromotive force induced in the circuit; U_1=voltage at the circuit's output

The circuit's impedance $\dot{Z}_k$ is

$$\dot{Z}_к = R_к + \frac{R'_к}{1 + \omega^2 C_к^2 R_к'^2} + j\omega\left(L_к - \frac{C_к R_к'^2}{1 + \omega^2 C_к^2 R_к'^2}\right). \tag{3.25}$$

We derive the circuit's load resistance $\dot{Z}'_k$ from (3.25), assuming that $R_k=L_k=0$:

$$\dot{Z}'_k = \frac{R'_k}{1+\omega^2 C_k^2 R_k'^2} - j\omega \frac{C_k R_k'^2}{1+\omega^2 C_k^2 R_k'^2}. \tag{3.26}$$

The receiving circuit is tuned in resonance with the proximity fuze's operating frequency ω_p. For a current at this frequency, the circuit is a purely effective resistance.

$$L_k - \frac{C_k R_k'^2}{1+\omega_p^2 C_k^2 R_k'^2} = 0.$$

From this, we find that the circuit's capacitance C_k is

$$C_k = \frac{1}{2\omega_p^2 L_k}\left(1 \pm \sqrt{1-\frac{4\omega_p^2 L_k^2}{R_k'^2}}\right). \tag{3.27}$$

Consequently, the resonance condition is satisfied by two different values of the capacitor's capacitance.

The receiving circuit's inductance is determined according to the empirical formula [3.3]

$$L_k = \frac{80\bar{D}_n^2 W_n'^2 10^{-9}}{3\bar{D}_k + 9b_k + 10a_k}, \tag{3.28}$$

where $\bar{D}_c$=average diameter of the winding; W_c=number of turns in the receiving coil; b_k=axial length of the winding; a_k=thickness of the winding.

The receiving circuit's amplifying properties are characterized by its Q-factor q_k:

$$q_k = \frac{|\dot{Z}'_k|}{|\dot{Z}_k|} = \frac{U'_{1m}}{E_{nm}}. \tag{3.29}$$

Since the coil is located in special vents in the warhead, it is screened by the body of this section and the circuit's Q-factor is reduced. In this case,

$$q_{kT} = (0{,}2 - 0{,}6)\, q_k. \tag{3.30}$$

The electromotive force of the effective signal in the receiver will be

$$E_n(t) = \mu_0 S_n \frac{d[H_{zn}(t)]}{dt}, \tag{3.31}$$

where μ_a=absolute magnetic permeability of the coil's core (for coreless coils, $\mu_a=\mu_0$); S_c=equivalent area of the receiving coil:

$$S_n = W_n S_t. \tag{3.32}$$

where S_t=area of an average turn in the coil.

After substituting the values from formula (3.16) into (3.31), and allowing for the fact that $K_k(t)$ changes slowly, we have

$$E_n(t) = \mu_a S_n H_{znm}(t)\,\omega_p \sin\left(\omega_p t + \varphi_z - \frac{\pi}{2}\right). \tag{3.33}$$

Consequently, considering (3.17) the amplitude of the electromotive force will change according to the rule

$$E_{nm}(t) = \mu_a S_n H_{z0n} K_k(t)\, K_z \omega_p. \tag{3.34}$$

The receiving circuit is inertialess, for all practical purposes.

Having substituted (3.34) into (3.29), with due consideration for (3.17) and (3.30), we obtain the receiving circuit's transmission factor:

$$K_n = \frac{U_{1m}}{H_{znm}} = q_{KT}\mu_a S_n \omega_p. \tag{3.35}$$

3.6. Amplifying Devices in Fuzes

The amplifying device boosts the alternating voltage that is sent from the receiving coils and converts the amplified alternating voltage into the direct current pulse that is needed to trigger the actuating relay, the electric primer's closing circuit, or the ignition device's electromagnets. It also provides noise stability for the proximity fuze.

The amplifying device contains a voltage amplifier, a phase discriminator, a differentiating circuit, and an electronic relay. Let us examine each of these units separately.

Voltage Amplifier

The basic requirement for this amplifier is that it be able to amplify signals in a rather narrow frequency band.

In principle, any amplifier can be used to amplify signals. However, choke-coupled and resistance amplifiers are used in proximity fuzes in practice. Schematic diagrams of these amplifiers are presented in Figures 3.12 and 3.13.

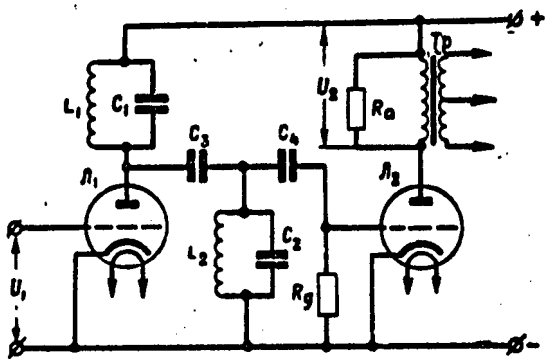

Figure 3.12. Schematic diagram of a choke-coupled amplifier.

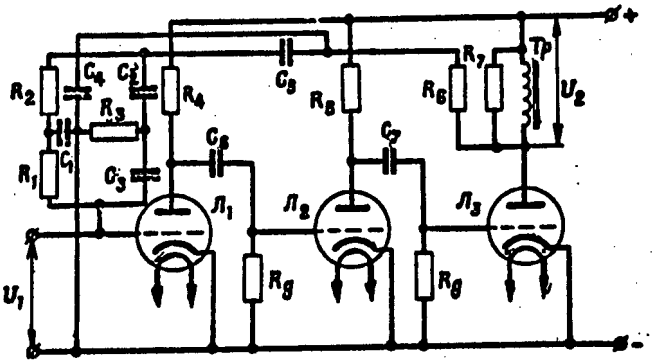

Figure 3.13. Schematic diagram of a resistance amplifier.

Two or three amplifier stages are adequate for the amplification of signals in a proximity fuze.

The L_1C_1 and L_2C_2 circuits of a choke-coupled amplifier are tuned to the fuze's operating frequency. Consequently,

$$\omega_p L_1 = \frac{1}{\omega_p C_1} \quad \text{and} \quad \omega_p L_2 = \frac{1}{\omega_p C_2}.$$

For a resistance amplifier, in which negative feedback in the form of a double T-shaped filter is used to impart frequency selectivity, the number of stages must be an odd number greater than one.

The voltage amplifier's transmission band is approximately 10% of the operating frequency. Under these circumstances, the amplifier's inertial

properties are expressed rather poorly and it can be regarded as an inertialess unit. In this case, the amplifier's transmission factor is equal to its amplification factor at the operating frequency:

$$K_y = \frac{U_{2m}^{\Phi}}{U_{1m}}. \tag{3.36}$$

Phase Discriminator

The phase discriminator gives a proximity fuze the property of phase selectivity. Its circuitry (Figure 3.14) consists of two symmetrical discriminator-tank circuits B_1 and B_2.

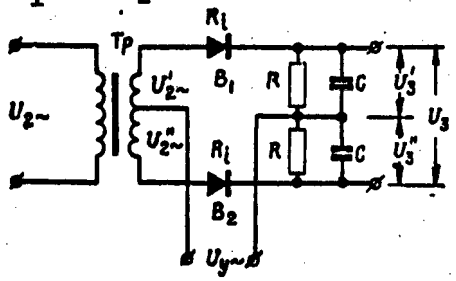

Figure 3.14. Schematic diagram of a phase discriminator.

The discriminator's input voltage is $U_{2\sim}$, which changes according to the harmonic rule

$$U_{2\sim} = U_{2m} \sin(\omega_p t + \varphi),$$

where ϕ=phase angle between voltages $U_{2\sim}$ and $U_{y\sim}$.

Voltage $U_{2\sim}$ is read at the voltage amplifier's output.

Transformer T_p has a transformation ratio of n=1, while its secondary winding is divided into halves. Therefore, only half of voltage $U_{2\sim}$ passes into each of the discriminators: $U'_{2\sim}=U''_{2\sim}=U_{2\sim}/2$.

In addition to voltage $U_{2\sim}$, the circuit receives controlling voltage $U_{y\sim}$, which is changed by a frequency equal to the operating frequency and which has a value that is considerably in excess of the input voltage: $U_{ym} \approx 40U_{2m}$. Voltage $U_{y\sim}$ is entered in such a fashion that it will be added to $U'_{2\sim}$ in circuit B_1 and subtracted from $U''_{2\sim}$ in B_2.

The total voltages in the upper ($U_{B1\sim}$) and lower ($U_{B2\sim}$) circuits are picked up as U'_3 and U''_3. The difference between these voltages is the phase discriminator's output voltage U_3.

In the theory of an ideal discriminator, it has been proven that if it has a load resistance R that is bridged by capacitance C, then the rectified voltage will be proportional to the amplitude of the rectifying voltage and the cosine of flow angle ψ.

Consequently,

$$U_3 = U_3' - U_3'' = (U_{B1m} - U_{B2m}) \cos \psi. \tag{3.37}$$

The flow angle depends only on the ratio of load resistance R to the internal resistance of the discriminator R_i and is independent of the applied voltage's amplitude. This function is transcendental [3.3]:

$$\frac{\pi \cos \psi}{\sin \psi - \psi \cos \psi} = \frac{R}{R_i}. \tag{3.38}$$

Angle ψ is determined approximately.

The difference between the amplitudes of voltages U_{B1m} and U_{B2m} can be determined by using the vector diagram of the discriminator represented by Figure 3.15:

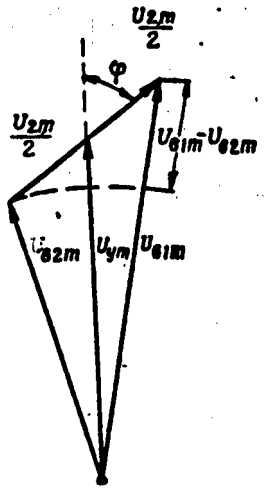

Figure 3.15. Vector diagram of the phase discriminator's operation.

$$U_{B1m} - U_{B2m} \approx U_{2m} \cos \varphi. \tag{3.39}$$

Substituting (3.39) into (3.37), we obtain

$$U_3 = U_{2m} \cos \psi \cos \varphi. \tag{3.40}$$

Assuming that $\phi=0$, from (3.40) it is obvious that the phase discriminator's transmission factor will be

$$K_{\phi\Delta} = \frac{U_3}{U_{3m}} = \cos\psi. \tag{3.41}$$

If the input signal's frequency differs from the controlling voltage's, then the phase discriminator will not rectify the alternating voltage, but will convert it into a difference frequency -- the beat frequency $\Delta\omega$

$$\Delta\omega = \omega - \omega_p. \tag{3.42}$$

This frequency's voltage can lead to triggering of the proximity fuze if it is low enough.

The phase discriminator's output contains capacitors C that, together with the internal resistance of the discriminators R_1 and the load resistances R, form a filter. The difference frequency's alternating voltage will be weakened considerably by this filter.

The phase discriminator's selective properties are characterized by the frequency characteristic

$$F(\Delta\omega) = \frac{1}{\sqrt{1+\left(\frac{\Delta\omega C R_1}{1+\frac{R_1}{R}}\right)^2}}. \tag{3.43}$$

The phase discriminator is an inertial component. It is difficult to evaluate its dynamic properties because of the rectifiers' nonlinearity.

For approximate calculations, its transient characteristic is determined on the basis of the applicable linearization:

$$h_{\phi\Delta}(t) = K_{\phi\Delta}\left(1-0{,}5e^{-\frac{t}{T_1}}-0{,}5e^{-\frac{t}{T_1}}\right), \tag{3.44}$$

where T_1 is the charge time constant of capacitor C:

$$T_1 = \frac{R_1 RC}{R_1+R}; \tag{3.45}$$

and T_2 is the discharge time constant of capacitor C:

$$T_2 = RC \tag{3.46}$$

The transient characteristic is the phase discriminator's reaction to a unit jump in voltage at its input while the phase remains the same.

Differentiating Circuit

The differentiating circuit imparts dynamicity to the fuze. This means that the proximity fuze can be triggered only when there is an increase in input signal $H_{zp}(t)$. Fuze triggering does not take place with as large an input signal as desired unless it changes with respect to time. This circuit protects the fuze from triggering in the presence of a natural constant disbalance.

Figure 3.16 is a diagram of the differentiating circuit.

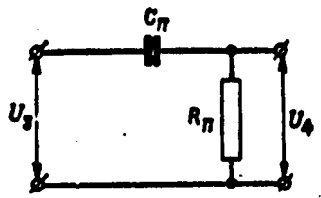

Figure 3.16. Schematic diagram of the differentiating circuit.

The voltage at this circuit's output will be

$$U_4 = U_3 \frac{R_п}{\sqrt{R_п^2 + \frac{1}{\Omega^2 C_п^2}}}, \tag{3.47}$$

where Ω=provisional frequency of the input signal's change with respect to its envelope:

$$\Omega = \frac{\pi}{t_и}. \tag{3.48}$$

From Figure 3.5,

$$t_и = \frac{3B_к}{V_т \sin\theta} < \frac{2a + B_к}{V_{тк}}. \tag{3.49}$$

Here,

$$V_{тк} = V_т + V_к \cos\theta, \tag{3.50}$$

where V_k=speed of the ship; a=fuze base.

From formula (3.47) we obtain the differentiating circuit's transmission factor

$$K_{дц} = \frac{U_4}{U_3} = \frac{T_3\Omega}{\sqrt{1 + T_3^2\Omega^2}}. \tag{3.51}$$

Here,

$$T_3 = R_c C_c, \tag{3.52}$$

where T_3=the circuit's time constant.

The differentiating circuit's dynamic characteristics are described by the transient characteristic

$$h_{ДЦ}(t) = e^{-\frac{t}{T_1}}. \tag{3.53}$$

Electronic Relay

On the one hand, the connection of capacitor C_p in parallel with the relay in the electronic relay's circuitry (Figure 3.17) leads to retardation of the fuze-triggering process and thereby protects it from short-pulse jamming; on the other hand, it increases the amount of time the relay's contacts are held in the closed state.

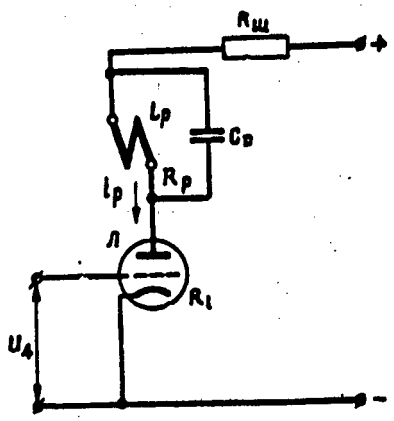

Figure 3.17. Schematic diagram of the electronic relay.

When the signals are building up rather slowly, the relay circuit's inductive and capacity reactances are small in comparison with the tube's internal resistance R_i. In this case, this component's transmission factor will be

$$K_{ep} = \frac{i_p}{U_4} = \frac{\mu}{R_i} = S_0 \tag{3.54}$$

where μ=the tube's static amplification factor; S_0=steepness of the tube's anode-grid characteristic at its operating point.

3.7. The Triggering Characteristic of Fuzes

A fuze's main characteristic is its triggering characteristic. It is the dependence of the current in the windings of the oeprating relays i_p on all of the fuze's parameters and characteristics when the external magnetic field's time change is governed by a specific law:

$$i_p(t) = F[V_т, V_к, B_к, K_к, e, \mu, f_p, H_т, \theta, M, a, h_{нв}(t)]. \tag{3.55}$$

The amount and nature of the current change in the relay are determined by the torpedo's tactical characteristics and specifications (V_T), target ship elements (V_k and B_k), medium parameters (α and μ), conditions of the torpedo's impact with the target (H_T and 0), and the fuze's parameters and characteristics (M, a, f_p, and $h_{pf}(t)$).

Since the receiving circuit, voltage amplifier, and electronic relay are inertial components for all practical purposes, $h_{pf}(t)$ can be obtained with the help of a Duhamel integral [3.8]:

$$h_{нв}(t) = K_в K_у K_{ор}\left[U_з(0)\, h_{ац}(t) + \int_0^t \frac{dU_з(u)}{du} h_{ац}(t-u)\, du\right]. \quad (3.56)$$

When $H_{zpm}(t)=1.0$ and $K_c=K_y=1.0$, it follows from formula (3.44) that $U_3(t)=h_{pD}(t)$.

Substituting the value of $h_{DC}(t)$ from (3.53), we have

$$h_{нв}(t) = 0{,}5\, K_в K_у K_{фз} K'_{ор} T_з \left[\frac{1}{T_з - T_1}\left(e^{-\frac{t}{T_з}} - e^{-\frac{t}{T_1}}\right) + \frac{1}{T_з - T_з}\left(e^{-\frac{t}{T_з}} - e^{-\frac{t}{T_з}}\right)\right]. \quad (3.57)$$

The proximity fuze's triggering characteristic is then determined analogously to formula (3.56):

$$l_p(t) = \left[H_{zпм}(0)\, h_{нв}(t) + \int_0^t \frac{dH_{zпм}(u)}{du} h_{нв}(t-u)\, du\right]. \quad (3.58)$$

Since function $H_{zpm}(t)$ is not described analytically, integral (3.58) can be solved either graphically or numerically (by an approximative method).

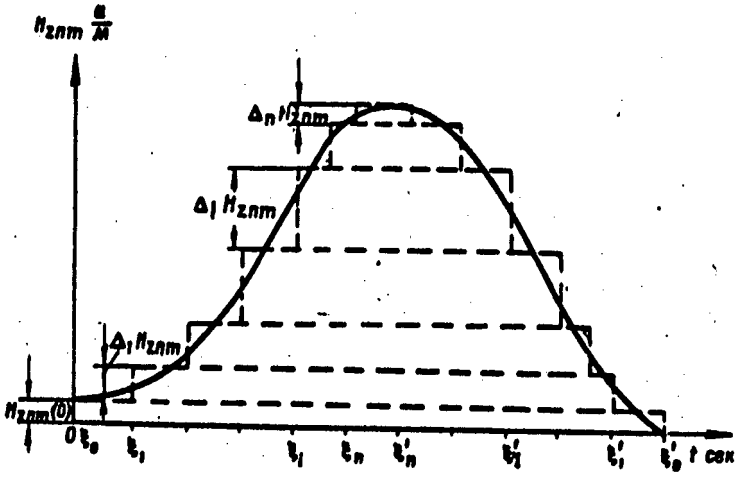

Figure 3.18. Approximation of the ship's effect when calculating an electromagnetic fuze's triggering characteristic.

Formula (3.58) is then replaced by an approximate formula (Figure 3.18):

$$i_p(t) \approx H_{zpm}(\xi_0)\left[h_{\text{нв}}(t) - h_{\text{нв}}(t-\xi_0')\right] + \sum_{i=1}^{n} \Delta_i H_{zpm}\left[h_{\text{нв}}(t-\xi_i) - h_{\text{нв}}(t-\xi_i')\right], \quad (3.59)$$

where $H_{zpm}(\xi_0)=H_{zpm}(0)$--initial value of the field; $\Delta_i H_{zpm}$=field jump during the i-th time interval; ξ_i=beginning time of the i-th field jump; ξ_i'=ending time of the i-th field jump.

When using formula (3.59) in practice, it should be kept in mind that at $(t-\xi)<0$, $h_{pf}(t-\xi)=0$.

It is most often the case that, instead of simply determining the current change $i_p(t)$, we have to select the voltage amplifier's amplification factor K_y such that the proximity fuze is triggered under completely specific conditions and by a certain triggering current i_{tr} in the operating relay.

3.8. Magnetic Proximity Fuzes

Magnetic fuzes belong to the passive type and are triggered when the torpedo enters the ship's magnetic field.

The ship's magnetic field is that space in which there is a measurable (or detectable) change in the Earth's magnetic field caused by the presence of the ship. The boundaries of a ship's magnetic field have not been defined mathematically. In practice, they are determined by the measuring instruments' sensitivity.

The dimensions of a ship's magnetic field are usually assumed to be

$$\left.\begin{aligned} X_к &= K_x L_к; \\ Y_к &= K_y B_к. \end{aligned}\right\} \quad (3.60)$$

where K_x and K_y are coefficients characterizing the extent of the ship's magnetic field with respect to its major dimensions.

On the one hand, one feature of a ship's field is that it is not temporarily stable, even when it is measured under similar conditions for the same ship. On the other hand, every ship has a field that is distinct from the fields of other ships -- even those of the same class.

At the same time, along with all the individuality of ships' magnetic characteristics, they are governed by a set of regularities.

A ship's magnetic field is formed as the resultant of the overlapping of several fields:

the permanent magnetization field;
the induced magnetization field;
the field of the bucking windings.

A ship acquires permanent magnetization under the influence of the terrestrial field -- primarily when it is being built -- and depends on:

the ship's heading and the latitude of the place where it was built;
the magnetic properties of the material's used in its hull (basically, on the amount of residual magnetization);
the ratio of the ship's major dimensions and the distribution and shapes of the ferromagnetic masses in it;
the method used to build the ship (the amount of reveting and welding).

The nature and amount of a ship's permanent magnetization can be changed significantly when the hull is subjected to severe shaking (nearby explosions, artillery fire, work being done of the hull, and so forth) or when the ship is based for a long period of time in an area where the Earth's magnetic field differs considerably from what it was where the ship was built.

In contrast to permanent magnetization, induced magnetization is wholly and completely determined by the geomagnetic field that is acting upon the ship at any given moment.

The main factors affecting a ship's induced magnetization are:

the ship's heading and latitude at the given moment;
the magnetic properties of the hull materials (primarily their magnetic permeability);
the ratio of the major dimensions and the distribution and shape of ferromagnetic masses in the ship.

A ship's magnetic field is represented by components along its main axes [2.1]:

$$\vec{H}_s = \vec{H}_z + \vec{H}_x + \vec{H}_y \tag{3.61}$$

where H_Z, H_X, and H_Y are the vertical, longitudinal, and transversal components, respectively, of a ship's magnetic field's strength.

The magnetic fields of ships cannot be calculated analytically. The values of H_Z, H_X, and H_Y are most frequently determined by measuring the field under the ship.

The field component values that are obtained by measurement serve as the basis for compiling magnetic charts of ships, from which the field curves are plotted.

The horizontal plane at the depth at which the measurements are taken is called the plane of measurements. The half-space lying below this plane

Consequently, if we assume that with an increase in depth intake pressure and back pressure increase by the same magnitude, engine effective horsepower will decrease, since the power increase due to increased intake pressure will not be compensated by power losses involved in overcoming back pressure forces in exhausting spent steam-gas from the torpedo even at constant rpm.

Engine rpm drops off with a drop in horsepower. If we assume a cube relationship between engine horsepower and rpm

$$N_e = K_n n^3, \qquad (5.11)$$

we can derive a formula for determining the law of change in engine effective horsepower with change in running depth.

Torpedo speed can be determined either by drop in horsepower

$$V_\tau^н = V_\tau^р \sqrt[3]{\frac{N_н}{N_р}}, \qquad (5.12)$$

or by rpm

$$V_\tau^н = V_\tau^р \cdot \frac{n_н}{n_р}, \qquad (5.13)$$

where $V_\tau^р$, $N_р$, $n_р$ — speed, horsepower and rpm at rated operating conditions;

$V_\tau^н$, $N_н$, $n_н$ — same, at given torpedo running depth.

As was indicated above, propulsive agent consumption will increase with an increase in torpedo running depth, with a decrease in time and consequently distance of torpedo run.

Engine operating time will also decrease because with a gaseous oxidizer an increase in back pressure leads to increased gas residual pressure in the tank and greater unutilized residual oxidizer.

Thus a decrease in torpedo range when running at greater depth will occur as a consequence of a drop in speed due to loss in power and decrease in running time as a consequence of an increase in per-second consumption and a decrease in quantity of consumed gaseous oxidizer.

In order to compensate for reciprocating engine power losses with an increase in running depth, it is necessary either to alter the law of gaseous oxidizer pressure regulation or select gas distribution phases in such a manner that average indicated pressure will be independent of torpedo running depth.

Example 5.4. Determine torpedo speed and range at a depth of 50 m in mode 1, if for rated engine operating conditions (running depth 10 m) pressure in the SGG P_1=28 dan/cm^2, exhaust back pressure P_4=3 dan/cm^2, and per-second steam-gas consumption is $m_{сек}^{н}$=1.1 kg/sec.

Solution. A change in running depth will lead to an increase in intake pressure and back pressure by one and the same amount. Engine horsepower under

the new conditions will be determined with formula (5.3), taking into consideration expressions (5.10), (5.11) and example 5.3; as a result we obtain

$$N_e = \frac{(0{,}84 \cdot 32 - 1{,}27 \cdot 7) \cdot 10^3 \cdot 3{,}14 \cdot 0{,}144^3 \cdot 0{,}15 \cdot 2 \cdot 2 \cdot 1440 \cdot N_e^{1/3} \cdot 0{,}87 \cdot 0{,}85}{4 \cdot 60 \cdot 345^{1/3}} = 295 \text{ kw.}$$

Consequently, at a depth of 50 meters the engine will develop power equal to 295 kw.

Torpedo running speed at a depth of 50 m will be

$$V_т = 25 \cdot \left(\frac{295}{345}\right)^{1/3} = 23{,}1 \quad \text{m/sec.}$$

Propulsion unit running time will be determined by available air supply. If we assume that steam-gas mixture consumption is proportional to pressure and rpm, then at a depth of 50 m it will be 1.26 kg/sec. Of this quantity, air accounts for

$$m_{сек}^{ок} = \frac{\nu_{ок} m_{сек}^{пг}}{1 + \alpha\nu_{ок} + \nu_в} = \frac{14{,}6 \cdot 1{,}26}{1 + 14{,}6 + 5{,}6} = 0{,}87 \quad \text{kg/sec.}$$

With a pressure differential between propulsion agent tanks of 7 dan/cm^2, total air consumption will be

$$m_{в.р}^{ок} = \frac{P_{нач} V_{вр}}{RT_{нач}} - \frac{P_{ост}(V_{вр} + V_{во} + V_{мб})}{RT_{ост}} = 112 \quad \text{kg.}$$

Torpedo running time will be

$$\tau = \frac{m_{в.р}^{ок}}{m_{сек}^{ок}} = \frac{112}{0{,}87} = 129 \quad \text{sec.}$$

Torpedo range at a depth of 50 meters will be

$$E_т = V\tau = 23{,}1 \cdot 129 = 3000 \quad \text{m.}$$

5.7. Features of Internal Combustion and Mixed Combustion Engines

One well-known method of improving the economy of heat engines is to raise the cycle maximum temperature. For the above reciprocal expansion-type engines a substantial elevation of steam-gas mixture temperature is possible only with solution of complex problems of ensuring adequate heat resistance and high-temperature corrosion resistance of the materials of which the engine is made. It was therefore logical to consider engines with combustion inside cylinders -- internal combustion engines. It is a well-known fact that fuel combustion in cylinders can occur with a constant volume, constant pressure, or in a combined manner.

Internal combustion engines operating on a cycle which involves the delivery of heat with a constant volume utilize for the most part readily-vaporizing fuels (usually gasoline) with spark ignition, in contrast to engines with combustion at a constant pressure, where heavier liquid fuels are employed (solar oil) with compression ignition.

Internal combustion engines are more economical than piston reciprocating engines as a consequence of the higher temperature of initiation of expansion and higher pressures.

The principal deficiencies which limit the use of internal combustion engines in torpedoes are the following: first, they are considerably more complex in design, chiefly in connection with the necessity of providing a starter system; second, as in a steam-gas expansion reciprocating engine, an increase in back pressure reduces rated work (the lower part of the indicator diagram is cut off) and cylinder filling; third, they have a low starting reliability.

In order to eliminate the drawbacks of the piston engine and the internal combustion engine (while retaining the advantages), British torpedoes employ an engine with a preheater and supplementary fuel feed (with a surplus of oxidizer in the preheater) into the expansion-type reciprocating engine (cycle B), where the operating process is almost the same as in internal combustion engines.

These engines are called mixed or combined combustion engines. They operate on the following principle. After the preheater, to which all oxidizer and only a part of the fuel is fed (combustion takes place with a high excess oxidizer ratio), the combustion products together with the excess oxidizer are fed into the expansion-type reciprocating engine. At the end of the process of intake of these products, the rest of the fuel is added, which, undergoing combustion, releases an additional amount of energy. An ideal indicator diagram has essentially the same form as for an expansion-type reciprocating engine, with the difference that heat f e e d partially occurs at constant pressure and partially at constant volume. An increase in initial temperature leads to a noticeable improvement in efficiency and decrease in summary consumption of propulsive agents.

The heater is made small, since it actually performs only the function of a starter device, while the working medium is finally prepared in the reciprocating engine cylinder.

The principal difficulties in performance of the operating process of these engines are, first of all, nonuniform mixing of oxidizer with combustion products prior to entry into the reciprocating engine; second, unreliable ignition of the gas mixture within the cylinder at one and the same moment and, as a result of this, instability of the operating process. However, the fact that only two propulsive agents are employed in the preheater and cylinders (fuel and oxidizer), and a third component is not required (water), gives these engines additional advantages over expansion-type reciprocating engines.

5.8. Fundamental Principles of Theory of Gas Flow

Study of the processes of the movement of gases along channels, accompanied by various transformations of energy, is of exceptional importance. Theory and calculations of gas turbines, reaction engines and other machines are built on the general data and principles of theory of gas flow.

We shall present some basic points of theory of flow of gases.

With steady-state flow, gas flow rate $m_{сек}$, flow section f, velocity C and density ρ in any section of the channel are connected with the continuity equation, in which the law of conservation of mass is expressed.

This equation is as follows:

$$m_{сек} = f\rho C = \text{const.} \qquad (5.14)$$

As gas expands, its rate of flow will increase and its density decrease. Therefore it is difficult directly to determine from equation (5.14) how f should change in order for gas continuously to increase its rate of flow. In order to answer this question we shall logarithmize equation (5.14) and present it in differential form:

$$\frac{df}{f} = \frac{dC}{C}\left(-\frac{d\rho}{\rho}\cdot\frac{C}{dC}-1\right).$$

Substituting in the expression in parentheses a value from the Bernoulli equation

$$dC = -\frac{dP}{\rho C},$$

we shall have

$$\frac{df}{f} = \frac{dC}{C}\left(\frac{C^2}{\frac{dP}{d\rho}}-1\right). \qquad (5.15)$$

We know from physics that speed of sound a is determined by expression

$$a = \sqrt{\frac{dP}{d\rho}}. \qquad (5.16)$$

In addition, designating the ratio of flow rate to speed of sound M, we shall have

$$\frac{df}{f} = \frac{dC}{C}(M^2-1). \qquad (5.17)$$

It is evident from equation (5.17) that:

in the subsonic region (M<1) acceleration of flow is possible only with a decrease in flow channel section;

in the supersonic region (M>1) flow acceleration will occur only with an increase in flow channel section;

at a flow rate equal to the speed of sound (M=1), the flow channel section will be at the extreme (minimum in this case), since

$$\frac{df}{f}=0.$$

Thus if we wish to have a flow which continuously accelerates from some initial subsonic to a supersonic speed, the flow channel section should at first be convergent, where the flow will be at subsonic speeds, subsequently widening, where the flow will be at supersonic speeds. At the boundary of these two areas, that is, at the narrowest section in the channel, flow rate will be equal to the speed of sound.

In order to produce supersonic flows, Swedish engineer Laval proposed a nozzle with an intercept (Laval nozzle).

To determine the rate of gas flow from a nozzle we shall apply the basic equation of the first law of thermodynamics for gas flows:

$$dq=di+d\left(\frac{C^2}{2}\right).$$

With adiabatic outflow, that is, in the absence of heat exchange, dq=0, consequently,

$$-di=CdC.$$

After integration we shall obtain

$$i_0-i_c=\frac{C_c^2}{2}-\frac{C_0^2}{2},$$

Whence, ignoring insignificantly small quantity C_0, we shall have

$$C_c=\sqrt{2(i_0-i_c)}=1{,}41\sqrt{C_p(T_0-T_c)}. \qquad (5.18)$$

where C_0, C_c, i_0, i_c — values of gas velocity and enthalpy at the beginning and end of the expansion process (entering and leaving the nozzle).

We see from equation (5.18) that the gas temperature drops off during adiabatic expansion.

Equation (5.18) for determining the velocity of gas outflow can be transformed, utilizing Meyer's equation and the adiabatic equation:

$$C_p-C_V=R;\ \frac{T_c}{T_0}=\left(\frac{P_c}{P_0}\right)^{\frac{K-1}{K}}.$$

After substituting these values in equation (5.18), we obtain

$$C_c=\sqrt{2\frac{K}{K-1}RT_0\left[1-\left(\frac{P_c}{P_0}\right)^{\frac{K-1}{K}}\right]}. \qquad (5.19)$$

We shall determine gas parameters in the nozzle critical and outlet sections.

We shall determine gas temperature in the critical section proceeding from the fact that flow velocity in this section is equal to the local speed of sound, that is,

$$C_{кр} = \sqrt{2\frac{K}{K-1}R(T_0 - T_{кр})} = \sqrt{KRT_{кр}},$$

hence

$$\frac{T_{кр}}{T_0} = \left(\frac{2}{K+1}\right). \qquad (5.20)$$

It is easy to determine pressure in the critical section, linking equation (5.20) with the adiabatic equation

$$\frac{P_{кр}}{P_0} = \nu_{кр} = \left(\frac{2}{K+1}\right)^{\frac{K}{K-1}}. \qquad (5.21)$$

Thus the critical ratio of pressures is determined solely by the adiabatic index.

It follows from equation (5.21) that if the ratio of pressure at the nozzle outlet to pressure at the inlet is greater than $\nu_{кр}$, a convergent nozzle should be employed and, on the other hand, if this ratio is less than $\nu_{кр}$, full gas expansion will take place only in the Laval nozzle.

We shall determine velocity at the critical section by substituting equation (5.20) into the formula for $C_{кр}$:

$$C_{кр} = \sqrt{2\frac{K}{K+1}RT_0}. \qquad (5.22)$$

Substituting in the continuity equation the velocity value according to formula (5.19), written for the current value along the nozzle, we shall obtain the area of any nozzle section:

$$f = \frac{m_{сек}}{\rho C} = \frac{m_{сек}RT}{P\sqrt{2\frac{K}{K-1}RT_0\left[1-\left(\frac{P_c}{P_0}\right)^{\frac{K-1}{K}}\right]}}. \qquad (5.23)$$

Utilizing the adiabatic equation and introducing designation

$$\beta = \sqrt{2\frac{K}{K-1}\left[\left(\frac{P}{P_0}\right)^{\frac{2}{K}} - \left(\frac{P}{P_0}\right)^{\frac{K+1}{K}}\right]}, \qquad (5.24)$$

we shall obtain

$$f = \frac{m_{сек}\sqrt{RT_0}}{\beta P_0}. \qquad (5.25)$$

For nozzle critical section

$$\beta_{кр} = \sqrt{K\left(\frac{2}{K+1}\right)^{\frac{K+1}{K-1}}}. \qquad (5.26)$$

For a given working medium, ignoring the relationship between specific heat and temperature, this value β_{kp} can be considered constant.

Therefore critical section quantity

$$f_{kr} = \frac{m_{cek}\sqrt{RT_0}}{\beta_{kp}p_0} \qquad (5.27)$$

is determined solely by gas flow and its initial parameters.

If the gas flow and nozzle parameters are known, then with formulas (5.25) and (5.27) we can determine the magnitude of per-second gas flow through this nozzle.

Determination of flow parameters in the presence of heat exchange (expansion on a polytropic curve) is extremely complex due to the difficulties of determining the magnitude of the polytropic curve index.

The ratio of actual gas velocity upon emerging from the nozzle to that velocity which can be obtained in the case of expansion without losses is called the gas nozzle velocity coefficient and is designated by ϕ. The value of the latter is usually determined experimentally.

If actual outflow velocity is substituted in the continuity equation, while still determining temperature with the adiabatic equation, we shall obtain formulas for determining an area of any section and critical nozzle section in the form of equations (5.25) and (5.27), in the denominator of which will appear additional term ϕ. The error is small and can be ignored.

5.9. Brief Data on Gas Turbines

The gas turbine is an engine which converts the thermal energy of a gas into mechanical work.

As a result of fuel combustion a high-temperature and pressure gas is produced, the potential energy of which is characterized by the values of parameters P and T.

Gas potential energy is converted in the nozzle box into kinetic energy.

Turbine engines are distinguished by the fact that they convert kinetic energy directly into mechanical work. A gas turbine consists of nozzle box 1 (Figure 5.5) and turbine wheel with blades.

A wheel which is single-forged with shaft 3 or placed on it, carries blades on its crown. Gas enters the nozzles and expands in them. During gas expansion its velocity increases from initial value C_0 to value C_c, that is there takes place transformation of potential into kinetic energy. Emerging from the nozzle at velocity C_c, the stream of gas hits the turbine blades, where its direction changes.

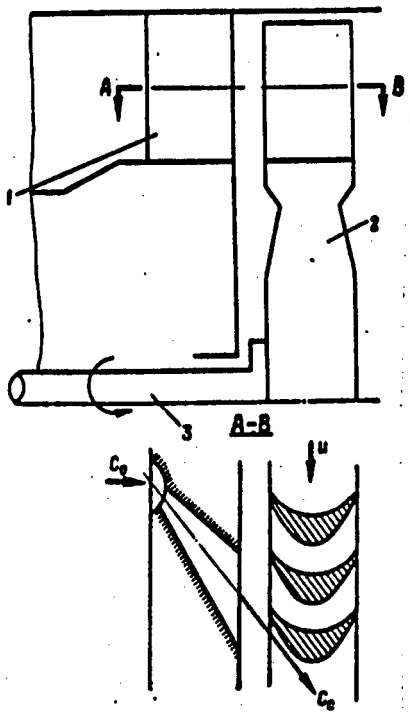

Figure 5.5. Diagram of Single-Stage Gas Turbine

When the gas stream turns in the channel between blades, centrifugal forces act on the gas particles, forces which seek to push them toward the concave part of the blades. The resultant of pressure forces on the blades generates torque which forces the turbine wheel to turn.

In recent years gas turbines have been in increasingly widespread use, both in industry and in military applications. This is due to the fact that gas turbines combine the advantages of internal combustion engines and steam turbines, and in addition possess substantial advantages over them, namely:

the working medium of a gas turbine is a gas which forms, as in internal combustion engines, directly in the combustion chamber, which is more efficient and much smaller than the boiler of steam turbine installations;

the installation as a whole is more sophisticated from a design standpoint, since its components perform only rotational motion; the number of moving parts is also smaller than in a reciprocating engine;

there is no rectilinear reciprocal motion, and consequently there is considerable uniformity of rotating parts and substantially less vibration loads;

a gas turbine, just like a steam turbine, can develop high rpm and generate high power in a single unit; reciprocating engines do not possess this advantage;

small size and unit weight.

The principal difficulty which impedes the development of gas turbines is the necessity of limiting the temperature of the gases which propel the turbine blades. High gas temperatures weaken the blading material and burn the blades. In connection with this the maximum allowable gas temperature ahead of the turbine should be selected on the basis of ensuring reliable operation of nozzle and rotor blades.

The following are differentiated in relation to the operating cycle which takes place in gas turbines:

turbines with constant combustion pressure (turbines P=const);

turbines with constant combustion volume (turbines V=const);

pulsating turbines.

In gas turbines with P=const the combustion process takes place in an open chamber at constant pressure, and therefore gas parameters ahead of the turbine will be fixed in time.

In gas turbines with V=const the combustion process takes place in a constant closed combustion chamber area. In these turbines, in conformity with the periodic character of the combustion process, initial gas parameters change cyclically in time. In spite of the fact that in turbines V=const specific power and thermodynamic efficiency are somewhat greater than in turbines P=const, they have not been utilized in aircraft engines, chiefly due to design complexity and difficulty of ensuring reliable operation of the valve system under high-temperature conditions.

An intermediate position between turbines P=const and V=const is occupied by pulsating turbines, which are designed to operate in a nonsteady flow. In particular, they include turbines employed in combined installations for utilization of the energy of exhaust gases.

The practical advantages of a cycle with combustion at constant pressure (high power at a given size and weight and simplicity of the entire unit) are so substantial that they overshadow the slight thermodynamic advantages of a cycle with combustion with constant volume. Therefore we shall henceforth be examining only turbines with constant combustion pressure.

Gas turbines are subdivided into high-temperature and low-temperature, single-stage and multistage (stage is defined as the aggregate of nozzle box and turbine wheel), action and reaction turbines.

An action turbine is a turbine in which transformation of thermal (potential) energy into kinetic energy takes place only in the nozzle box.

In reaction turbines transformation of potential into kinetic energy in the nozzle box takes place only partially, with the process being completed on the rotor wheel blading.

We shall examine the features of operation of a single-stage action or impulse turbine.

Figure 5.6 shows change in gas velocity when passing through the turbine wheel blading.

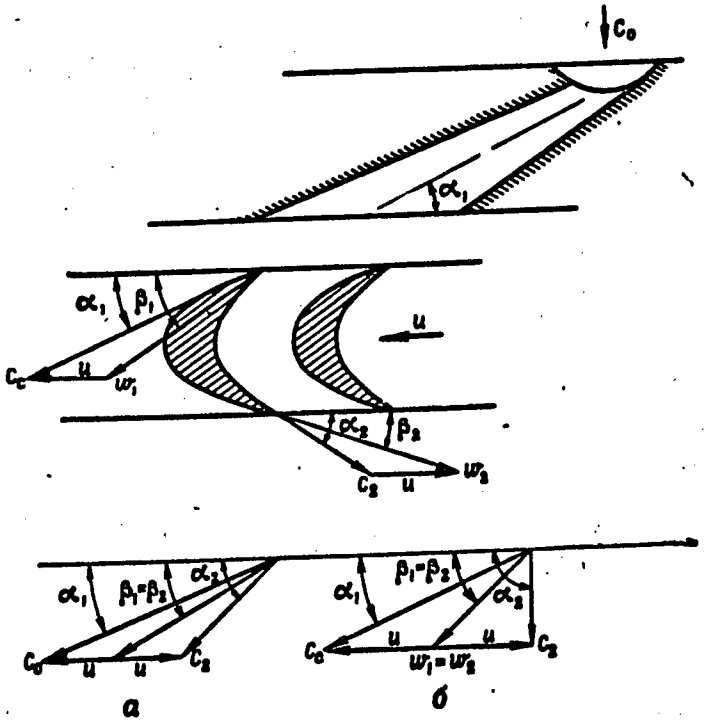

Figure 5.6. Velocity Triangles on Entering and Leaving the Rotor Wheel of a Single-Stage Impulse Turbine

Gas leaves the nozzle at velocity C_c, entering the blading at relative velocity w_1, which is obtained by subtracting from absolute velocity C_c velocity of transient motion, that is, blading tip speed u:

$$u = \frac{\pi D_{cp} n}{60}, \qquad (5.28)$$

where D_{cp} — rotor diameter measured at blading height midpoint; n — rotor rpm.

Gas emerges from the rotor blades at relative velocity w_2, which in an impulse turbine would be equal to w_1 if it were not for losses on the rotor blades. Adding w_2 to tip speed u, we find absolute discharge velocity C_2. The vector of relative velocity w_1 comprises together with the vector of tip speed angle β_1; the blade leading edge is positioned at approximately the same angle. The average direction of w_2 at discharge is characterized by angle β_2, which is approximately equal to the pitch angle of the blade trailing edges.

Assuming $\beta_2=\beta_1$ and $w_2=w_1$ (for the ideal case of a turbine without losses), we obtain a combined velocity triangle (Figure 5.6a).

The greater C_2, the smaller the quantity of kinetic energy imparted by the gas to the turbine, since the difference in kinetic energy of 1 kg of gas prior to entering the blading and after emerging from it constitutes gas energy transformed into turbine mechanical work:

$$L_u = \frac{C_c^2 - C_2^2}{2}.$$

The least velocity value C_2 and consequently the greatest stage efficiency will occur when $\alpha_2=90°$.

From the velocity triangles we find (Figure 5.6)

$$\left(\frac{u}{C_c}\right)_{опт} = \frac{\cos\alpha_1}{2}. \qquad (5.29)$$

Nozzle angle of inclination α_1 is selected at 15-20° from practical considerations; therefore the ratio of tip speed u to gas velocity C_c should equal approximately 0.5, which dictates the high rpm of gas turbines. For example, if gas leaves the nozzles at a velocity of C_c=1000 m/sec, u should be equal to 500 m/sec. Utilization of such velocity at the present time in turbines with small values D_{cp} is hampered by the high stresses produced in the rotor wheel and blades by centrifugal forces.

Thus a single-stage action or impulse turbine possesses the following characteristic features:

transformation of gas potential energy into kinetic energy takes place only in the nozzles;

the absolute velocity of gas entry into the blading corresponds to the velocity of gas outflow from the nozzle;

no change in gas state takes place in the blading; pressure remains constant and equal to back pressure; therefore action or impulse turbines constitute equal-pressure turbines which are not subjected to axial stresses;

relative velocity remains practically unchanged in the blading; the mechanical work of the turbine wheel is generated by a reduction in gas absolute velocity;

a turbine will be most economical with the ratio $\frac{u}{C_c}=0.5$.

A single-stage reaction or pressure turbine is most economical with a ratio $\frac{u}{C_c}=\cos\alpha_1$, which at the present time is difficult to achieve in practice.

In order for turbines with a substantial heat drop to be able to operate economically at a moderate tip speed, velocity stages or pressure stages are employed.

A single-stage impulse turbine can also operate with a small $\frac{u}{C_c}$ ratio, but velocity C_2 increases with a decrease in this quantity below optimal, and consequently efficiency drops. The greater velocity C_2 can be utilized on a second turbine wheel, for which a row of guide vanes must be placed forward of this wheel's blading, turning the gas stream and feeding it to the blading at the requisite angle. If gas velocity is still substantial upon leaving the second stage, a third stage can be added, etc. Thus output loss can be reduced to a minimum even with a small $\frac{u}{C_c}$ ratio (with low tip speed).

A turbine with velocity stages consists of a nozzle box, in which complete gas expansion takes place (transformation of potential into kinetic energy), and several turbine wheels (one wheel with several rows of blades), in which velocity is sequentially converted into work. Usually two velocity stages are employed, since turbine efficiency drops off with a greater number of stages (each stage produces additional losses in the guide vanes and turbine blades).

One can prove that for ideal (without losses) turbines with velocity stages the optimal $\frac{u}{C_c}$ ratio is inversely proportional to the number of stages z, that is,

$$\left(\frac{u}{C_c}\right)_{\text{опт}}=\frac{\cos\alpha_1}{2z}. \qquad (5.30)$$

Another method of reducing turbine tip speed is the employment of pressure stages. A turbine with pressure stages is a combination of several single-stage (impulse or pressure) turbines in a single unit.

The tip speed of a turbine with pressure stages is inversely proportional to the square root of the number of stages:

$$\left(\frac{u}{C_c}\right)_{\text{опт}}=\frac{\cos\alpha_1}{2\sqrt{z}}. \qquad (5.31)$$

Multistage turbines can have counterrotating wheels. If there are two wheels in a turbine, it is called a birotational turbine. On the basis of available data, such turbines are employed as engines in U.S. Navy gas-steam torpedoes. They do not differ fundamentally from turbines with two velocity stages, and ratio (5.30) also applies to them.

One drawback of multistage turbines is the retention of high gas temperature in several stages. While in a single-stage turbine gas enters the blading at a temperature appreciably reduced during expansion in the nozzles, in a multistage turbine with pressure stages such a drop in temperature is achieved only in several stages, which complicates the design of blading cooling. In addition, employment of a multistage design makes it necessary to increase the length of the turbine.

5.10. Gas Turbine Thermodynamic Cycle

A gas turbine is a heat engine variant, in the investigation of which, as we know, one usually examines its thermodynamic cycles, which give a graphic picture of the operation and basic features of the given heat engine.

The processes which take place in a gas turbine reduce to the following (Figure 5.7). Fuel, consisting of fuel and oxidizer, is fed by pumps or by another method (for example, by compressed gas) into the combustion chamber. Fuel pressure is raised thereby from initial pressure P_H to combustion chamber pressure P_0.

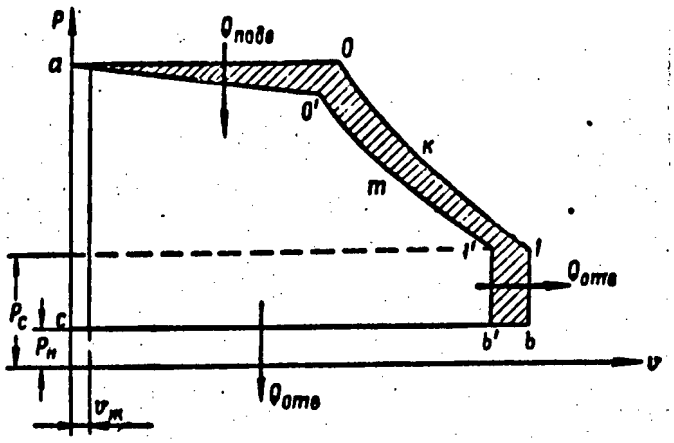

Figure 5.7. Gas Turbine Thermodynamic Cycle

Fuel, entering the combustion chamber in liquid form, is heated, vaporizes and burns at almost constant pressure. As a result of this the temperature and specific volume of the working medium increase (line a-0). Adiabatic expansion of the constant-composition working medium then begins, from pressure P_0 to pressure P_c, which is established at the nozzle exit (in the general case it may differ from ambient pressure P_H).

In order for the working medium to return to its initial state, it must be cooled and condensed to the original volume by means of isochor (line 1-b) and isobar (line b-c) heat removal. The obtained closed cycle a01bca will be the ideal compressorless gas turbine cycle.

An ideal cycle, simplifying the actual processes, gives simple computation relations which make it possible to elucidate those factors which affect engine operation and to determine ways to improve engine efficiency.

The difference between the actual and the ideal cycle consists primarily in the following:

the work expended on the process of compression and propulsive agent feed is not equal to zero;

with the ideal cycle energy losses in the combustion process are not taken into account, as a result of which the temperature of the working medium is lower in the actual cycle;

as a consequence of heat exchange, friction and other losses, the expansion process takes place not on an adiabatic but a polytropic curve.

For the most part these losses are determined experimentally.

The principal quantity which characterizes the ideal engine cycle is thermal efficiency. This efficiency takes into account only losses of heat which cannot be converted to work in conformity with the second law of thermodynamics.

For the ideal cycle thermodynamic efficiency is

$$\eta_t = \frac{Q_1 - Q_2}{Q_1},$$

where Q_1 — quantity of heat applied to the working medium; Q_2 — quantity of heat removed from the working medium.

In our case

$$Q_1 = C_p(T_0 - T_a);$$
$$Q_2 = C_v(T_1 - T_b) + C_p(T_b - T_c);$$
$$\eta_t = 1 - \frac{1}{K}\left(\frac{P_c}{P_0}\right)^{\frac{K-1}{K}}\left[(K-1)\frac{P_H}{P_c} + 1\right]. \qquad (5.32)$$

It is evident from formula (5.32) that thermodynamic efficiency is determined by degree of expansion $\frac{P_c}{P_0}$, the ratio of ambient pressure and nozzle exit pressure, and gas adiabatic expansion index K.

For rated operating conditions where $P_c = P_H$, thermodynamic efficiency will be determined by a simpler formula:

$$\eta_t = 1 - \left(\frac{P_c}{P_0}\right)^{\frac{K-1}{K}}. \qquad (5.33)$$

With an increase in ratio $\frac{P_c}{P_0}$ and adiabatic index K, the cycle thermodynamic efficiency increases, approaching 1 at the maximum. Employment of fuel the combustion products of which consist of gases with low molecular weight increases thermodynamic efficiency, all other conditions being equal.

A gas turbine can also operate under conditions other than rated, which occur both with a change in running depth and with a change in fuel consumption. Two types of operating conditions other than designed are possible:

incomplete expansion, when nozzle exit pressure is greater than ambient pressure, that is, $P_c > P_H$;

overexpansion, when pressure at the nozzle exit is less than ambient pressure, that is, $P_c < P_H$.

For a fixed nozzle, that is, a nozzle with fixed critical and outlet section values, and consequently a fixed degree of expansion, formula (5.32) is transformed as follows:

$$\eta_t = \alpha - \beta\left(\frac{P_H}{P_0}\right), \qquad (5.34)$$

where

$$\alpha = 1 - \frac{1}{K}\left(\frac{P_c}{P_0}\right)^{\frac{K-1}{K}}; \quad \beta = \frac{K-1}{K}\left(\frac{P_0}{P_c}\right)^{\frac{1}{K}}.$$

Thus a gas turbine's thermodynamic efficiency changes by linear law from the ratio $\frac{P_H}{P_0}$. Quantity $\frac{P_0}{P_c}$ leads to a sharper dependence of thermodynamic efficiency on ratio $\frac{P_H}{P_0}$, since the value of coefficient β increases thereby.

5.11. Work Performed By Gas on Turbine Wheel Periphery

As a result of gas dynamic effect on the turbine blades, a circumferential force is applied to the turbine wheel which is dictated by change in quantity of motion during gas flow through the wheel.

The product of the circumferential force and tip speed constitutes work performed by the gas on the wheel periphery, that is, work performed by the gas.

Determination of the force acting on a blade on the basis of distribution of pressures on the blade surface constitutes a very complex and laborious problem. This problem becomes considerably simplified if one applies the theorem formulated by Leonard Euler in 1755, applied to steady-state flow of liquid and gaseous bodies in the following manner.

The resultant of all forces applied to the surface of a tube is equal to the per-second quantity of motion of inflowing liquid (gas) minus the per-second quantity of motion of outflowing liquid (gas).

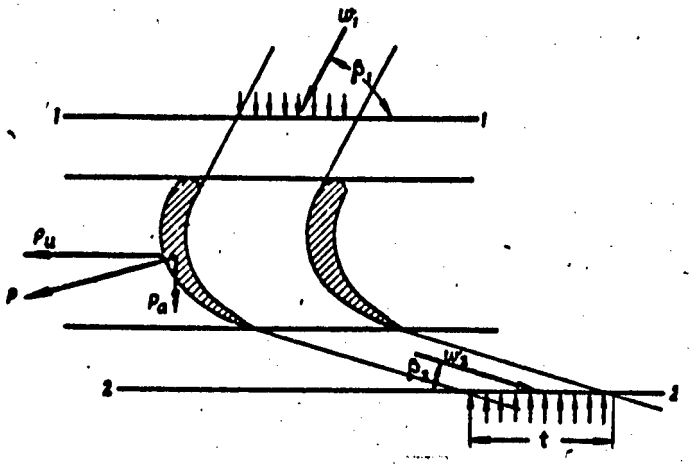

Figure 5.8. Determining Work Performed by Gas on Turbine Wheel Periphery

To determine circumferential force and work on the turbine wheel periphery we shall set apart with sections 1-1 and 2-2 that segment of the flow which fills the cavity between two blades (Figure 5.8). We shall disregard the remaining mass of gas beyond these boundaries and replace its action with pressure forces. We shall run sections 1-1 and 2-2 fairly far from the blades (theoretically to infinity) in order to consider the flow parameters in these sections identical.

Applying Euler's theorem in a projection onto the direction of the circumferential velocity of the gas, taking into account the fact that the projection of the pressure forces onto the direction of the circumferential velocity is equal to zero, and considering the height of the isolated volume equal to 1, we shall have

$$P'_u = m'_{cek}(w_1 \cos \beta_1 + w_2 \cos \beta_2).$$

Axial force

$$P'_a = m'_{cek}(w_1 \sin \beta_1 - w_2 \sin \beta_2) + t(P_1 - P_2),$$

where m'_{cek} — per-second gas flow per blade; t — distance between adjoining blades; P_1 — pressure on entry into blading; P_2 — pressure at exit from blading.

For action or impulse turbines $P_1 = P_2$.

The circumferential force acting on all blades when m_{cek}=1 kg/ sec is computed with the formula

$$P_u = \sum P'_u = w_1 \cos \beta_1 + w_2 \cos \beta_2. \qquad (5.35)$$

Work on the turbine wheel periphery is determined with formula

$$L_u = P_u u = u(w_1 \cos \beta_1 + w_2 \cos \beta_2). \qquad (5.36)$$

From the velocity triangles of a single-stage action turbine we have:

$$w_1 \cos \beta_1 = C_c \cos \alpha_1 - u; \quad w_2 \cos \beta_2 = C_2 \cos \beta_2 + u.$$

Taking this into account, the expression for work on the turbine wheel periphery can be rewritten as follows:

$$L_u = u (C_c \cos \alpha_1 + C_2 \cos \alpha_2). \qquad (5.37)$$

Thus the work of 1 kg of gas on the turbine wheel periphery is equal to the product of the circumferential velocity of rotation times the algebraic sum of circumferential components of absolute velocities.

The same work can be expressed in the form of the difference in kinetic energies possessed by a gas when entering and exiting from the blading, that is

$$L_u = \frac{C_c^2 - C_2^2}{2}. \qquad (5.38)$$

5.12. Losses in the Turbine

We shall call the difference between work performed by an ideal turbine operating without losses with adiabatic gas expansion, and work performed by an actual turbine losses in the turbine (stage).

We differentiate the following losses:

from gas friction, vortex formation, and flow separation in the nozzle blade channels;

from friction, vortex formation, and flow separation on the turbine wheel blades;

losses with exit velocity;

losses connected with gas overflow through clearance gaps;

losses from wheel-gas friction;

ventilation losses;

mechanical losses.

The first three losses comprise so-called losses on the turbine crown. They are of determining significance and affect turbine efficiency more than all other losses.

With the exception of mechanical losses, all the rest are internal losses, taking place within the turbine housing and directly affecting the state of the gas.

Mechanical losses usually include power losses in overcoming friction in the engine bearings and reduction gears, as well as losses in driving feed (fuel and oil pumps) and control devices.

We shall briefly examine the nature and procedure of figuring in each of the above-enumerated losses.

Losses in the Nozzle Box

Losses in the nozzle box (nozzles) take place due to friction between gas particles and the nozzles as well as each other, due to vortex forming, shock waves, etc. As a consequence of this the actual gas velocity of exit from the nozzle will be less than the velocity it would possess in the absence of losses:

$$C_c = \varphi C_t$$

where ϕ — nozzle velocity coefficient; C_t — theoretical gas outflow velocity.

Energy losses in the nozzle are determined with the formula

$$\Delta L_c = \frac{C_t^2}{2} - \frac{C_c^2}{2} = \xi_c \frac{C_t^2}{2} = \xi_c L_0 \qquad (5.39)$$

where $\xi_c = 1 - \varphi^2$ — coefficient of energy loss in the nozzle; L_0 — available energy (work).

For gas turbines losses in the nozzle boz comprise from 10 to 20% of available work.

One should bear in mind that the value of the velocity coefficient is determined by blade height and profile, which restricts the channel.

The precise value of coefficient ϕ for a given nozzle or nozzle cascade can be determined only experimentally, observing similarity criteria. Losses in the nozzle box increase particularly sharply with nondesigned operating conditions, such as with increased back pressure, for example.

Losses on the Turbine Blades

According to modern concepts of gas movement through blade rows, the phenomena which take place in the turbine nozzle and turbine wheel channels have much in common. In both cases gas flows around the shaped blades with gas expansion in the channels formed by the blades.

An important factor which distinguishes flow through rotor blades is the fact that these blades are turning. In addition, gas velocity on entering the blading is usually higher than at nozzle blade entry, while there is always a radial clearance between blades and turbine housing, which may not be the case in the nozzles.

Due to losses, actual relative gas exit velocity from the turbine wheel will be less than theoretical:

$$w_2 = \psi w_{2t},$$

where ψ — turbine blade velocity coefficient.

For the case of a purely action turbine $w_2 = \psi w_1$, while energy losses on the blades are

$$\Delta L_{p.\,a} = \frac{w_{2t}^2 - w_2^2}{2} = \xi_{p.\,a} \frac{w_1^2}{2}, \qquad (5.40)$$

where $\xi_{p.\,a} = 1 - \psi^2$ — coefficient of energy loss on turbine blades.

For modern gas turbines, even with an optimal ratio of turbine wheel circumferential velocity to gas velocity at nozzle exit, energy losses on the turbine blades comprise 5-10% of available work.

The coefficient of energy loss on the blades is determined by the following factors.

By channel curvature or by fluid deflection, which is equivalent to the sum of angles $\beta_1+\beta_2$. With an increase in this sum ψ increases, and consequently $\xi_{p.л}$ decreases. This is due to the fact that the more curvilinear the channel, the greater the possibility of flow separation. In general the conditions of obtaining a slightly-curved blade, a channel of a converging shape, thicker leading edge and thinner trailing edge are achieved considerably more easily in a reaction blade row than in an action row, in view of the fact that losses in reaction blade rows are considerably less than in action rows.

By blade height. Energy losses increase sharply with a decrease in blade height, since the Reynolds number decreases with a decrease in blade height, and relative vortex pair losses increase.

By blade pitch (solidity). The smaller the blade pitch, the greater the number of blades and consequently the greater the number of rubbing surfaces. Maximum lift is generated with an optimal pitch value, and energy losses are reduced to a minimum.

By Reynolds number, with an increase in which ψ increases.

When $Re > 5 \cdot 10^5$ the turbine blade is operating in the so-called self-similar region, where ψ no longer is determined by the sum of angles $\beta_1+\beta_2$.

Losses with Exit Velocity

These losses are caused by the fact that on exiting from the turbine blades the gas possesses a certain velocity C_2, and consequently kinetic energy as well:

$$\Delta L_{вых} = \frac{C_2^2}{2}. \qquad (5.41)$$

Since this portion of gas kinetic energy was not utilized in the given stage, it must be added to losses, even if it is utilized in the succeeding stage or, for example, to produce reaction thrust.

In any of these cases the power produced by the given stage is reduced by the magnitude of exit loss, which comprises 5-15% of available heat drop (available work).

Efficiency on Wheel Periphery

If we subtract from the quantity of available work the magnitude of losses in the nozzles, blades and exit losses, we shall obtain work on wheel periphery L_u.

The ratio of work at wheel periphery to available work is called efficiency at wheel periphery. For a single-stage action turbine with symmetrical blades $\beta_1=\beta_2$:

$$\eta_u = \frac{L_u}{L_0} = 2\varphi^2(1+\psi)\left(\cos\alpha_1 - \frac{u}{C_c}\right)\frac{u}{C_c}. \qquad (5.42)$$

The above equation indicates that efficiency at the wheel periphery η_u is determined by nozzle and turbine blade velocity coefficients, the ratio $\frac{u}{C_c}$ and angle α_1 between the direction of flow after the nozzle box and the plane of rotation. These quantities are usually specified when designing a turbine, proceeding from specific considerations.

The basic factor which determines efficiency at the wheel periphery and turbine efficiency as a whole is the ratio $\frac{u}{C_c}$. Therefore function

$\eta_u = f\left(\frac{u}{C_c}\right)$ is of the greatest importance in turbine theory.

We shall determine ratio $\frac{u}{C_c}$ at which η_u possesses maximum value. For this we shall take the first derivative of the expression for η_u with $\frac{u}{C_c}$ and equated to zero, whence

$$\left(\frac{u}{C_c}\right)_{опт} = \frac{\cos\alpha_1}{2}.$$

Maximum value η_u corresponds to obtained value $\frac{u}{C_c}$:

$$\eta_{u\,max} = \frac{1}{2}\varphi^2(1+\psi)\cos^2\alpha_1. \qquad (5.43)$$

It follows from the expression for $\eta_{u_{max}}$ that the nozzle, not the turbine wheel is more important for a turbine from the standpoint of economy. In fact, a change in nozzle velocity coefficient ϕ by one one hundredth produces a change in efficiency of approximately 1.5-2%, while with the same change in turbine wheel velocity coefficient efficiency changes 0.5%.

Losses in Radial Clearance

Quantity L_u computed by us is work performed on the rim of a turbine without radial clearance betweer. blades and housing. In actuality this clearance is unquestionably necessary to avoid the blades hitting the housing, which can cause turbine failure. In view of the particularly stringent demands in regard to operational re. iability imposed on any engine, these clearances must be fairly substantial.

Losses in the radial clearance occur as a consequence of a portion of the gas passing through the radial clearance. In addition, as a consequence of a pressure gradient in the interblade channels, gas seeks to pass from the high-pressure region to the low-pressure region. This flow causes additional friction, vortex formation and related losses. Blades are shrouded to reduce these losses.

The amount of losses through the clearance is determined by the ratio of clearance amount δ_p to blade height l:

$$\bar{\delta}_p = \frac{\delta_p}{l}.$$

The greater δ_p, the greater the losses.

According to the data of S. M. Dorofeyev and V. Kh. Abiants, clearance losses are determined by clearance efficiency $\eta_з$, which constitutes the ratio of work on the rim L_u of a turbine with radial clearance to work on the rim L_u of a turbine without radial clearance, that is,

$$\eta_з = \frac{L_u - \Delta L_з}{L_u}, \qquad (5.44)$$

whence

$$\Delta L_з = (1 - \eta_з) L_u. \qquad (5.45)$$

Losses to Disk-Gas Friction and Fan Losses

Fan losses and losses to friction on ambient medium particles occur during turbine wheel rotation.

Disk friction losses are caused by the fact that gas particles surrounding the disk and blades acquire a certain velocity under the influence of friction against the disk surface, on which a portion of energy is expended.

We know that action turbines are made with partial admission of working medium. The nozzles occupy only part of the circumference of the nozzle ring, as a

consequence of which each blade channel during each revolution enters and leaves the sphere of effect of the working medium flow.

Fan losses are caused by phenomena which accompany blade rotation of a turbine with partial admission. These losses are caused, in the first place, by the fan action of the turbine blades which at a given moment are not receiving a flow of working medium; second, by the suction of inert gas from the clearances by the working medium, the flows of which are separated from one another as a consequence of the partial admission and, in the third place, by expenditure of energy on expelling particles of nonworking gas remaining in the blade channels before the turbine blade reaches the nozzle ("tear-out" losses).

Empirical formulas are normally employed to determine losses due to disk-gas friction and fanning $\Delta L_{т.в}$.

5.13. Turbine Power

If other internal losses are taken from work on the wheel periphery, that is, fan, disk-gas friction, and leakage, we obtain turbine internal work

$$L_i = L_u - \Delta L_в - \Delta L_{т.в}.$$

Corresponding to this work is internal or indicated turbine (stage) power N_i:

$$N_i = m_{сек} L_i. \tag{5.46}$$

The ratio of internal work to available work is called relative internal (power) efficiency, that is,

$$\eta_{oi} = \frac{L_i}{L_0}. \tag{5.47}$$

If we consider mechanical losses $\Delta L_м$, effective turbine work L_e will be equal to

$$L_e = L_i - \Delta L_м. \tag{5.48}$$

Corresponding to it is turbine effective power or shaft power

$$N_e = m_{сек} L_e. \tag{5.49}$$

The ratio of effective power to internal power or, what is the same thing, the ratio of effective to internal work, is called mechanical efficiency:

$$\eta_м = \frac{N_e}{N_i} = \frac{L_e}{L_i}. \tag{5.50}$$

The ratio of effective work to available work is called relative effective efficiency:

$$\eta_e = \frac{L_e}{L_0}. \tag{5.51}$$

This coefficient characterizes the degree of turbine sophistication and indicates what part of available gas energy is transformed into useful work on the turbine shaft.

Effective turbine power is

$$N_e = m_{сек} L_0 \eta_e \qquad (5.52)$$

5.14. Torpedo Reaction Engines

The idea of applying the reaction principle of motion in torpedoes arose and was developed simultaneously with the appearance and evolution of torpedoes. For example, as early as 1879 inventor A. I. Shpakovskiy presented to the Russian navy's technical committee the plans for a rocket-propelled torpedo, to be powered by a special rocket device. Numerous attempts to employ reaction engines in torpedoes were also made in other countries. However, these projects were either abandoned prior to completion or failed to produce satisfactory results. In addition, continuous improvement of conventional types of engines made it possible to provide torpedoes with the range and speed required by tactical considerations.

A reciprocating engine or turbine rotates the propellers, which propel the water mass in a direction opposite to the torpedo's direction of travel. According to the law of equal action and reaction, thrust of equal magnitude impels the torpedo forward.

The thrust of a jet or rocket engine is reaction imparted to the engine structure as a result of ejection of combustion products at high velocity from the combustion chamber through an exhaust nozzle. Thus reaction engines are engines which propel an object (torpedo, aircraft) as a result of the reaction force of an outflowing substance (gas, steam-gas, liquid).

There exist two types of reaction engines:

rocket engines, the operation of which involves the ejection of a substance located within the traveling object (torpedo, projectile, aircraft);

w a t e r j e t (air-reaction for an air environment) engines, in which the ambient medium passes through the engine and is accelerated to increase the quantity of motion with the aid of various mechanical or thermal devices.

The basic difference between reaction engines and equipment with reciprocating or turbine engines consists in the fact that thrust is independent of velocity. In addition, they possess significant size and weight advantages in comparison with reciprocating and turbine engines.

Figure 5.9 contains a diagram of a solid-fuel rocket engine. The combustion chamber contains solid fuel 1, which at the present time as a rule consists of special kinds of gunpowder-type propellant.

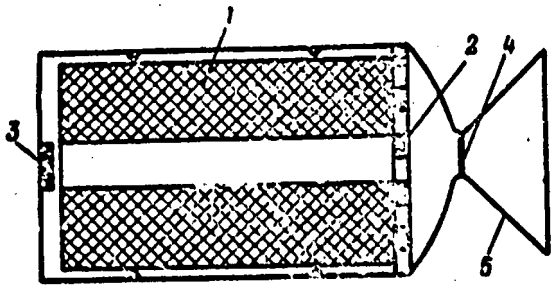

Figure 5.9. Diagram of Solid-Fuel Rocket Engine

There exist two basic types of solid propellant charges: with burning on part of the surface and on the entire surface. In charges of the first type part of the external surface (the outer surface and one of the ends) is covered with a substance which inhibits burning, or as they say, restricts, as a consequence of which the burning of such a charge can take place only on the surface not covered with this substance. Charges with burning on a part of the surface frequently burn like a cigarette, from one end to the other.

In solid propellant charges with any burning surface, when necessary support surfaces and ends are restrictive-treated.

Charges which burn only at one end burn for a longer time than charges with a total burning surface. Nevertheless it is difficult to delineate the areas of application of engines with charges of these two types, and a selection can be made only by taking the specific operating conditions in each individual case into account.

During engine operation solid-propellant charges are kept from collapsing by special diaphragm aperture 2.

Propellant ignition is effected either with explosive charge 3 or with a metal filament heated by an electric current. The role of the ignition device consists in elevating the propellant temperature to the combustion point and generating in the combustion chamber a pressure which can ensure normal burning. In order to obtain a faster pressure increase, diaphragm 4 is placed in the nozzle, which is destroyed when a certain pressure is reached.

The combustion products are ejected at high velocity through exhaust nozzle 5, generating engine thrust.

The principal feature of rocket engines is their simplicity. They contain no tanks, pipes, valves, injectors or fuel feed systems. However, the lack of efficient methods of recharging combustion chambers limits the time of continuous operation of a modern solid-fuel rocket engine to the burning time of the propellant charge.

Liquid fuel rocket engines operate on liquid fuel which is fed under pressure from tanks to the combustion chamber.

Fuels for liquid-fuel rocket engines usually consist of a liquid oxidizer (nitric acid, for example) and a liquid fuel (kerosene, for example). As a result of a chemical reaction between oxidizer and fuel in the combustion chamber, high-temperature gases are formed which are ejected at high velocity through the nozzle, producing thrust.

The high fuel combustion temperatures dictate the necessity of cooling the engine, which is usually effected by one of the fuel components. Entry of fuel components into the combustion chamber is effected either with pumps or by pressure exerted by compressed gas in special tanks. A solid-reactant or liquid-reactant gas generator can be employed in place of a compressed-gas cylinder. A device which generates gas to force fuel from the tanks by the burning of a solid-propellant charge or liquid fuels is called a solid (liquid)-reactant gas generator.

Substantial fuel consumption and the necessity of maintaining a constant fuel composition, high pressure in the combustion chamber, as well as the necessity of controlling the engine and ensuring safe engine operation have led to a situation where modern liquid-fuel rocket engines are very complicated devices with highly-sophisticated automatic control.

Thrust in hydrojet engines is produced by ejecting water through a nozzle at high velocity, water which enters the engine from the exterior. Seawater can be utilized both as an oxidizer and to increase the ejected mass. In utilizing seawater to increase thrust it is necessary to impart to it a certain quantity of kinetic energy. This can be achieved either by altering the thermodynamic parameters of the water by heating and vaporization or by power effect. The former method is most efficient in utilizing seawater as an oxidizer. In this case certain metals and compounds which vigorously react with water, releasing a large quantity of heat and gases, can be employed as fuel.

Power effect on water can be achieved either with the aid of special mechanical devices (of the water jet type) or by direct contact of gases fed into the engine or generated in it.

Hydrojet engines can be of various design.

CHAPTER 6. ELECTRIC TORPEDO ENERGY SOURCES AND MOTORS

6.1. General Description of Electric Torpedo Propulsion Systems

Alongside various types of torpedoes equipped with heat engines, electric torpedoes have been widely used, torpedoes which travel at a specified velocity and a specified range through the employment of electric power obtained from batteries, while its conversion to mechanical work of rotating propellers is effected with the aid of special DC motors. The propulsion system of electric torpedoes consists of the following principal components: a source of electric power, an electric motor, and propellers.

Electric power first began to be employed in torpedoes after World War I (beginning in the thirties) and was connected with solving the problem of eliminating the torpedo's bubble wake, a problem which was attacked from two directions: a search for fuels and oxidizers the combustion products of which readily dissolve in water, and the utilization of electric power in torpedoes.

Science and technology of the time proved to be more prepared to go the second route, which led to the development of electric torpedoes.

The development of such torpedoes, in combination with a system of torpedo launching without the release of telltale bubbles, as well as other measures, sharply improved concealment of submarine torpedo attacks.

Today the problem of running concealed has also been solved for torpedoes propelled by heat engines. However, this does not exclude the development and improvement of electric torpedoes, for the following reasons.

The speed and range of gas-steam torpedoes decrease with increased running depth. The power output of electric motors is independent of depth, which ensures constant speed and range for electric torpedoes at any depth.

Another important advantage of electric propulsion systems is the ease of providing an electric power supply for various influence systems, ease of changing running speed, and highly economical operation.

All these factors are to the advantage of electric propulsion systems over thermal systems and create prospects for extensive utilization. At the same time electric propulsion systems are inferior to heat engines in a number of indices: they are of lower power (as a result of which the speed and range of electric torpedoes are less than those of torpedoes propelled by heat engines) and they are more complex in operation (requiring comparatively frequent recharging and torpedo battery ventilation, insulation measurements, etc).

Chemical sources of electrical energy are principal components of an electric torpedo propulsion system.

Devices which convert chemical into electrical energy are called chemical current sources. Such an energy conversion can be performed by various types of devices. They are divided into two basic groups, in relation to character of chemical reactions: primary cells and storage batteries. The primary cells convert chemical energy into electrical energy only one time, after which they become unusable, since some chemical reactions are irreversible. In storage batteries energy is converted by means of reversible reactions, that is, storage batteries can be recharged, which means that they can be utilized time and time again.

Of the great diversity of existing storage batteries, chiefly lead-acid batteries are used as torpedo electric power sources.

Other chemical sources of electrical current are not employed in torpedoes for various reasons, the most important of which is unsatisfactory characteristics during discharge at high amperage.

In addition to this important requirement, torpedo power supplies must meet the following requirements:

convenience in utilization;

capable of operating across a broad temperature range;

provide maximum energy return per unit of weight and volume, as well as minimum loss of electric power;

a long service life and high mechanical strength.

Usually chemical electric power supplies, including torpedo storage batteries, are connected into banks of batteries. The number of storage batteries contained in a bank as well as their manner of connection into groups are determined by the electric motor's power requirements and total operating time, that is, the specified torpedo operating conditions. The properties of the individual storage battery in turn are determined by the quantity and quality of reacting chemical substances, and are also determined by its specifications.

The simplest storage battery is a vessel filled with electrolyte, containing a number of metal plates with grids filled with chemicals. One group of plates constitutes the positive electrode and another the negative. Isolating partitions -- separators -- are installed to eliminate the possibility of contact between plates of opposite charge. The separator material should be stable in regard to the electrolyte, and when impregnated by the latter should acquire porosity and low electrical resistance. A number of materials possess such qualities, particularly specially-processed thin sheets of wood (Siberian stone pine, alder, basswood), microporous rubber (porous ebonite), and polychlorvinyl resin.

The grids of positive and negative plates in various storage batteries may substantially differ i n size, type of material and design, but in all cases they serve to hold active chemical substances in the plates and to achieve uniform current distribution along the entire plate surface.

The most common form of grids which satisfy these requirements is in the form of mutually-intersecting lengthwise and crosswise rods. In some cases, to improve current discharge, the lengthwise rods are replaced by inclined bundles converging at the terminal end of the plate. The plate grids of lead-acid storage batteries are made of an alloy of 94-95% pure lead and 6-5% antimony added to improve the fluidity of the molten material and strength of the cast grids.

As for active chemical substances, that is, those materials which directly participate in the reactions, specially-prepared pastes are employed, applied to the plates, and electrolyte. The pastes of the positive and negative plates differ in chemical composition and method of preparation. Without going into detail on their composition and method of preparation, we shall note that in a charged lead-acid battery the active material of the negative plate is spongy lead -- Pb, and that of the positive plate is lead dioxide -- PbO_2. An aqueous solution of sulfuric acid, H_2SO_4, serves as electrolyte.

In order to increase the contact surface between plates and electrolytes, sotrage batteries contain several positive and negative plates which are connected in parallel and then soldered to two opposite-sign polar leads.

Torpedo electric motors are designed to convert the electrical energy of the storage battery into mechanical energy to turn the propellers. Such an energy conversion can be performed both by DC and AC motors. Since choice of type of motor is determined by the available type of current, DC motors are employed in electric torpedoes.

Torpedo electric motors have the following features in contrast to conventional motors:

brevity of operation (in the order of 10-15 minutes);

short service life (30-50 operating cycles);

limited operating voltage.

The following principal requirements are imposed on torpedo electric motors:

capability of producing high output at minimum weight and size; this is important because the motor's power is proportional to the cube of the torpedo's speed;

capability of startup without a rheostat; this requirement proceeds from the necessity of reaching the designed torpedo running speed as quickly as possible;

the electric motor should not spark during operation; this is dictated by safety considerations, since gases may be given off and an explosive mixture formed in the process of battery operation; in addition, sparking on the commutator generates additional electrical interference, which can have a negative effect on the operation of influence systems.

The operating principle of torpedo electric motors differs in no way from conventional electric motors, and therefore there is no need to study them. We shall merely note some of their specific and design features.

Of all energizing methods, only the series method is employed in electric torpedo motors, since it most fully satisfies all the requirements imposed on torpedo motors.

Alongside unary rotation motors, in which only the armature turns, motors of a differential type are also employed in electric torpedoes, where both the armature and magnet system rotate.

Differential motors are more powerful than conventional motors of the same size. This is due to the higher relative armature rotation speed in respect to the magnet system, in direct proportion to which motor output increases. Another advantage is the absence of a differential and reduction gear, which reduces torpedo noise and simplifies design. But the design of differential motors is more complex. They contain additional assemblies: a fixed housing, slip rings and twice as many bearings and brushes.

6.2. Electrical Characteristics of Storage Batteries

The useful work which a storage battery can perform is equal to the product of quantity of electricity It times voltage U. The quantity of electricity supplied by a battery and the voltage in turn are determined by load current and duration, electromotive force, internal resistance, and efficiency. These quantities are designated the electrical characteristics of a storage battery.

Battery emf and voltage. Battery emf E comprises the difference in electrode potentials with an open external circuit, that is,

$$E=E_{(+)}-E_{(-)},$$

where E_+ and E_- are the potentials of the positive and negative terminals respectively.

The magnitude of potential difference is determined by the quantity of ions contained in the electrolyte and free charges on the electrodes. And this is determined by the nature of the electrodes, electrolyte concentration and temperature, and can be computed for each of the electrodes according to the following analytical relation:

$$E_{(+)} = \frac{RT}{nF} \ln \frac{P_0}{P_э}, \qquad (6.1)$$

where R -- ion gas constant, equal to 8.3 $\frac{J}{g \cdot mole \cdot degr}$; T -- system absolute temperature; n -- electrode metal valance; P_0 and $P_э$ -- electrolyte ion osmotic pressure and metal diffusion elasticity respectively.

The shape, dimensions and quantity of masses both of electrodes and electrolyte do not affect quantity E.

Elevation of electrolyte temperature produces an increase in molecule kinetic energy, due to which the number of molecules dissociated into ions also increases. The latter increases ion osmotic pressure in solution P_0, and consequently E as well. However, an emf change by 1°C, that is,

$$\frac{dE}{dT}$$

for lead-acid batteries, does not exceed a few millivolts.

Storage battery emf (E) changes more substantially with electrolyte concentration. An increase in electrolyte concentration raises degree of dissociation α, which increases ion osmotic pressure P_0 and E.

An increase in E caused by an increase in concentration can be computed with formula (6.1). However, since P_0 measurement requires a considerable amount of time and its magnitude is in direct relation to electrolyte density d, one can figure in the influence of electrolyte concentration on E by quantity d, which is very simple to determine.

There exists the following Doletsaleka empirical formula, which links the emf value of a lead-acid battery with density d:

$$E=0.84+d. \qquad (6.2)$$

This formula gives fairly accurate results for d values of 1.1-1.3.

It is evident from expression (6.2) that quantity E increases with increase in electrolyte density d. In spite of this fact in most cases there is no sense in elevating d, because with an increase in d, battery internal resistance r_i increases, and voltage on high-amperage discharge may drop, since $U=E-Ir_i$.